R-09-36

Effects on surface hydrology and near-surface hydrogeology of an open repository in Laxemar

Results of modelling with MIKE SHE

Erik Mårtensson, Lars-Göran Gustafsson
DHI Sverige AB

Emma Bosson, Svensk Kärnbränslehantering AB

October 2009

Svensk Kärnbränslehantering AB
Swedish Nuclear Fuel
and Waste Management Co

Box 250, SE-101 24 Stockholm
Phone +46 8 459 84 00

ISSN 1402-3091
SKB Rapport R-09-36

Effects on surface hydrology and near-surface hydrogeology of an open repository in Laxemar

Results of modelling with MIKE SHE

Erik Mårtensson, Lars-Göran Gustafsson
DHI Sverige AB

Emma Bosson, Svensk Kärnbränslehantering AB

October 2009

Abstract

This report presents the methodology and the results from the modelling of an open repository for spent nuclear fuel in Laxemar. Specifically, the present work analyses the hydrological effects of the planned repository during the construction and operational phases when it is open, i.e. air-filled, and hence may cause a disturbance of the hydrological conditions in the surroundings. The numerical modelling is based on the SDM-Site Laxemar MIKE SHE model.

The modelling was divided into three steps. The first step was to update the SDM-Site Laxemar model with a new hydrogeological bedrock model (the bedrock model had been updated after the data delivery to the SDM-Site MIKE SHE model). The other main updates were an increase of the depth of the MIKE SHE model domain, enhanced vertical computational resolution and that the drainage of the Äspö Hard Rock Laboratory was included in the model. The resulting model was used to simulate undisturbed natural conditions.

The next step was to describe the open repository conditions, using Laxemar layout D2 (version 1.0, from February 2009), by implementing the access tunnel, the repository tunnels and shafts in the model, and to simulate the consequences for the surface hydrology caused by an open repository under different conditions. The final step was a sensitivity analysis that aimed to investigate the sensitivity of the modelled effects of the open repository to the hydrogeological properties of the bedrock and the Quaternary deposits, the sediments under the sea, and changes in boundary conditions.

The model covers an area of 34 km^2. The groundwater divides were assumed to coincide with the surface water divides; thus, a no-flow boundary condition was used at the horizontal boundaries, except in the Quaternary deposit layers towards the sea where a time-varying boundary condition describing the sea-level in the area was used. In the bedrock layers, however, a no-flow boundary condition was applied. Also the bottom boundary was described as a no-flow boundary. The transient top boundary condition was based on meteorological data gathered at the local SKB stations during the period 2004–2006.

The groundwater modelling was performed with the MIKE SHE code, a process-based modelling tool that calculates the groundwater flow in three dimensions. It takes the whole hydrological cycle into consideration and describes the water flow from rainfall to river flow. The coupling to the pipe flow model MOUSE was used to implement the repository. A development of the coupling code, compared to the code used in earlier open repository modelling, was made. The repository was described as a number of pipe links in MOUSE and the inflow of water from MIKE SHE to MOUSE, i.e. the flow of water from the aquifer to the tunnels, was calculated. The shafts were described as cells with atmospheric pressure.

The results from the updated MIKE SHE model for undisturbed conditions agrees with the results obtained from the SDM Laxemar model presented in the final (SDM-Site) version of the site description. The average specific runoff in the simulation for the year 2006 was calculated to 139 mm and the total evapotranspiration to 398 mm. The groundwater table in the area is rather deep; the mean depth to the groundwater table for the year 2006 was calculated to 3.7 m below ground surface (the sea area excluded). The discharge in the water courses is transient during the year and is dependent on the meteorological conditions.

The impact of the open repository on the groundwater table position is extensive, which is also the case with the head change in the bedrock, and reaches the model boundary in the northern and southern parts of the model domain. The largest drawdown of the groundwater table is developed above the central parts of the repository.

The calculated groundwater table drawdown and the size of the associated influence area (here defined as the area where the drawdown is larger than 0.3 m) are somewhat dependent on the level of grouting in the access tunnel and the deposition tunnels. Three levels of grouting were tested corresponding to hydraulic conductivities (K) of $1 \cdot 10^{-8}$ m/s in all tunnels, or $1 \cdot 10^{-9}$ m/s or $1 \cdot 10^{-10}$ m/s in deposition tunnels and $1 \cdot 10^{-8}$ m/s elsewhere. The lowest level of grouting leads to an influence

area of 16.7 km^2, as an average for 2006 (the last year in the simulation period). When the highest level of grouting is applied in the repository, the average influence area is calculated to 13.9 km^2 for the year 2006.

The temporal variation of the influence area during a year is rather small, with small differences in influence areas between most months in 2006. However, periods with heavy rain or snowmelt decrease the influence areas and cause a large difference between the maximum and minimum influence areas. The water level in Lake Frisksjön, as well as the discharges in the water courses, are affected by the open repository; for example, the average water level of Lake Frisksjön decreases with 0.1 m and the mean discharge of Laxemarån decreases with 8% compared to undisturbed conditions, with a grouting level of $K=1 \cdot 10^{-8}$ m/s.

The simulated total inflows to the open repository vary between 88 L/s and 55 L/s depending on the applied level of grouting. More than two thirds of the repository inflow comes from an increased vertical inflow from the land area. The influence areas and inflows specified above refer to a case with the whole repository open, i.e. with all the transport and deposition tunnels open at the same time. However, this is a hypothetical worst case scenario, because the repository will be constructed and taken into operation in five development phases. In the present modelling study, the second of these development phases and the initial construction phase were investigated in separate open repository simulations and the results compared to those obtained with the whole repository open at the same time.

Sammanfattning

Denna rapport ger en presentation av metodiken och resultaten från modelleringen av ett öppet förvar i Laxemar. Det huvudsakliga syftet var att beskriva effekterna av tillfartstunneln, det öppna slutförvaret och hiss- och luftschakt på grundvattenförhållandena och den ytnära hydrologin inom modellområdet. Den numeriska modelleringen baseras på MIKE SHE-modellen från SDM-Site Laxemar, vilket är den ythydrologiska modell som togs fram som en del den sista platsbeskrivande modellen av Laxemar (SDM-Site) som producerades under platsundersökningsskedet.

Modelleringen har delats in i tre huvuddelar. Första delen utgjordes av en uppdatering av den hydrogeologiska bergmodellen jämfört med den som använts i den sista versionen av platsbeskrivningen. Andra större uppdateringar bestod främst i att komplettera modellen med data för det djupa berget ner till nivån 1 190 meter under havet, att förfina modellens vertikala indelning i beräkningslager, samt att inkludera dräneringen av Äspölaboratoriet i modellen. Denna modell användes sedan för att simulera opåverkade (av förvaret) förhållanden.

Nästa steg var att beskriva det öppna förvaret, varvid Laxemar layout D2 användes (version 1.0, från februari 2009), med tillfartstunnlar och schakt i modellen, samt att simulera och beskriva effekterna på den ytnära hydrologin av det öppna förvaret under olika förhållanden. Slutligen gjordes en känslighetsanalys som syftade till att undersöka modellens känslighet för bergets egenskaper, egenskaperna hos jordlagren, sedimenten under havet, samt förändrade randbetingelser med avseende på ett antal parametrar som beskriver omgivningspåverkan från ett öppet förvar.

Modellen täcker ett område på 34 km^2. Yt- och grundvattendelare antas sammanfalla. Därför har en tät rand (en rand med nollflöde) ansatts vid de horisontella ränderna, förutom i jordlagren mot havet där en tidsvarierande tryckrand lika med uppmätt havsnivå ansatts. I berget har dock en tät rand använts. Även bottenranden har beskrivits med en tät rand. Det övre randvillkoret beskrivs med hjälp av nederbörd och potentiell avdunstning. Meteorologidata från SKB:s lokala väderstationer för åren 2004–2006 har använts som indata.

Grundvattenmodelleringen har genomförts med modellkoden MIKE SHE, ett processbaserat modellverktyg som beräknar grundvattenflödet i tre dimensioner. MIKE SHE beskriver hela den hydrologiska cykeln, från nederbörd till avrinning i bäckar och vattendrag. Kopplingen till modellverktyget MOUSE (utvecklat för beskrivning av ledningsnät) användes för att implementera förvaret i modellen. Jämfört med tidigare modelleringar av öppet förvar med MIKE SHE, har en uppdatering av kopplingskoden genomförts. Förvaret beskrivs som ett antal ledningar i MOUSE och vattenflödet mellan MIKE SHE och MOUSE, d.v.s. vattenflödet från akviferen till tunnlarna, beräknades. Hiss- och ventilationsschakt beskrevs i modellen som celler med atmosfärstryck.

Resultaten från den uppdaterade MIKE SHE-modellen, som syftar till att beskriva hydrologin i området under ostörda förhållanden, stämmer bra överens med de resultat som presenterades i platsbeskrivningen SDM-Site Laxemar. Avrinningen för år 2006 beräknades till 139 mm och den totala evapotranspirationen till 398 mm. Grundvattenytan i området ligger ganska långt under markytan; medeldjupet till grundvattenytan i hela modellområdet (exklusive havet) för den simulerande perioden 2006 är 3,7 m under markytan. Flödena i områdets vattendrag varierar mycket under året och starkt kopplade till de meteorologiska förhållandena i området.

Påverkan av det öppna förvaret på grundvattenytan i jordlagren är, liksom portrycksändringen i berget, betydande och det påverkade området når modellranden i både norr och söder. Den största avsänkningen av grundvattenytan sker i förvarets centralområde.

Avsänkningen av grundvattenytan och storleken på påverkansområdet, vilket här definieras som det område där grundvattenytan sänks av mer än 0,3 m, visade sig vara beroende av vilken grad av tätning som appliceras på tunnelväggarna. Tre tätningsfall testades motsvarande hydrauliska konduktiviteter (K) på $1\cdot10^{-8}$ m/s, $1\cdot10^{-9}$ m/s eller $1\cdot10^{-10}$ m/s i den tätade zonen runt tunnlar och schakt. I de två sistnämnda fallen var tätningen $1\cdot10^{-8}$ m/s runt alla tunnlar förutom runt deponeringstunnlarna där tätning motsvarande $1\cdot10^{-9}$ m/s eller $1\cdot10^{-10}$ m/s antogs. För den lägsta tätningsnivån med K=$1\cdot10^{-8}$ m/s beräknades påverkansområdet till i medeltal ca 16,7 km^2 för år

2006 (sista året i simuleringsperioden). När den högsta tätningsnivån tillämpades på tunnelväggarna i modellen ($K=1\cdot10^{-10}$ m/s runt deponeringstunnlarna och $1\cdot10^{-8}$ m/s runt övriga tunnlar) erhölls ett påverkansområde på i medeltal ca 13,9 km^2 för år 2006.

Påverkansområdets tidsmässiga variation var generellt ganska liten under ett år, med små skillnader i påverkansområdet mellan månaderna under modellåret 2006. Resultaten visade dock att ett kraftigt regn eller snabb snösmältning kan orsaka stora skillnader mellan det minsta och det största påverkansområdet. Såväl nivåerna i Frisksjön som flödet i vattendragen påverkas i relativt stor omfattning av förvaret. Som exempel kan nämnas att den beräknade medelvattennivån i Frisksjön minskar med 0,1 m och medelflödet i Laxemarån med 8 % jämfört med ostörda förhållanden när tätningsnivån $K=1\cdot10^{-8}$ m/s tillämpas i modellen.

De beräknade totala inflödena till det öppna förvaret varierar mellan 55 L/s och 88 L/s beroende på vilket tätningsfall som studeras. Mer än två tredjedelar av inflödet till förvaret härstammar från ett ökat vertikalt inflöde från landområdet. De angivna påverkansområdena och inflödena ovan baseras på ett beräkningsfall där hela djupförvarsanläggningen antas vara öppen, vilket innebär att alla transport- och deponeringstunnlar är öppna samtidigt. Detta är dock ett hypotetiskt värsta fall som inte kommer att inträffa i verkligheten. Förvaret kommer att anläggas och tas i drift i fem utbyggnadsfaser. Beräkningsfall som beskriver effekterna av enskilda utbyggnadsfaser har därför också studerats i modelleringen.

Contents

1 Introduction

1.1 Background

The Swedish Nuclear Fuel and Waste Management Company (SKB) has performed site investigations at two different locations in Sweden, referred to as the Forsmark and Laxemar-Simpevarp areas, with the objective of siting a final repository for high-level radioactive waste (spent nuclear fuel). Data from the site investigations are used in a variety of modelling activities, and the results are utilised within the frameworks of Site Descriptive Models (SDM), Safety Assessment (SA), and Environmental Impact Assessment (EIA). The SDM provides a description of the present conditions at the site, which is used as a basis for developing models intended to describe the future conditions in the area. This report presents results of numerical flow modelling of surface water and near-surface groundwater, with the aim to quantify the effects of an open repository at the Laxemar site.

The numerical modelling was performed using the modelling tools MIKE SHE and MOUSE, and is based on the conceptual description of the Laxemar site presented in /Werner 2009/. The modelling performed in this project is based on the SDM Laxemar MIKE SHE model /Bosson et al. 2009/. The results from all the different modelling disciplines within the site descriptive modelling project are summarised in /SKB 2009/ and the surface system is described in /Söderbäck and Lindborg (eds) 2009/.

During the construction and operation phases, there will be atmospheric pressure in the open tunnels and shafts and rock caverns in the repository. This will cause disturbances in the pressure field around the subsurface constructions and inflow of groundwater. The size of this inflow and its possible effects on surrounding groundwater and surface water systems need to be quantified. The issues related to the effects of the open repository concern both the conditions in the repository (inflows and hydrochemical conditions) and in the surrounding environment (groundwater levels, surface water levels and discharges). Thus, the open repository modelling will deliver results to both SA and EIA. The modelling presented in this report is focused on the effects on the surface hydrology and near-surface hydrogeology, i.e. on the surrounding environment and produces input primarily to the EIA activities.

1.2 Scope and objectives

Using the MIKE SHE SDM-Site Laxemar model as a starting point, the present modelling work can be subdivided into the following three parts:

1. Update the SDM-Site Laxemar model in /Bosson et al. 2009/ (new hydrogeological bedrock model, increased depth of the model domain, enhanced vertical resolution in the numerical model, and inclusion of the drainage of the Äspö Hard Rock Laboratory), and simulation of undisturbed conditions.
2. Implementation of the open repository description in the flow model, and analysis of the hydrogeological and hydrological effects of the open repository (effects on surface hydrology and the hydrogeological conditions in the Quaternary deposits and the bedrock).
3. Analyses of the sensitivity of the model to the hydrogeological properties of the bedrock, the properties of the Quaternary deposits, the model boundary conditions, and the sediments under the sea, with respect to the effects of the open repository.

The general objectives of the present modelling are the following:

- Develop and present an open repository flow model based on the MIKE SHE SDM-Site Laxemar model.
- Provide qualitative and quantitative results to be used primarily the EIA for analysing the impact of the repository during the construction and operation phases.

- Evaluate the influence of the open repository on groundwater levels, surface water levels and surface water discharges within the model area.
- Evaluate the inflow to different parts of the open repository construction under different conditions; in particular for three different levels of grouting.

1.3 Setting

The Laxemar area is located approximately 320 km south of Stockholm, in eastern Småland within the municipality of Oskarshamn. Figure 1-1 shows the regional model area and the local model area of SDM-Site Laxemar. Also some lakes and other objects of importance for the hydrological modelling are shown in the figure.

During the period from 2002 to 2007, site investigations were conducted mainly within a square-shaped area referred to as the Laxemar-Simpevarp regional model area, covering approximately 273 km^2. The local model area is the area prioritised for potentially hosting the geological repository, which means that the repository possibly could be built somewhere within this area (not that it would occupy the whole area). This implies that more detailed investigations have been performed within the local model area, at least for some of the site investigation disciplines, see /SKB 2009/ for details. The local model area is situated to the west, in close vicinity of the Oskarshamn nuclear power plant.

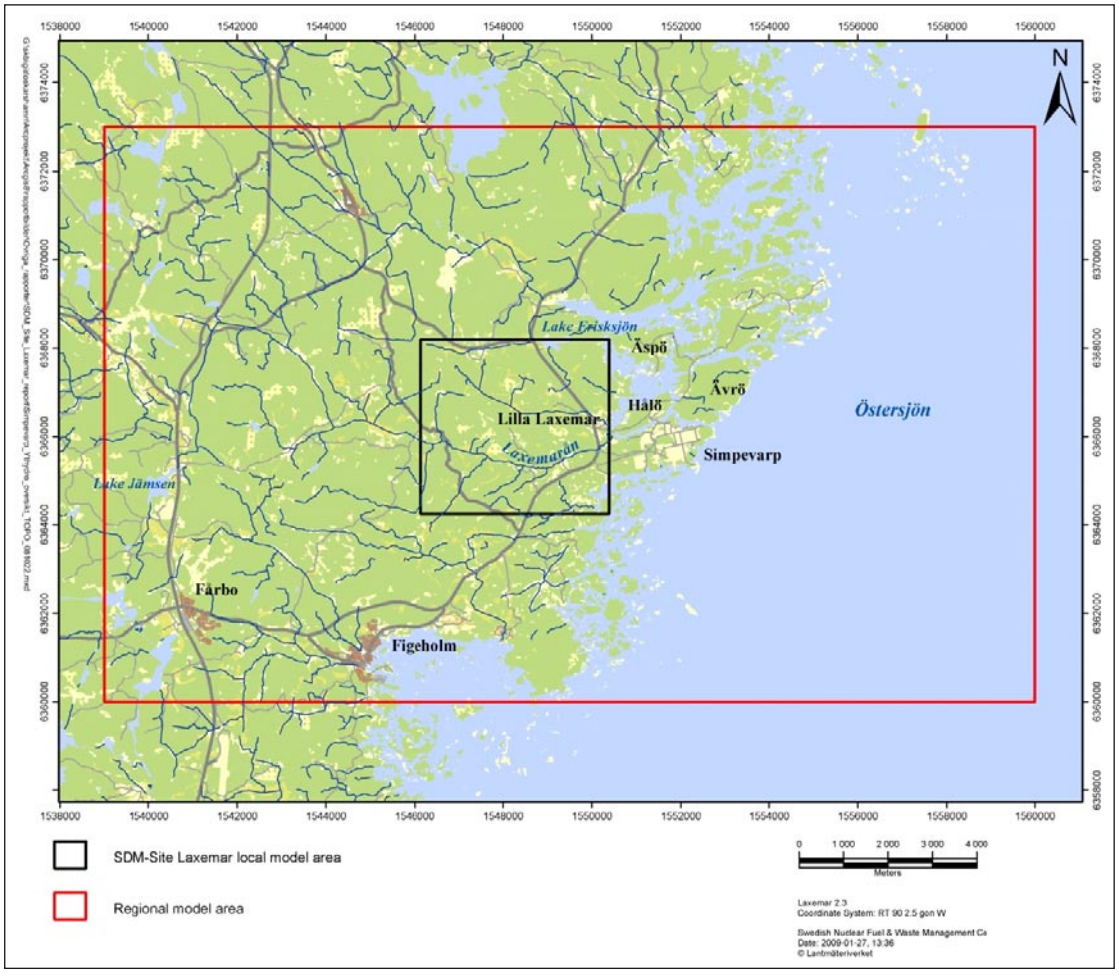

Figure 1-1. *Overview map of the Laxemar-Simpevarp regional model area and the SDM-Site Laxemar local model area.*

In this report, the datum plane is RHB 70. Depending on type of data presented, levels will be given in metres above sea level, abbreviated m.a.s.l., or metres below sea level, m.b.s.l., according to RHB 70.

A description of the climate and the hydrological and hydrogeological conditions in the Laxemar-Simpevarp area is presented in /Werner 2009/. The main surface system report produced as a part of SDM-Site Laxemar /Söderbäck and Lindborg (eds) 2009/ gives a description of the whole surface and near-surface system, including the most recent models of, e.g. the topography and the Quaternary deposits.

1.4 Modelling procedure

The present modelling work is based on the SDM-Site Laxemar MIKE SHE model /Bosson et al. 2009/. A reference simulation was defined as an updated version of the calibrated final model version described in /Bosson et al. 2009/. The reference simulation was used as a base model for the tunnels, shafts and rock caverns introduced into the modelling work to investigate how these constructions would affect the surface hydrology and near-surface hydrogeology in the model area. The last step was a sensitivity analysis which aimed to investigate the sensitivity to the level of grouting of the tunnel walls.

1.5 Related modelling activities

Several modelling activities have provided the various external input data and models required for the present modelling. Whereas most of these inputs are described in /Bosson et al. 2009/, we discuss here briefly the interactions with the hydrogeological activities that consider flow modelling of the integrated rock-Quaternary deposits system and the modelling activities analysing the influences of an open repository and the design work of the planned repository.

The numerical model was developed using the MIKE SHE tool, coupled with the modelling tool MOUSE describing the geometry of the repository and its interactions with the surrounding groundwater system. The ground surface, as obtained from the topographical model (DEM) of the site, is the upper model boundary and the lower boundary is set at 1,190 m.b.s.l. The modelling activities that provided inputs to the various parts of this work can be summarised as follows:

- The SDM Laxemar hydrogeological modelling performed with the ConnectFlow modelling tool /Rhén et al. 2009/ delivered the description of the hydrogeological properties of the bedrock.
- The SDM-Site conceptual modelling of the surface hydrology and near-surface hydrogeology at the Laxemar site /Werner 2009/ provided a basic hydrogeological parameterisation and a hydrological-hydrogeological description to be tested in the numerical modelling. The relations between the near-surface and bedrock hydrogeological models are discussed in /Söderbäck and Lindborg (eds) 2009/.
- The MIKE SHE SDM-Site Laxemar numerical modelling of the hydrology and near-surface hydrogeology /Bosson et al. 2009/ provided the numerical model used as a starting point for the present modelling. All the simulations in this report are based on an update of the final version of the MIKE SHE model described in /Bosson et al. 2009/.
- The repository design work provided the repository layout, i.e. the geometrical description of tunnels and shafts, also input to the selection of grouting levels, i.e. the thickness and hydraulic conductivities of the grouted zone in the different simulation cases studied.

Another related modelling activity is the ongoing open repository simulations performed using the DarcyTools code. The DarcyTools modelling is focused on the bedrock and the conditions at repository depth, with detailed studies of the inflow to tunnels and the resaturation after repository closure. Although not providing input data to the present MIKE SHE modelling, the results of the DarcyTools modelling will be useful for making comparisons and consistency checks in connection with the Environmental Impact Assessment.

1.6 This report

This report provides an integrated presentation of the modelling activities listed in Section 1.2. Chapter 2 describes the modelling tool and the numerical flow model. In Chapter 3, the model updates, simulation specifications as well as the conditions and simulation cases for disturbed conditions, with the open repository included in the model, are presented. The results of a reference simulation for undisturbed conditions are presented in Chapter 4. Chapter 5 presents results from simulations of disturbed conditions. In Chapter 6 input data, simulation cases and results of simulations with different meteorological input data are presented. Chapter 7 describes and presents results from a sensitivity analysis investigating various hydraulic parameters and boundary conditions, and Chapter 8 presents the conclusions of the work.

2 Overview of modelling tools

2.1 MIKE SHE

MIKE SHE (Système Hydrologique Europeen) is a physically based, distributed model that simulates water flows from rainfall to river flow. It is a commercial code, developed by the Danish Hydraulic Institute (DHI). This sub-section summarises the basic processes and the governing equations in MIKE SHE. The code used in this project is software release version 2008. For a more detailed description, see the user's guide and technical reference /DHI Software 2008a/.

MIKE SHE describes the main processes in the land phase of the hydrological cycle. The precipitation can either be intercepted by leaves or fall to the ground. The water on the ground surface can infiltrate, evaporate or form overland flow. Once the water has infiltrated the soil, it enters the unsaturated zone. In the unsaturated zone, it can either be extracted by roots and leave the system as transpiration, or it can percolate down to the saturated zone (Figure 2-1). MIKE SHE is fully integrated with a channel-flow code, MIKE 11. The exchange of water between the two modelling tools takes place during the whole simulation, i.e. the two programs run simultaneously.

MIKE SHE is developed primarily for modelling of groundwater flow in porous media. However, in the present modelling the bedrock is also included. The bedrock is parameterised by use of data from the SDM Laxemar groundwater flow model /Bosson et al. 2009/.

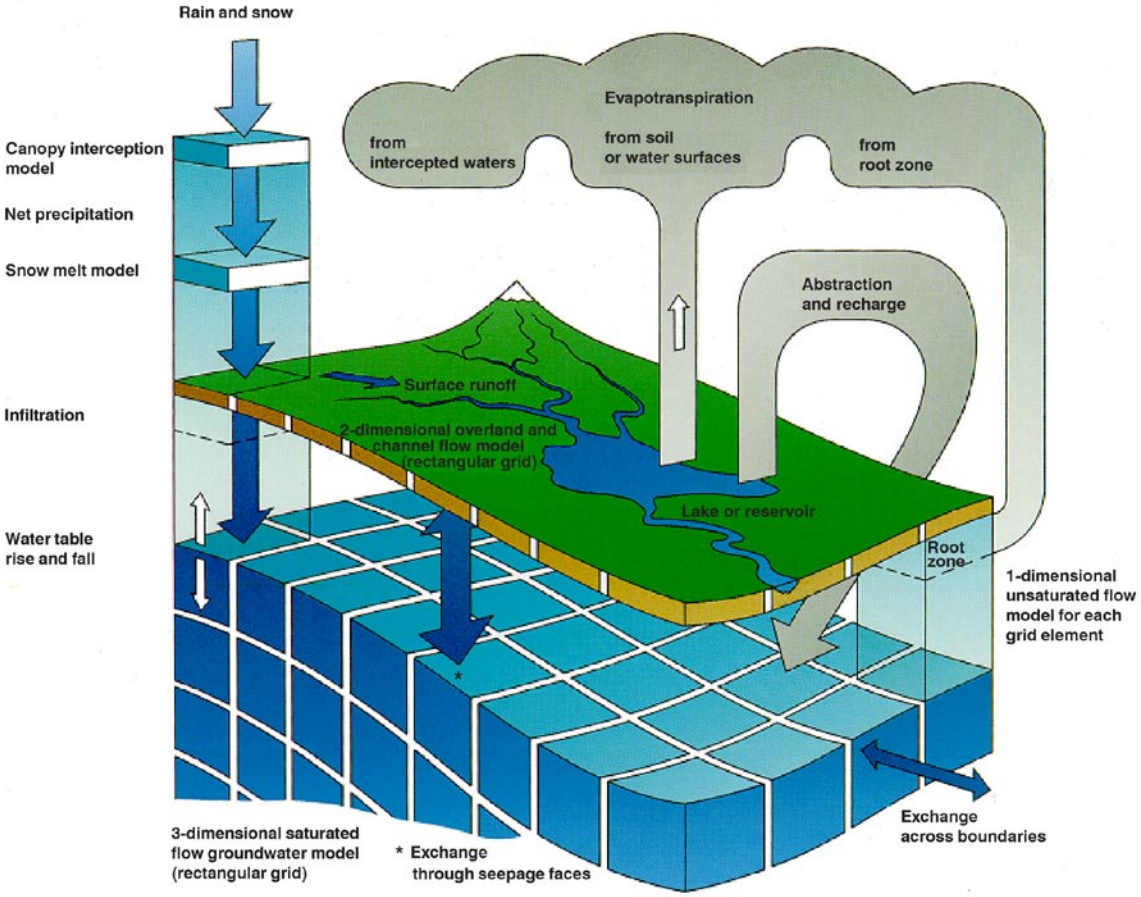

Figure 2-1. *Overview of the MIKE SHE model /DHI Software 2008a/.*

MIKE SHE consists of the following model components:

- Precipitation (rain or snow).
- Evapotranspiration, including canopy interception, which is calculated according to the principles of /Kristensen and Jensen 1975/.
- Overland flow, which is calculated with a 2D finite difference diffusive wave approximation of the Saint-Venant equations, using the same 2D mesh as the groundwater component. Overland flow interacts with rivers, the unsaturated zone, and the saturated (groundwater) zone.
- Channel flow, which is described through the river modelling component, MIKE 11, which is a modelling system for river hydraulics. MIKE 11 is a dynamic, 1D modelling tool for the design, management and operation of river and channel systems. MIKE 11 supports any level of complexity and offers simulation tools that cover the entire range from simple Muskingum routing to high-order dynamic wave formulations of the Saint-Venant equations.
- Unsaturated water flow, which in MIKE SHE is described as a vertical soil profile model that interacts with both the overland flow (through ponding) and the groundwater model (the groundwater table provides the lower boundary condition for the unsaturated zone). MIKE SHE offers three different modelling approaches, including a simple two-layer root-zone mass balance approach, a gravity flow model, and a full Richards's equation model.
- Saturated (groundwater) flow, which allows modelling of 3D flow in a heterogeneous aquifer, with conditions shifting between unconfined and confined. The spatial and temporal variations of the dependent variable (the hydraulic head) are described mathematically by the 3D Darcy equation and solved numerically by an iterative implicit finite difference technique.

For a detailed description of the processes included in MIKE SHE and MIKE 11, see /DHI Software 2008a/.

2.2 The coupling between MIKE 11 and MIKE SHE

The coupling between MIKE 11 and MIKE SHE is made via so-called river links, which are located on the edges that separate adjacent grid cells. The location of each river link is determined from the co-ordinates of the MIKE 11 river points. Since the MIKE SHE river links are located on the edges between grid cells, the details of the MIKE 11 river geometry can be only partly included in MIKE SHE, depending on the grid size. The smaller the grid size, the more accurately the river network can be reproduced. This also leads to the restriction that each MIKE SHE grid cell can only couple to one coupling reach in MIKE 11 per river link in MIKE SHE.

2.2.1 Overland water

In this version of the Laxemar model, a one-way communication from overland flow to the streams is applied. Consequently, this option does not allow river water to spill onto the MIKE SHE model as overland flow.

If water levels are such that water flows to the river, overland flow to the river is added to MIKE 11 as lateral inflow. If the water level in the river is higher than the level of ponded water, there will be no overland flow to the river, but instead an increase of the ponded water around the river, until the level of ponded water again is higher than in the river.

2.2.2 Groundwater

The communication between the river network and the groundwater aquifer is calculated in the same way as for previous versions of the code /DHI Software 2008a/. The groundwater coupling between MIKE 11 and MIKE SHE is made via river links, which are located on the edges that separate adjacent grid cells. The exchange flow between a saturated zone grid cell, with contact to the river system, and a river link is included as a source/sink term in the governing flow equation

for three-dimensional saturated flow. The exchange flow (Q_{cell}) is calculated as a conductance (C) multiplied by the head difference (dh) between the river and the grid cell according to Equation 2-1. The principle is illustrated in Figure 2-2.

$$Q_{cell} = dH \cdot C \qquad \text{(Equation 2-1)}$$

Q_{cell} Exchange flow from one neighbouring grid cell to the river link (m^3/s).

dh Head difference between the river link and the neighbouring grid cell (m).

C Total conductance (m^2/s).

Note that Equation 2-1 is calculated twice – once for each cell on either side of the river link. This allows for different flow to/from each side of the river if there is a groundwater head gradient across the river, or if the aquifer properties are different.

The conductance C between the grid cell and the river link is a function of the water level in the river, the river width, the elevation of the riverbed, as well as the hydraulic properties of the riverbed and the aquifer material, according to Equation 2-2 and Figure 2-2.

$$C = \frac{1}{\frac{ds}{K_h \cdot da \cdot dx} + \frac{1}{LC \cdot P \cdot dx}} \qquad \text{(Equation 2-2)}$$

K_h Horizontal hydraulic conductivity (m/s).

da Vertical surface available for exchange flow (m).

dx Grid size (m).

ds Average flow length (m), i.e. the distance from the grid node to the middle of the river bank.

P Wetted perimeter of the cross-section (m), assumed to be equal to the sum of the vertical (da) and horizontal (lh) lengths available for exchange flow (Figure 2-2).

LC Leakage coefficient of the bed material (s^{-1}).

The MIKE 11 hydraulic model uses the precise cross-sections, as defined in MIKE 11, for calculating the river water levels and the river volumes. However, the exchange of water between MIKE 11 and MIKE SHE is calculated based on the river link cross-section, which is a simplified, triangular cross-section. The top width is equal to the distance between the left and right banks of the cross-section. The elevation of the bottom of the triangle equals the lowest level of the MIKE 11 cross-section, see Figure 2-2.

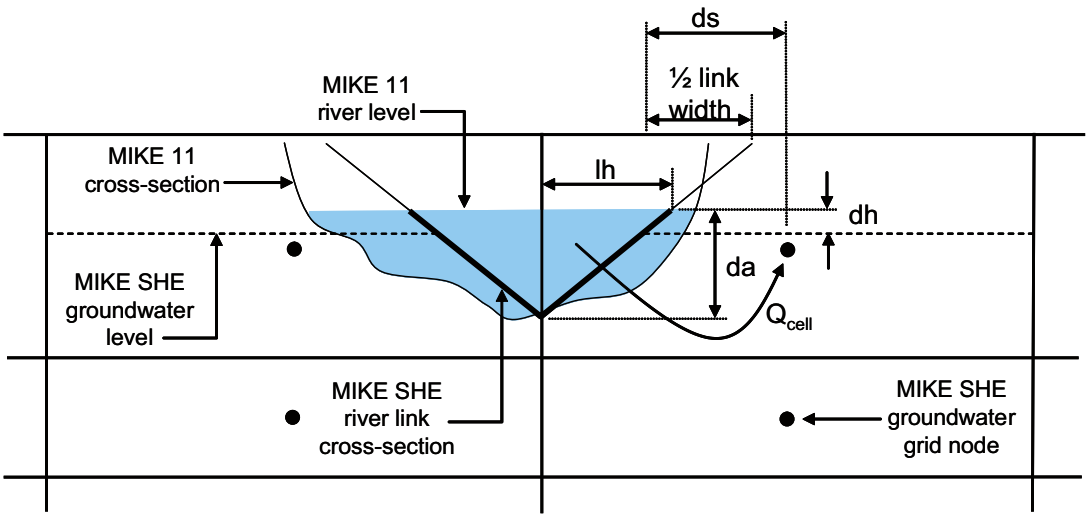

Figure 2-2. *Illustration of the groundwater coupling between MIKE11 and MIKE SHE, and representation of relevant parameters used for calculating the exchange of water.*

2.3 The coupling between MOUSE and MIKE SHE

In the present open repository modelling, the program MOUSE /DHI Software 2008b/ has been used for modelling the inflow to the repository tunnels. MOUSE is a modelling tool developed for urban hydrology and pipe flow hydraulics. The coupling between MOUSE and MIKE SHE is primarily used for calculating groundwater infiltration to sewers. In this project, the access tunnel from the ground down to the repository, the tunnels and rock caverns in the central area, the transport tunnels and the deposition tunnels have been described as a number of pipe links in MOUSE. The program calculates the flow of water between the MIKE SHE groundwater model and the MOUSE model, i.e. the inflow of water to the tunnels, according to Section 2.3.1.

In the present version of the coupling between MOUSE and MIKE SHE, inflow of water to vertical shafts (manholes in MOUSE) is not allowed. Therefore, the inflow of water to the shafts is calculated in MIKE SHE only, as described in Section 2.3.2.

2.3.1 Description of different levels of grouting for tunnels

The results of the comparison between an analytical solution and the numerical MIKE SHE and MOUSE coupling in /Gustafsson et al. 2009/ showed that the flow between MIKE SHE and MOUSE was underestimated in the numerical model. A development of the code, compared to the one used in /Bosson 2006, Gustafsson et al. 2009/, and in all other previous open repository modelling, has therefore been performed for the present modelling work. The improved code described below is used in all simulations presented in this report.

The exchange flow between a saturated zone grid cell (MIKE SHE) and a tunnel link (MOUSE) intersecting the grid cell, is included as a source/sink term in the governing flow equation for three-dimensional saturated flow. The exchange flow is calculated according to Equation 2-3. The principle is illustrated in Figure 2-3.

$$Q_{cell} = dh \cdot \frac{K \cdot 2 \cdot \pi}{\ln(\frac{r + d_{grout}}{r})} \cdot L \qquad \text{(Equation 2-3)}$$

Q_{cell} Leakage flow from grid cell to tunnel (m^3/s).

dh Head difference between groundwater head, h_{aq} (in the grid cell where the tunnel is located), and the water head in the tunnel link, h_t (m).

L Length of a tunnel segment intersecting the grid cell (m).

K Hydraulic conductivity (m/s).

r Tunnel radius (m).

d_{grout} Thickness of the grouted zone (m).

The level of grouting and the "ungrouted" hydraulic conductivity, in both the vertical and the horizontal direction, of the bedrock are taken into consideration by setting the hydraulic conductivity, K, in Equation 2-3, according to Equation 2-4.

$$K = \min[K_{grout}, \max(K_h, K_v)] \qquad \text{(Equation 2-4)}$$

K_{grout} Hydraulic conductivity of the grouting level, i.e. the conductivity of the bedrock after grouting to a certain level (m/s).

K_h Horizontal hydraulic conductivity of the bedrock grid cell (m/s).

K_v Vertical hydraulic conductivity of the bedrock grid cell (m/s).

Equation 2-4 governs whether the hydraulic conductivity of the grouting material, K_{grout}, or the aquifer, K_h or K_v, should be used when calculating the total inflow to the tunnel (Equation 2-3). The hydraulic conductivity of the aquifer varies with depth and is set according to the conductivity in the actual calculation layer. The exchange of water also depends on the head difference between the tunnel and the aquifer, as well as the tunnel radius (Equation 2-3). The only input data needed for the coupled MOUSE-MIKE SHE simulation, except for the geometry and location of the tunnel,

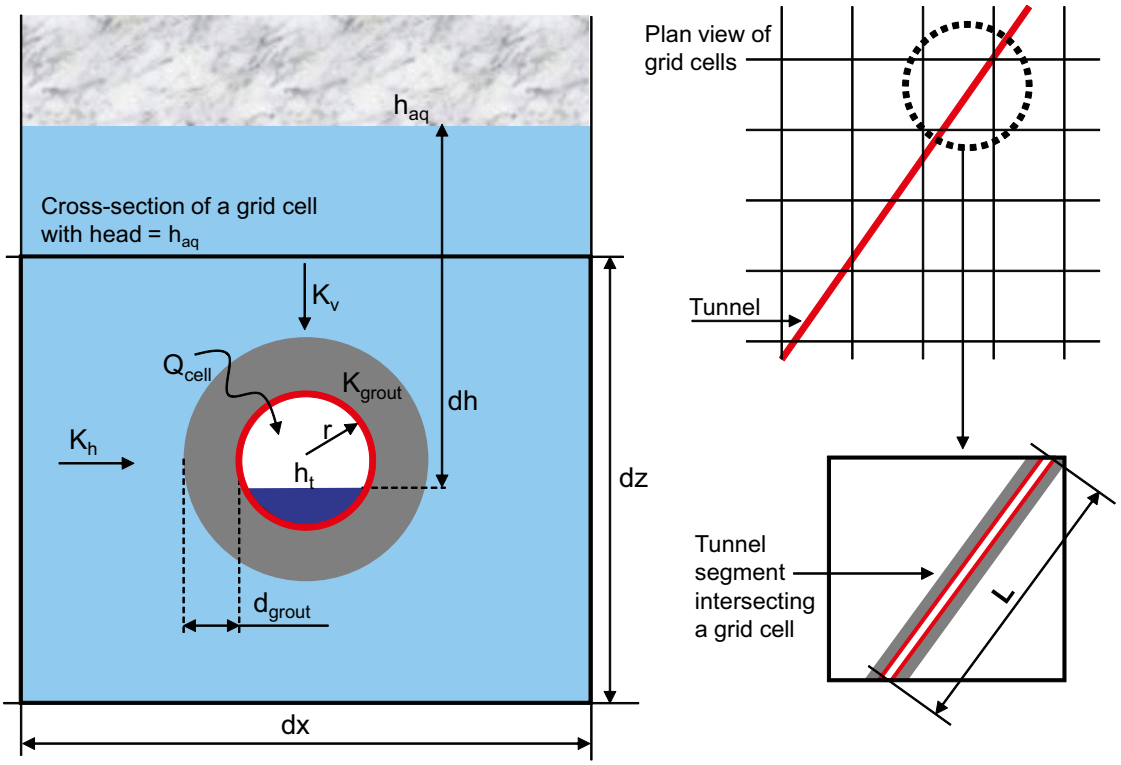

Figure 2-3. *Illustration of the groundwater coupling between MOUSE and MIKE SHE, and representation of relevant parameters used for calculating the exchange of water.*

is the grouting conductivity of the tunnel, K_{grout}, and the thickness of the grouted zone, d_{grout}, which may be specified as a unique value for each tunnel link.

In the present open repository modelling work, different levels of grouting, formulated as different hydraulic conductivities of the grouted zone, have been applied in the description of the repository. These different grouting cases are described in Section 3.3.

2.3.2 Description of different levels of grouting for shafts

The shafts are described as grid cells in MIKE SHE with a specified head, corresponding to atmospheric pressure, in the calculation layers intersected by the shafts. The leakage flow from the aquifer to a shaft is then calculated as the sum of flows from all calculation layers intersecting the shaft, based on a specified conductance, C, for each calculation layer. The leakage flow from a saturated zone grid cell, containing one or several shafts, is included as a sink term in the governing flow equation for three-dimensional saturated flow. The leakage flow is calculated according to Equation 2-5. The principle is illustrated in Figure 2-4.

$$Q_{cell} = dH \cdot C \qquad \text{(Equation 2-5)}$$

Q_{cell} Leakage flow from grid cell containing the shaft (m^3/s).

dh Difference (m) between the calculated head in the grid cell containing the shaft and the specified head boundary (equal to the lower level of the calculation layer when the shaft is deeper than the lower level of the calculation layer, and equal to the bottom of the shaft if the bottom is above the lower level of the calculation layer).

C Total conductance (m^2/s).

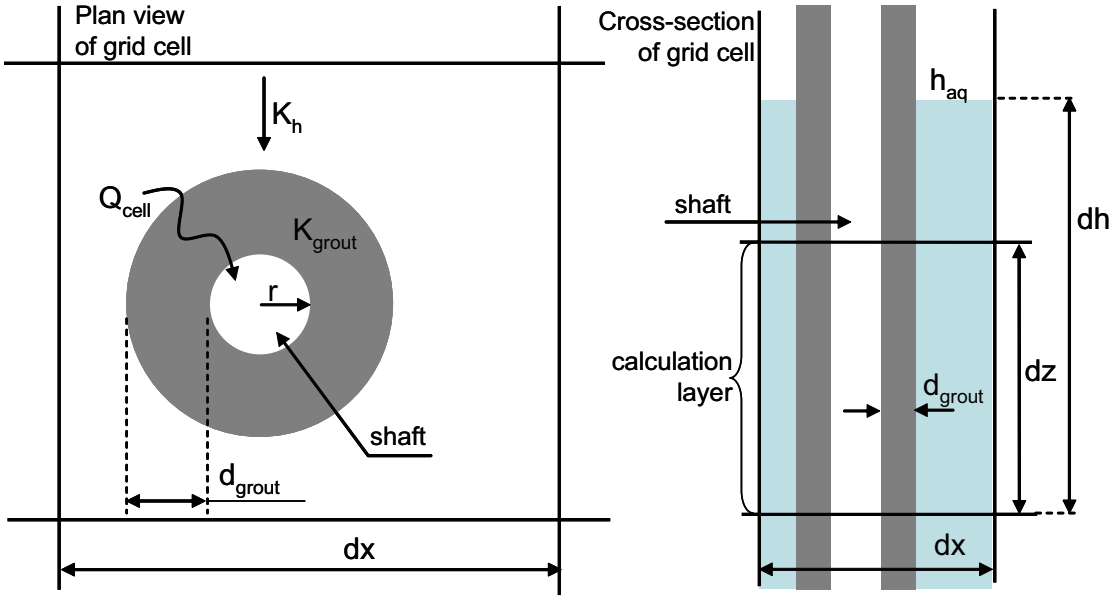

Figure 2-4. *Illustration of how the exchange of water is calculated for the shafts.*

The total conductance, C, is calculated according to Equation 2-6.

$$C = \frac{K \cdot 2 \cdot \pi}{\ln\left(\frac{r + d_{grout}}{r}\right)} \cdot dz \qquad \text{(Equation 2-6)}$$

K Hydraulic conductivity (m/s).

dz Height of calculation layer (or height of the shaft contained in the layer, if the shaft bottom is above the lower level of the calculation layer) (m).

r Radius of the shaft (m).

d_{grout} Thickness of the grouted zone (m).

The level of grouting and the "ungrouted" hydraulic conductivity of the bedrock are both taken into consideration by setting the hydraulic conductivity, K, in Equation 2-6 to the lowest value of the two, as shown in Equation 2-7.

$$K = \min[K_{grout}, K_h) \qquad \text{(Equation 2-7)}$$

K_{grout} Hydraulic conductivity of the grouting level, i.e. the conductivity of the bedrock after grouting to a certain level (m/s).

K_h Horizontal hydraulic conductivity of the grid cell (m/s).

3 Description of models and simulation cases

The first step in the modelling process was to update the MIKE SHE SDM-Site Laxemar model /Bosson et al. 2009/. The main model updates were performed with respect to the bedrock part of the hydrogeological model, see Section 3.1, as well as the vertical extent of the model volume, Section 3.2. The depth of the hydrogeological model and its vertical resolution in terms of computational layers were updated, see Section 3.2.1. These changes were made in order to avoid boundary effects of the repository being situated close to the original bottom boundary. The simulation period and chosen initial conditions are described in Section 3.2.2. In Table 3-1 the updates of the SDM Laxemar model are summarized.

A reference simulation with the above mentioned updates of the SDM-Site Laxemar model was run for the chosen simulation period. The results from these simulations are presented in Chapter 4.

The second step in the modelling process was to describe the conditions for the open repository by implementing the access tunnel, the repository tunnels and shafts in the model, and to analyse the consequences for the surface hydrology caused of the open repository under different conditions. The geometrical descriptions of the tunnels and shafts are presented in Section 3.3.1 and the different simulation cases for open repository conditions in Section 3.3.2. The results from these simulations are presented in Chapter 5.

3.1 Input data updates

A new hydrogeological model of the bedrock, compared to the one used in the MIKE SHE SDM-Site Laxemar model /Bosson et al. 2009/, was delivered from the ConnectFlow modelling team /Rhén et al. 2009/ and implemented in the MIKE SHE model, see Table 3-1. The data set delivered from ConnectFlow contains data on the horizontal and vertical hydraulic conductivities, the specific storage and the porosity. The bedrock models produced and delivered from the ConnectFlow team are specified in terms of "identification strings", which essentially specify the various sub models, initial and boundary conditions used in each model. The specifications of the bedrock models used in the present model and the preceding SDM-Site Laxemar model are given in Table 3-1.

The geometric mean values of the horizontal and vertical hydraulic conductivities (K_h and K_v) in each layer in the upper 200 m of the model volume are given in Table 3-2. The mean values for all the layers down to 200 m depth are $1.76 \cdot 10^{-7}$ m/s and $3.06 \cdot 10^{-7}$ m/s for the horizontal and vertical hydraulic conductivity, respectively. Compared to the SDM-Site Laxemar model the bedrock is less permeable; the corresponding mean values in the SDM-Site model are $2.64 \cdot 10^{-7}$ m/s and $4.09 \cdot 10^{-7}$ m/s for the horizontal and vertical hydraulic conductivity, respectively.

Table 3-1. Summary of updates of the SDM Laxemar model.

	SDM-Site Laxemar model	Present open repository model
Hydrogeological bedrock model	POM23_PWH_HCD7_HRDopo-sc1r2-10_HSD2_BC3	POM23f_PALAEO_HCD12_HRDopo-sc1-28phiF10_HSD3b_BC4b_IC4_24
Location of bottom boundary	600 m.b.s.l.	1,190 m.b.s.l.
Number of computational layers	13	25
Simulation period	Oct. 10, 2003– Dec. 31, 2007	Jan. 1, 2004– Dec. 31, 2006
Drainage of Äspö Hard Rock Laboratory	Not included	Included

Table 3-2. Geometric mean values of K_h and K_v in the upper 200 m of the bedrock model.

Layer	Mean elevation, m.b.s.l.	Geometric average of K_h, m/s	Geometric average of K_v, m/s
1	10	$2.85 \cdot 10^{-7}$	$5.23 \cdot 10^{-7}$
2	50	$3.01 \cdot 10^{-7}$	$5.18 \cdot 10^{-7}$
3	90	$3.04 \cdot 10^{-7}$	$5.19 \cdot 10^{-7}$
4	130	$6.92 \cdot 10^{-8}$	$1.16 \cdot 10^{-7}$
5	170	$4.97 \cdot 10^{-8}$	$8.52 \cdot 10^{-8}$
6	210	$4.47 \cdot 10^{-8}$	$7.59 \cdot 10^{-8}$

The drainage of the Äspö Hard Rock Laboratory (HRL) is included in the base case of the MIKE SHE model in this report. The drainage was described as a number of wells on different levels along the tunnel construction. Monitoring data on the inflow to the Äspö HRL have been used when describing the inflow to the construction. All point inflows larger than 0.3 L/s have been taken into consideration, meaning that 85% of the total measured inflow is included in the model. The total water extraction in the model is c 14.2 L/s. A more detailed description of the implementation of the drainage of the Äspö HRL is found in /Bosson et al. 2009/ where it was studied as a sensitivity case. The locations of the wells describing the drainage are shown in Figure 3-1.

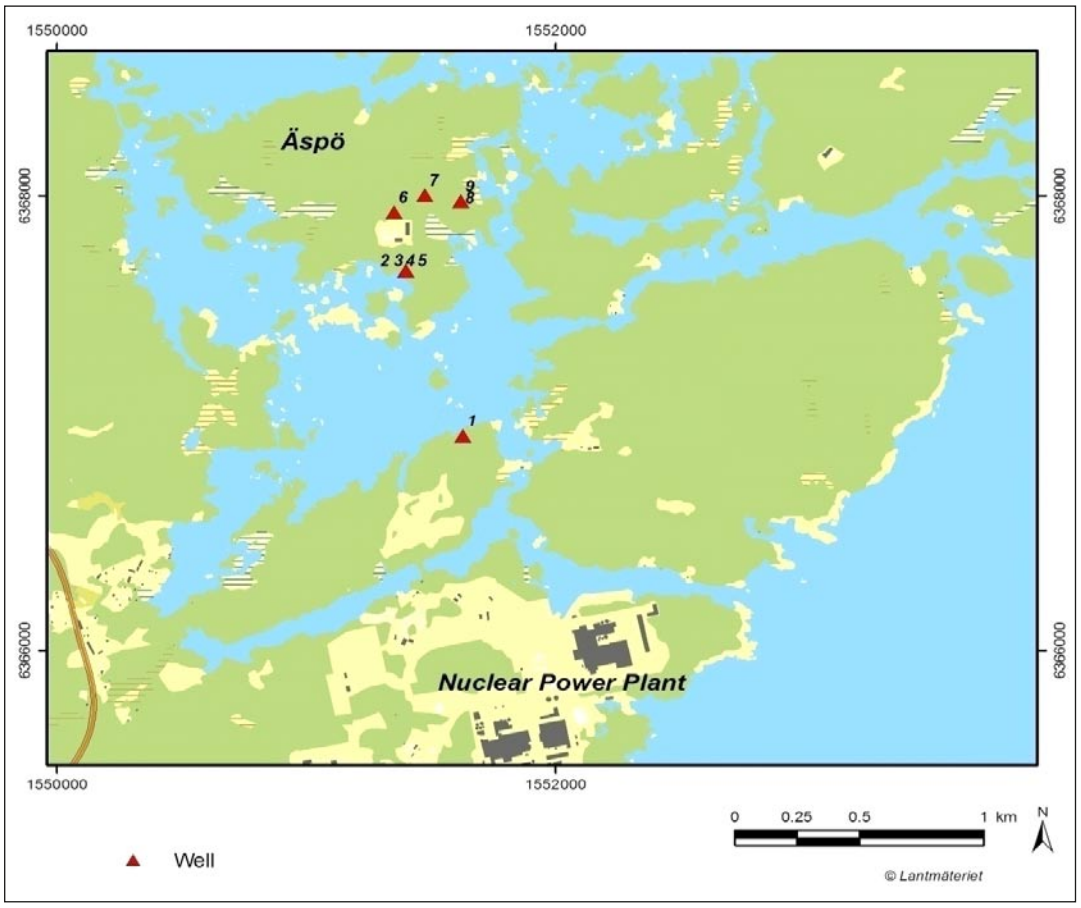

Figure 3-1. *Locations of the wells describing the inflow of water to the Äspö Hard Rock Laboratory.*

3.2 Description of the numerical model and initial base case

3.2.1 Boundaries and grid

The MIKE SHE model area, which has a size of 34 km^2, is shown in Figure 3-2. It can be seen that the SDM-Site Laxemar local model area is included. Furthermore, the MIKE SHE model area extends some distance into the sea, although the offshore part of the MIKE SHE area is much smaller than that of the regional model area (see Figure 1-1). Only the central part of the Laxemar-Simpevarp regional model area is included in the MIKE SHE model area considered in the present work. The southern and north-western boundaries follow the water divide towards the stream Laxemarån catchment. However, the model area intersects this water divide along the western boundary of the model area. The boundary of the model area follows the boundary of sub-catchments within the Laxemar catchment as much as possible. The northern boundary follows the catchment of the stream Kärrviksån.

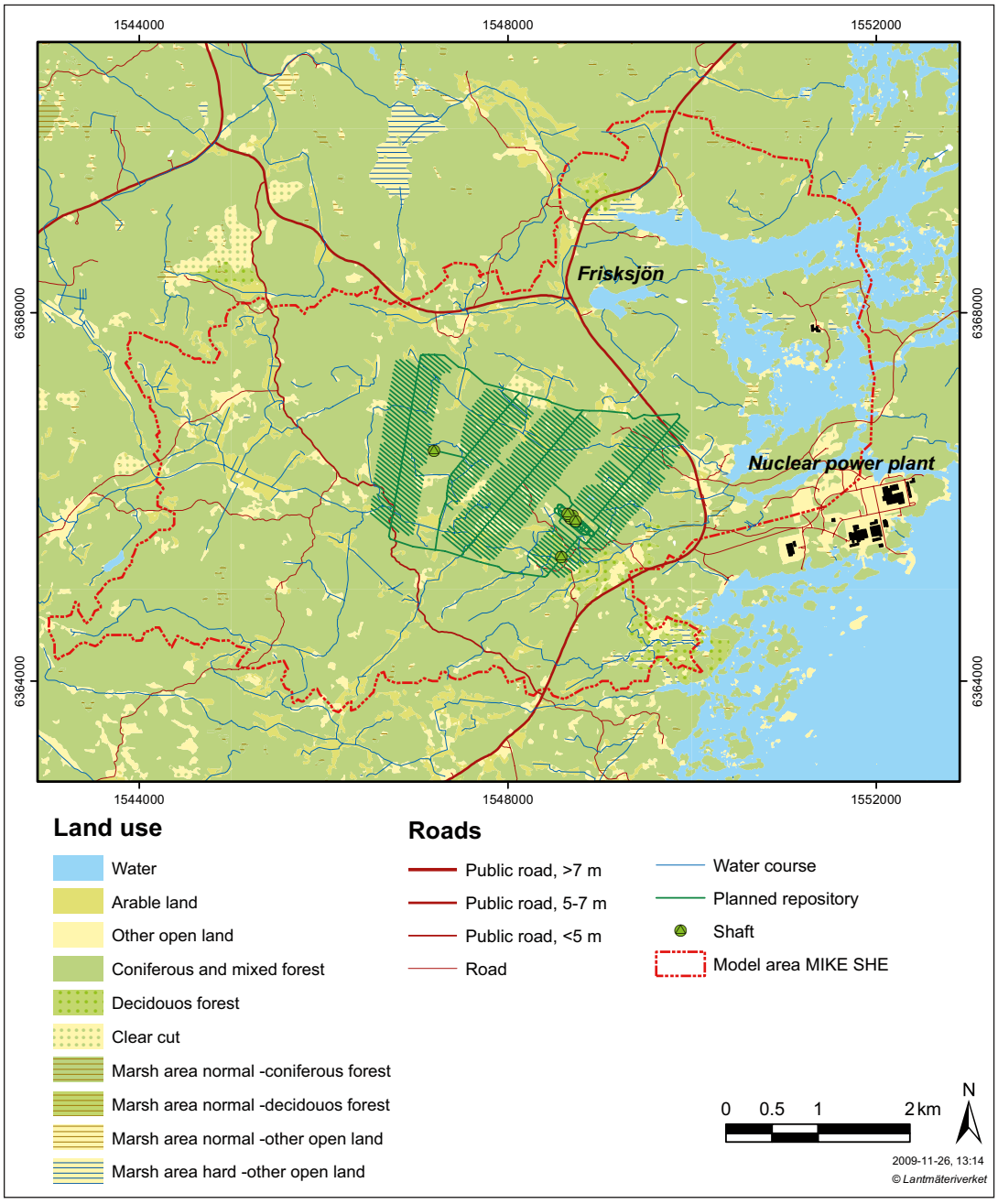

Figure 3-2. The MIKE SHE model area and the repository (Laxemar layout D2, version 1.0).

When defining the horizontal extent of the model area, the local model area and the surface water divides were taken into consideration. The surface water divide of the Laxemarån catchment is an appropriate boundary for the south western part of the model area and the water divide of the Kärrviksån water course is an appropriate boundary in the northern part of the model area.

The vertical extent of the reference setup of the model has been extended from 600 m.b.s.l. to 1,190 m.b.s.l. The computational layers were adjusted to follow the geological layers down to layer 19, where the deepest six geological layers in the model were included as three computational layers. The horizontal resolution of the calculation grid is 40 m by 40 m in the whole model area. A detailed description of the geological layers and calculation layers included in the Laxemar SDM-Site model is given in /Bosson et al. 2009/.

The groundwater divides are assumed to coincide with the surface water divides; the latter are reported in /Brunberg et al. 2004/. Thus, a no-flow boundary condition is used for the on-shore part of the model boundary. The sea forms the uppermost calculation layer in the off-shore parts of the model. The sea is represented by a geological layer consisting of highly permeable material. The hydraulic conductivity of this material is set to 0.001 m/s. The sea part of the uppermost calculation layer has a time-varying boundary condition. The measured time-varying sea level /Werner et al. 2008/ is used as input data.

Only small parts of the model area are exposed towards the sea. Therefore, a no-flow boundary is specified also for the off-shore parts of the model. In the QD-layers the boundary towards the sea is the time-varying boundary condition describing the sea-level in the area but in the bedrock layers there is a no-flow boundary condition. A sensitivity analysis was performed to analyse the effect of different boundary conditions towards the sea. This is further described in Chapter 6.

The top boundary condition is expressed in terms of the precipitation and potential evapotranspiration (PET). There is a gradient in the precipitation from the coast to the more inland parts of the model area. Therefore, the model area has been divided into three precipitation zones, as further described in /Bosson et al. 2009/. The actual evapotranspiration is calculated during the simulation.

A no-flow bottom boundary condition is applied to the model. Below 650 m.b.s.l. the hydraulic conductivities in the bedrock hydrogeology model are very low, which means that a no-flow boundary condition is considered a good approximation at 1,190 m.b.s.l.

3.2.2 Initial condition and handling of temporal variations

The simulation period covers three years, from the 1th of January 2004 to the 31th of December 2006. All of the simulations in the Open Repository modelling work have been performed using meteorological site data for these three years /Bosson et al. 2009/.

The years of 2004 and 2005 was used as an initialization phase and results presented in this report are derived from 2006 only. The year 2006 contains both very dry conditions during the dry summer of 2006 and a wet period in connection with distinct snowmelt that took place in the spring of 2006.

3.3 Input to simulations of open repository conditions

3.3.1 Geometry of the tunnels and shafts

The open repository layout version “Laxemar layout D2, version 1.0” from February 2009 (SKBdoc ID: 1185003 and DFX-ID: 191BAB00_8X01.dxf) has been used in the present modelling. The layout includes a 20% loss of deposition holes. The positions of the tunnels and shafts are shown in Figure 3-3. The layout of the access tunnel from the ground surface down to the central area, the tunnels and rock caverns in the central area, the transport tunnels and the deposition tunnels is shown in Figure 3-4.

The repository is described as a number of pipe links in the modelling tool MOUSE (described in Section 2.3.1). Table 3-3 shows the geometry of the tunnels included in the model. The total length of tunnels is c 113 km, with the majority located at approximately 500 m.b.s.l.

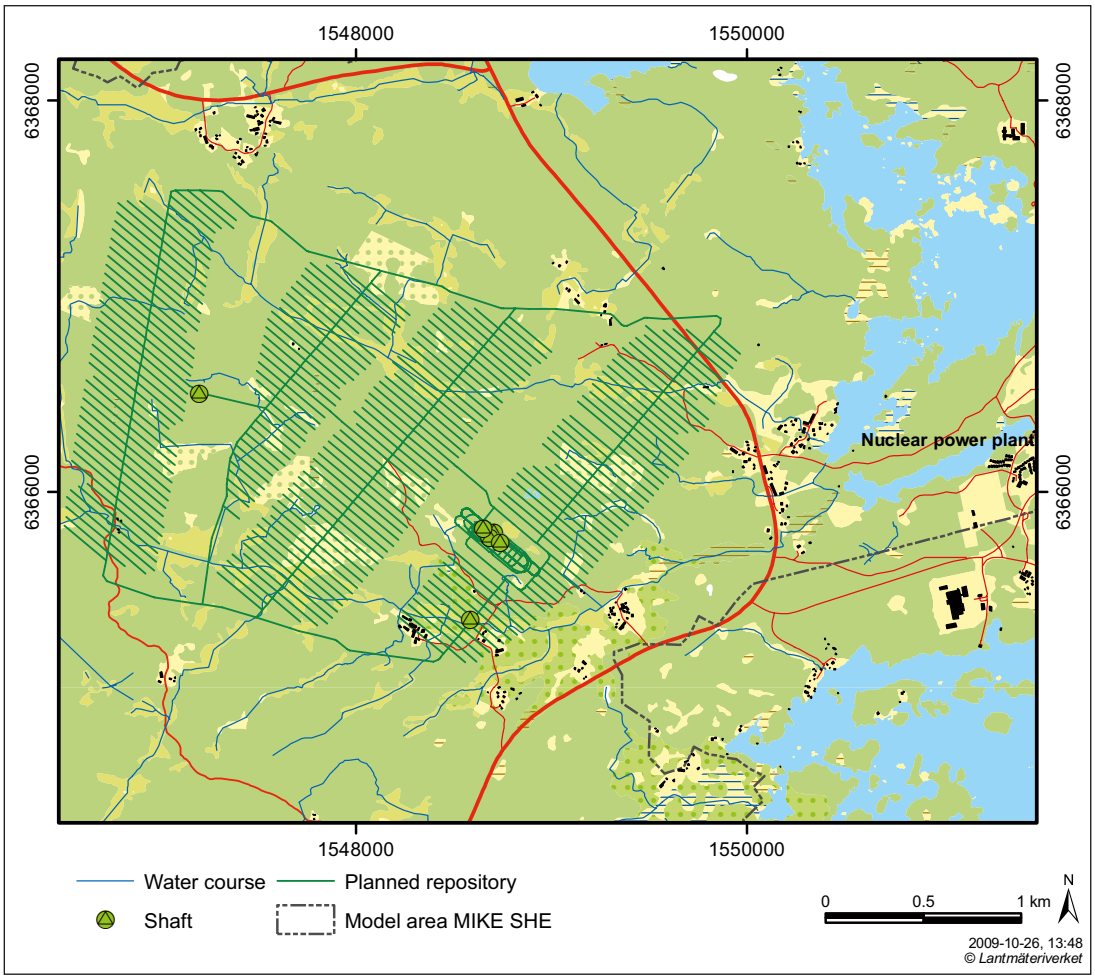

Figure 3-3. *Positions of the tunnels and the shafts of the planned repository.*

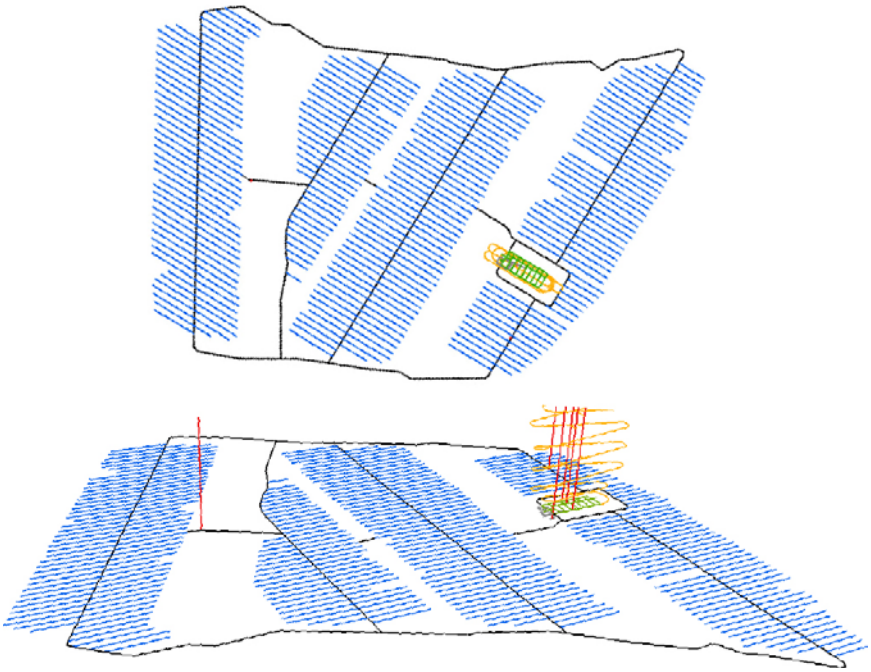

Figure 3-4. *Layout of the access tunnel from the ground surface and down to the repository (yellow line), the tunnels and rock caverns in the central area (green lines), the transport tunnels (black lines), the deposition tunnels (blue lines) and the shafts (red lines).*

There are totally six shafts. These are described as cells with atmospheric pressure in MIKE SHE (described in Section 2.3.2). Table 3-4 gives the bottom level, location, diameter and circumference of the shafts. The total conductances, C (Equation 2-6, Section 2.3.2), for all calculation layers are listed in Appendix 1 for each shaft and for the different grouting cases.

3.3.2 Simulation cases

Three different cases have been defined according to different levels of grouting (with different hydraulic conductivities, K). The thickness of the grouted zone in the bedrock is set to 5 m (Sten Palmer, personal communication). The three grouting levels are:

1. $K=1\cdot10^{-8}$ m/s → for all tunnels and shafts
2. $K=1\cdot10^{-8}$ m/s → for all tunnels and shafts except deposition tunnels
   $K=1\cdot10^{-9}$ m/s → for deposition tunnels
3. $K=1\cdot10^{-8}$ m/s → for all tunnels and shafts except deposition tunnels
   $K=1\cdot10^{-10}$ m/s → for deposition tunnels

It should be noted that the inflow to the repository is calculated based on both the grouting leakage coefficient and the conductivities in the surrounding bedrock (see Section 2.3.1 for details). This means that when the bedrock has a lower conductivity than the grouting, the bedrock conductivity controls the inflow, and vice versa.

Table 3-3. Geometry of tunnels in the repository, as described in the model (layout D2, version 1.0, from February 2009). The access tunnel goes from layer 1 and down to layer 16.

Calculation layer	Lower level, m.b.s.l.	Tunnel segment length, m	Tunnel casing area, m²
Layer 1–3	–10	31	506
Layer 4	–8	21	338
Layer 5	30	460	7,610
Layer 6	70	563	9,358
Layer 7	110	508	8,282
Layer 8	150	413	6,767
Layer 9	190	433	7,138
Layer 10	230	510	8,275
Layer 11	270	489	8,066
Layer 12	310	508	8,282
Layer 13	350	413	6,767
Layer 14	390	433	7,138
Layer 15	430	508	8,281
Layer 16	470	423	7,022
Layer 17	510	71,111	1,124,027
Layer 18	550	35,686	580,384
Layer 19	590	121	1,926
Layer 20	630	0	0
Layer 21	670	0	0
Layer 22	720	0	0
Layer 23	870	0	0
Layer 24	1,030	0	0
Layer 25	1,190	0	0
Sum		**112,628**	**1,800,168**

Table 3-4. Geometry of shafts in the repository, as described in the model.

Shaft	Lower level, m.b.s.l.	X-coordinate, m	Y-coordinate, m	Diameter, m	Circumference, m
SA01	508.80	1548584	6365346	3.00	9.42
SA02	507.68	1547200	6366501	3.00	9.42
SB00	529.72	1548737	6365742	6.00	18.85
SC00	553.76	1548651	6365810	5.00	15.71
SF00	477.22	1548684	6365765	2.50	7.85
ST00	477.59	1548706	6365792	3.50	11.00

The different grouting levels have been applied in simulation cases where the full construction has been modelled as an open repository, i.e. with all the deposition tunnels open at the same time. The results presented in Chapter 5 are based on this assumption, unless otherwise stated (i.e. the results in Section 5.4.3 and selected parts of Section 5.2). This is, however, a hypothetical worst case scenario. The repository will be constructed and taken into operation in five development phases. The description of the development phases used as an input to the present modelling was obtained from the SKB-internal document "Laxemar Layout 3D-modell SR-Site PM1" (SKBdoc ID no 1187028).

Figure 3-5 shows the two phases of the construction that will be modelled individually in this report, the initial construction phase (denoted 0 in Figure 3-5) and development phase 2. Results are presented in Section 5.4.3. The initial construction phase is the initial phase when only the ramp, tunnels and shafts within the central area will be open. In development phase 2 some sections of the deposition tunnels and the surrounding access and transport tunnels will be open together with the central area, see Figure 3-5. In the last development phases (phases 3-5), which will not be modelled and therefore are not shown in Figure 3-5, the remaining deposition, transport and access tunnels will be opened gradually. The deposition tunnels will, however, only be open a few sections at a time. The two different phases have been simulated with a grouting level of $K=1\cdot10^{-9}$ m/s in the deposition tunnels and $K=1\cdot10^{-8}$ m/s in all other tunnels and shafts.

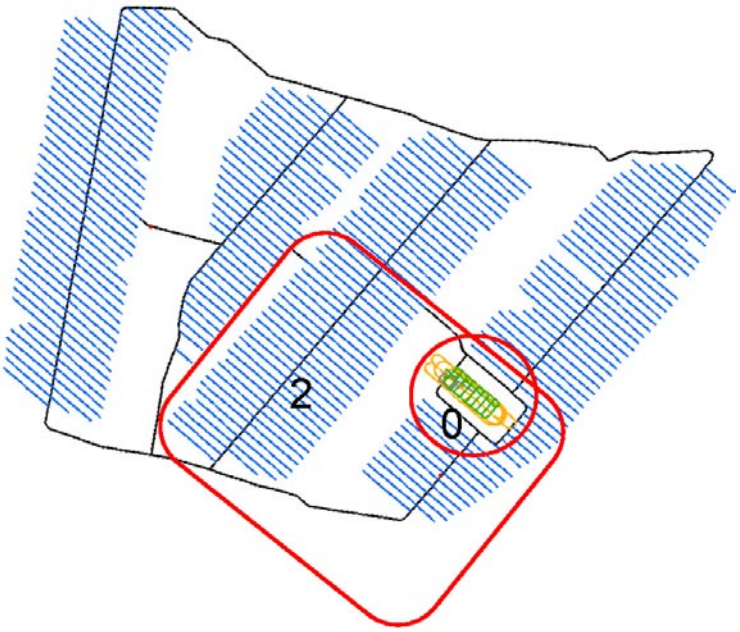

Figure 3-5. *Initial construction phase (0) and development phase 2 in the construction of the open repository.*

The same initial conditions and meteorological data as described for the reference simulation (Section 3.2.2) are applied to the simulation cases with an open repository. The meteorological data cover observed daily values from the years 2004 to 2006, which means that seasonal variations are included in all simulation cases. In all simulations, results are evaluated from 2006 which is characterized by a heavy snowmelt in the spring and a dry summer and beginning of the autumn. The total precipitation during 2006 is considered to be rather normal. In Chapter 6 the effects of different meteorological conditions are further investigated.

Two longer simulations were carried out, one reference case and one based on a grouting level of $K=1\cdot10^{-9}$ m/s in the deposition tunnels and $K=1\cdot10^{-8}$ m/s in all other tunnels and shafts, where the 3 year simulation (2004–2006) period was repeated to represent a period of totally 9 years. This was done in order to evaluate the development of the groundwater table drawdown over a longer period (results are presented in Section 5.4.6).

Finally, a simulation was carried out to evaluate the recovery of the drawdown of the groundwater table, after the operational phase of the open repository is finished and the repository is closed. The simulation was done without tunnels and shafts, but initialised from the conditions with an open repository. The initial conditions were taken from simulations with a grouting level of $K=1\cdot10^{-9}$ m/s in the deposition tunnels and $K=1\cdot10^{-8}$ m/s in all other tunnels and shafts, after the third three-year cycle. The simulation was done for a nine-year period (using data from 2004–2006), and compared with a parallel reference simulation with undisturbed conditions, when calculating the drawdown of the groundwater table (results are presented in Section 5.4.7). All simulation cases presented above are summarized in Table 3-5.

Table 3-5. Summary of the different simulation cases. Results are evaluated from the highlighted years.

Simulation case	Grouting level, all tunnels and shafts except deposition tunnels	Grouting level, deposition tunnels	Meteorological data											
Development phase 0	K=1·10^{-8} m/s	K=1·10^{-9} m/s	2004	2005	2006									
Development phase 2	K=1·10^{-8} m/s	K=1·10^{-9} m/s	2004	2005	2006									
Full construction	K=1·10^{-8} m/s	K=1·10^{-8} m/s	2004	2005	2006									
Full construction	K=1·10^{-8} m/s	K=1·10^{-9} m/s	2004	2005	2006	2004	2005	2006	2004	2005	2006			
Full construction	K=1·10^{-8} m/s	K=1·10^{-10} m/s	2004	2005	2006									
Recovery after closing the repository (initial conditions from K=1·10^{-8}, K=1·10^{-9} m/s)	No repository											2004	2005	2006
Reference simulation	No repository		2004	2005	2006	2004	2005	2006	2004	2005	2006	2004	2005	2006
	Simulation cycle		1st			2nd			3rd			4th – 6th		

4 Results for undisturbed conditions

This chapter gives a short presentation of the results for undisturbed conditions. The natural conditions are needed as a reference to the simulations where the tunnel, shafts and rock caverns have been implemented in the model. The presentation includes calculated water balances, surface water discharges and groundwater levels. For a detailed presentation of the results for undisturbed conditions, the reader is referred to /Bosson et al. 2009/. The updates made in the present reference simulation of undisturbed conditions (described in Chapter 3) are considered to give only very small changes compared to the results described in /Bosson et al. 2009/.

4.1 Water balance

The water balance presented here represents a sub-volume within the total model volume. Since the sea is represented as a highly conductive geological layer with a fixed head, the sea and the model volume covered by the sea are not included in the water balance calculations. Thus, the water balance is calculated for the land part of the model area, including the islands of Hålö and Äspö. In /Bosson et al. 2009/ these areas outside the coastline are not included in the water balance calculations.

The calculated water balance for the year 2006 for undisturbed conditions is presented in Figure 4-1 and Table 4-1. All water balance components are expressed as area-normalised total volumetric discharges, i.e. in mm (mm/year in this case). The accumulated precipitation during the modelled period is 591 mm. The total evapotranspiration is calculated to 398 mm. Compared to the results in /Bosson et al. 2009/ both the precipitation and the evapotranspiration are slightly smaller. This can be explained by the different evaluated time periods; the calendar year of 2006 in this report and the hydrological year (i.e. October to September) in /Bosson et al. 2009/.

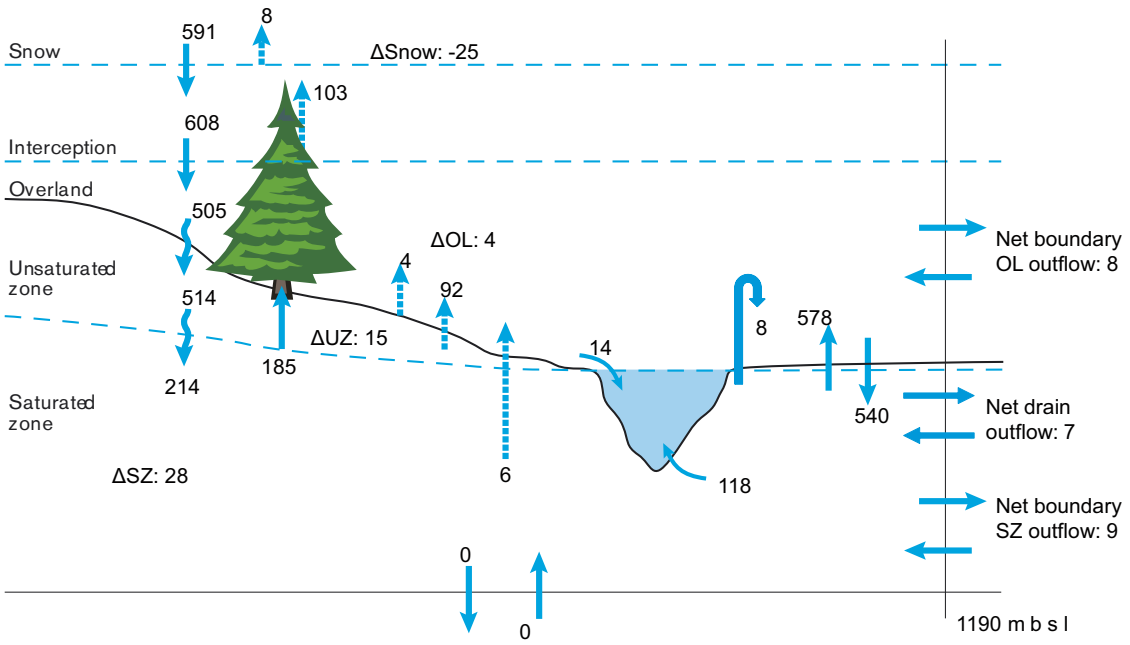

Figure 4-1. *Calculated water balance for 2006 for the Laxemar area under undisturbed conditions (mm).*

Table 4-1. Annual total accumulated water balance (mm) for the land part of the model area, reference simulation.

Date	Precipitation	Canopy storage change	Evapo-transpiration	Snow storage change	Overland storage change	Overland boundary inflow	Overland boundary outflow	Overland to streams	Subsurface storage change	Subsurface boundary inflow	Subsurface boundary outflow	Drain to streams	Drain outflow
2005-12-31	0	0	0	0	0	0	0	0	0	0	0	0	0
2006-01-30	–30.2	–0.1	0.1	19.8	–0.3	0	0	0.3	–0.8	1.1	1.3	1.7	0.1
2006-03-01	–92.7	–0.3	1.3	53.8	0.4	0	0.2	0.6	7.5	2.1	3.1	6.2	0.3
2006-03-31	–150.8	–0.1	10.5	41.5	7.6	0	0.9	1.2	36.2	3.1	5.4	15.3	1.3
2006-04-30	–204	1.4	47.3	–25.1	14.2	–0.4	6.9	11.7	27.8	4.3	11.6	59.4	5.4
2006-05-30	–256.1	2.3	122.0	–25.1	8.7	–0.4	7	12.4	17.5	5.7	13.3	62	5.5
2006-06-29	–278.9	–0.3	221.0	–25.1	3.6	–0.4	7.1	12.7	10.1	7.2	14.5	62.7	5.6
2006-07-29	–288.4	–0.3	289.2	–25.1	–0.3	–0.4	7.1	12.8	5.6	8.8	15.4	62.9	5.6
2006-08-28	–376.7	1.5	339.6	–25.1	–0.6	–0.4	7.1	12.8	3.5	10.2	16.5	63.2	5.6
2006-09-27	–390.1	–0.3	390.2	–25.1	–1.8	–0.4	7.1	12.9	0.3	11.5	17.3	63.4	5.6
2006-10-27	–439.1	2.1	398.3	–25.1	–1.3	–0.4	7.1	13	–0.3	12.7	18.4	64	5.6
2006-11-26	–566.2	0	398.3	–25.1	3	–0.4	7.5	13.3	22.8	13.8	21.3	73	6
2006-12-31	–591.2	–0.1	398.3	–25.1	3.6	–0.5	7.9	13.8	27.7	15.1	23.9	80.9	6.6

The total evapotranspiration is a sum of the different evaporation components. The transpiration from plants is 185 mm, the evaporation from soil is 92 mm, the evaporation from snow is 8 mm and the evaporation from flooded areas is 4 mm. The amount of water intercepted by plant leaves is calculated to 103 mm and the evaporation from the saturated zone is 6 mm.

The total runoff is calculated to 156 mm, with 14 mm from overland flow to rivers, 118 mm from groundwater flow to rivers (81 mm drain flow from the upper soil layer and 37 mm by leakage from the aquifer), and 24 mm (8+7+9) through net boundary outflow to the sea. The infiltration from the overland compartment to the unsaturated zone is 514 mm and the groundwater recharge, defined as the water flow from the unsaturated to the saturated zone, is 214 mm.

The large flows between the saturated zone (SZ) and overland water (OL), 578 mm from SZ to OL and 540 mm from OL to SZ, can be explained by the activated drainage function in agricultural areas. This is further explained in /Bosson et al. 2009/.

The quite large snow storage change is an effect of the chosen period for the water balance calculation, which is the year 2006. This comes from storage of snow during December 2005, whereas no snow was present in the end of December 2006. The large storage change in both the unsaturated (UZ) and saturated zone can also be explained by the evaluated time period. If a water balance is extracted for 2005–2006 the storage components are +1 mm in the unsaturated zone (UZ) and –7 mm in SZ.

The bent arrow in Figure 4-1 indicates the water drained through the sinks/wells representing the Äspö Hard Rock Laboratory, which together extract water at a rate corresponding to 8.4 mm/year (8.6 L/s). However, not all wells are included when only the land part of the model is included in the calculations. In Section 5.1 the extraction for the whole model area is presented.

4.2 Surface water levels and discharges

As described above, the runoff is calculated as the net flow of water to the MIKE 11 model plus the water that leaves the model area as overland flow and groundwater flow. MIKE 11 calculates the discharges and water levels in the water courses. The calculated discharge and water level in a water course varies during the year. Figure 4-2 shows the positions of the discharge gauging stations considered in the present study.

Figure 4-3 shows the calculated and measured discharges at the station in Laxemarån during 2006. In April 2006, a distinct snowmelt resulted in high peak discharges. The summer of 2006 was very dry, including a dry beginning of the autumn, followed by a sudden switch to a rather wet last part (November and December) of 2006. The model captures the overall runoff dynamics during both the wet and the dry periods. Figure 4-4 shows the measured and calculated water level at Lake Frisksjön during 2006. The measured water levels are generally underestimated in the model due to a large boulder situated downstream of the lake outlet, restraining the discharge from Lake Frisksjön. The overall results of the surface water levels and surface water discharges are in accordance with the results in /Bosson et al. 2009/, where a more detailed comparison between calculations and measured data is presented.

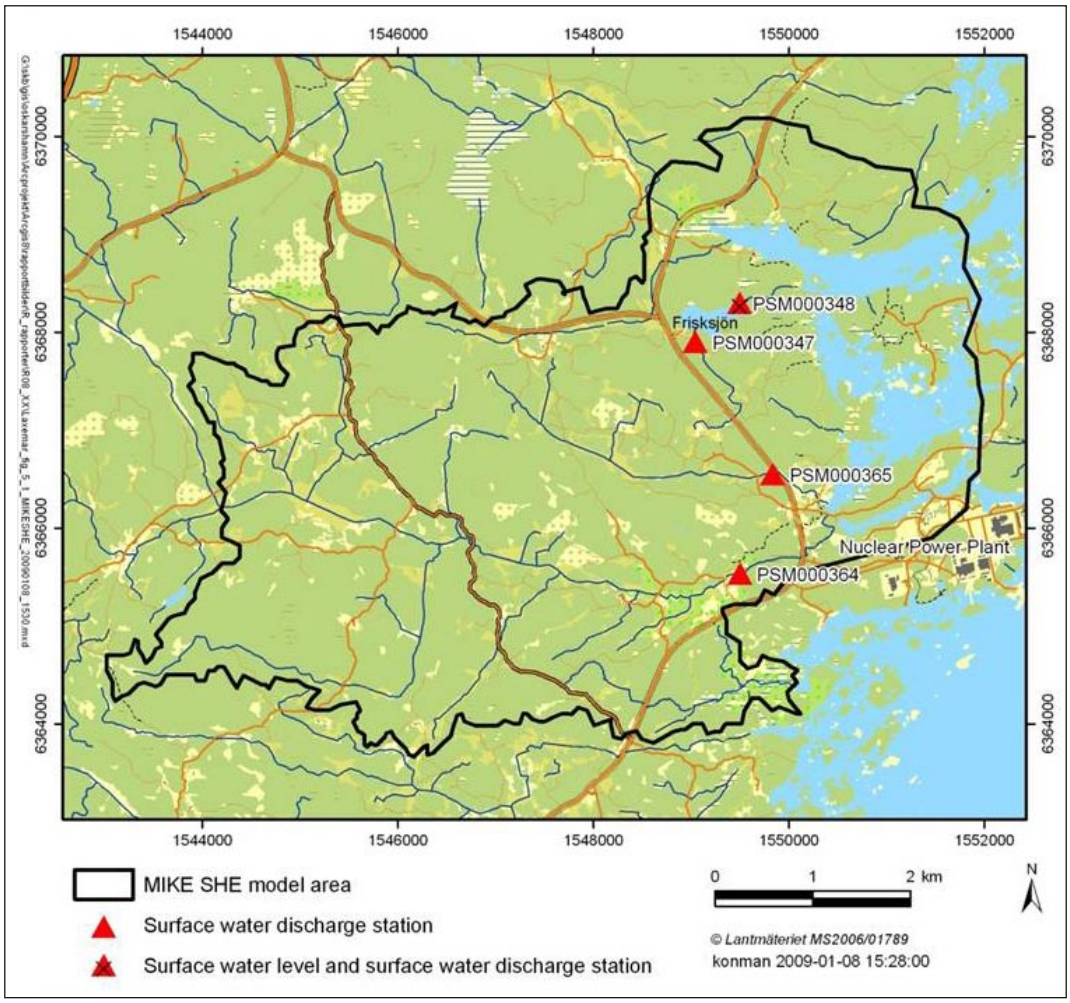

Figure 4-2. *Position of the surface water discharge gauging stations PSM000347 (upstream Lake Frisksjön), PSM000348 (downstream Lake Frisksjön), PSM000364 (Laxemarån) and PSM000365 (Ekerumsbäcken) and the surface water level station PSM000348 (at the outlet from Lake Frisksjön).*

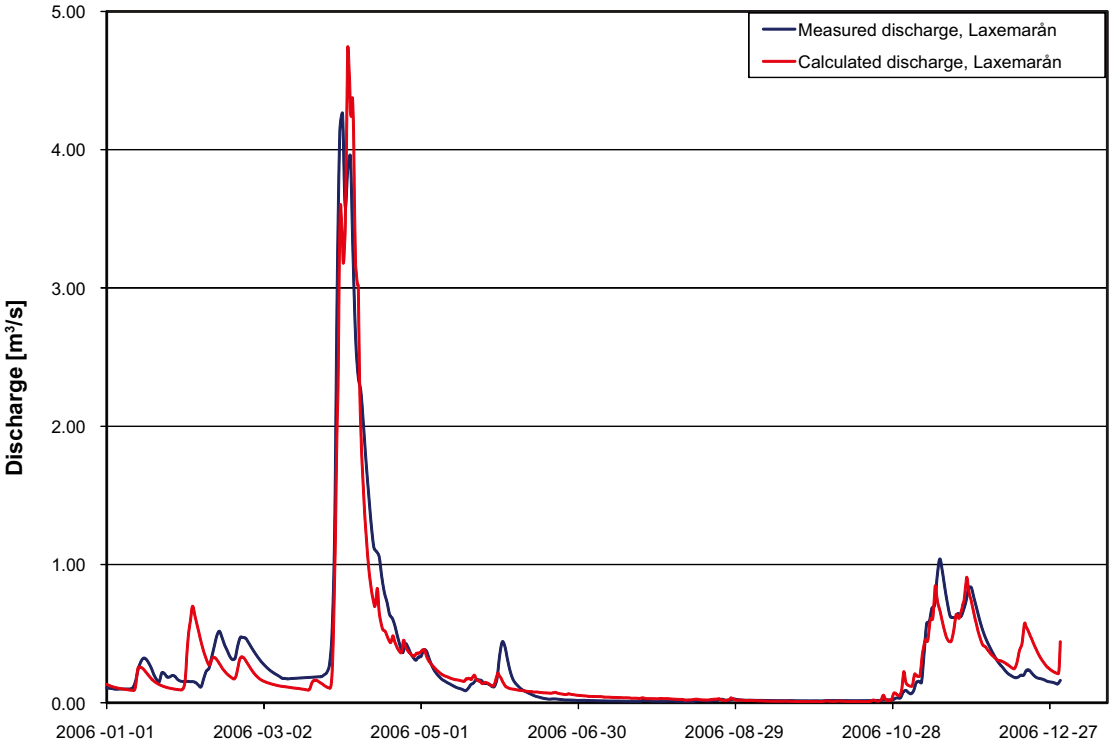

Figure 4-3. *Measured and calculated discharges in Laxemarån, reference simulation.*

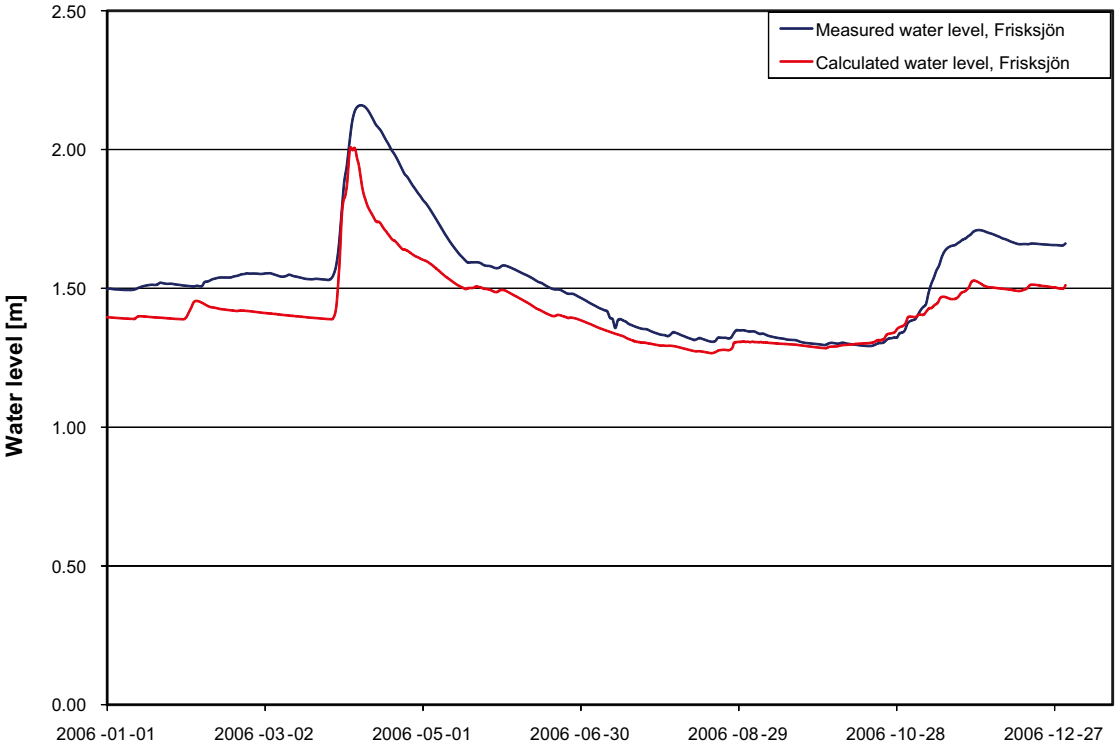

Figure 4-4. *Measured and calculated water levels in Lake Frisksjön, reference simulation.*

4.3 Groundwater table

Figure 4-5 shows the calculated elevation (m.a.s.l.) of the groundwater table in the model area as an average for 2006. The model area is characterised by topographical high-altitude conditions for large parts of the area. About 75% of the land area has a groundwater elevation higher than 5 m.a.s.l. as a mean for 2006. Consequently, the groundwater table elevation will only be affected by the sea level variation in areas in close proximity to the sea.

Figure 4-6 shows the calculated depth to the groundwater table in the model area as an average for 2006. As can be seen in the figure, the groundwater table is rather deep and located more than 2.0 m below ground in most of the model area, with a mean depth of 3.7 m below ground surface (the sea area excluded). The deepest groundwater levels are mainly found in high-altitude areas, associated with groundwater recharge near the groundwater divides. There are also areas with a groundwater pressure head above the ground surface for which the calculated overland water level is presented. Hence, these are groundwater discharge areas, including Lake Frisksjön and areas in the vicinity of the water courses located in the north eastern parts of the model area.

Since the Quaternary deposits are thin in large parts of the model area, the relatively large depth to the groundwater table implies that it is located in the bedrock in most of the area. Figure 4-7 shows the calculated depth to the groundwater table in areas where it is located in the Quaternary deposits. The mean depth in these areas is 1.7 m below ground surface (the sea area excluded).

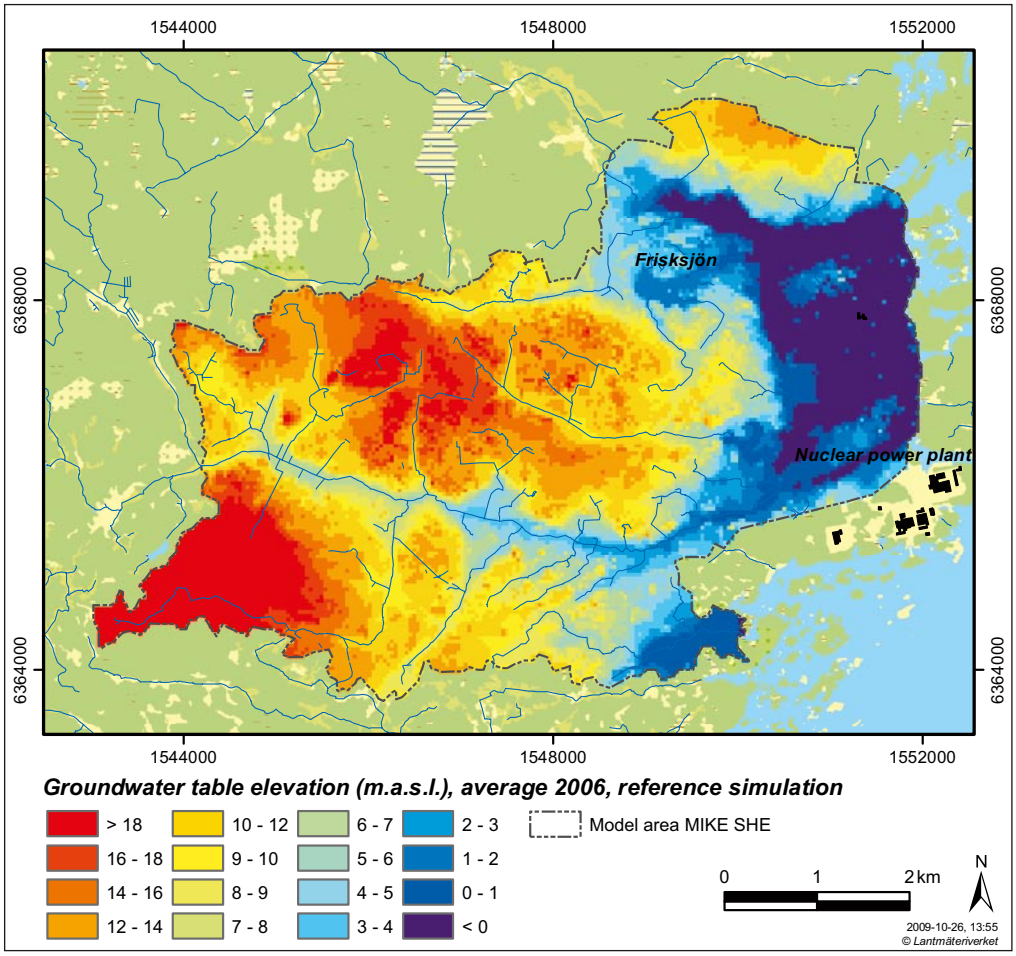

Figure 4-5. *Calculated elevation (m.a.s.l.) of the groundwater table as an average for 2006, reference simulation.*

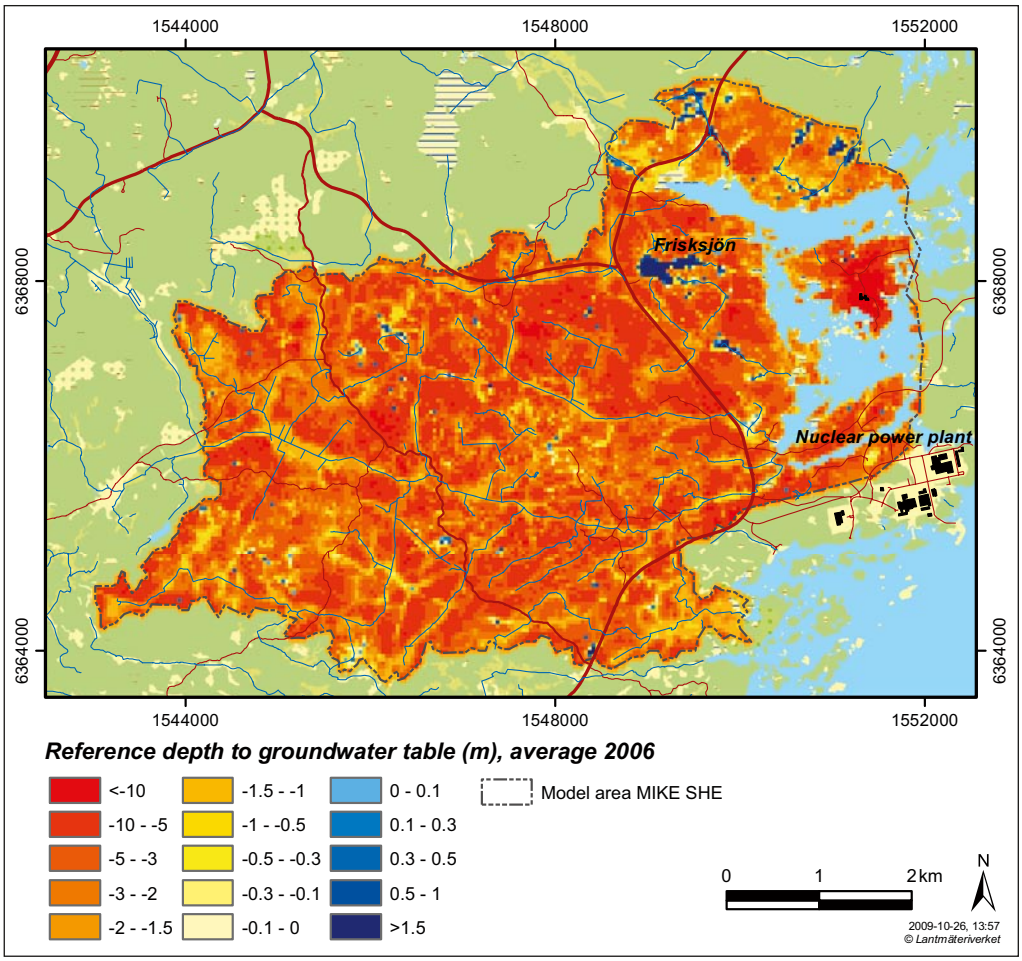

Figure 4-6. *Calculated depth to the groundwater table as an average for 2006, reference simulation. Positive depths (blue colours on land; the depth scale is not applicable in the sea) indicate areas with water above the ground surface.*

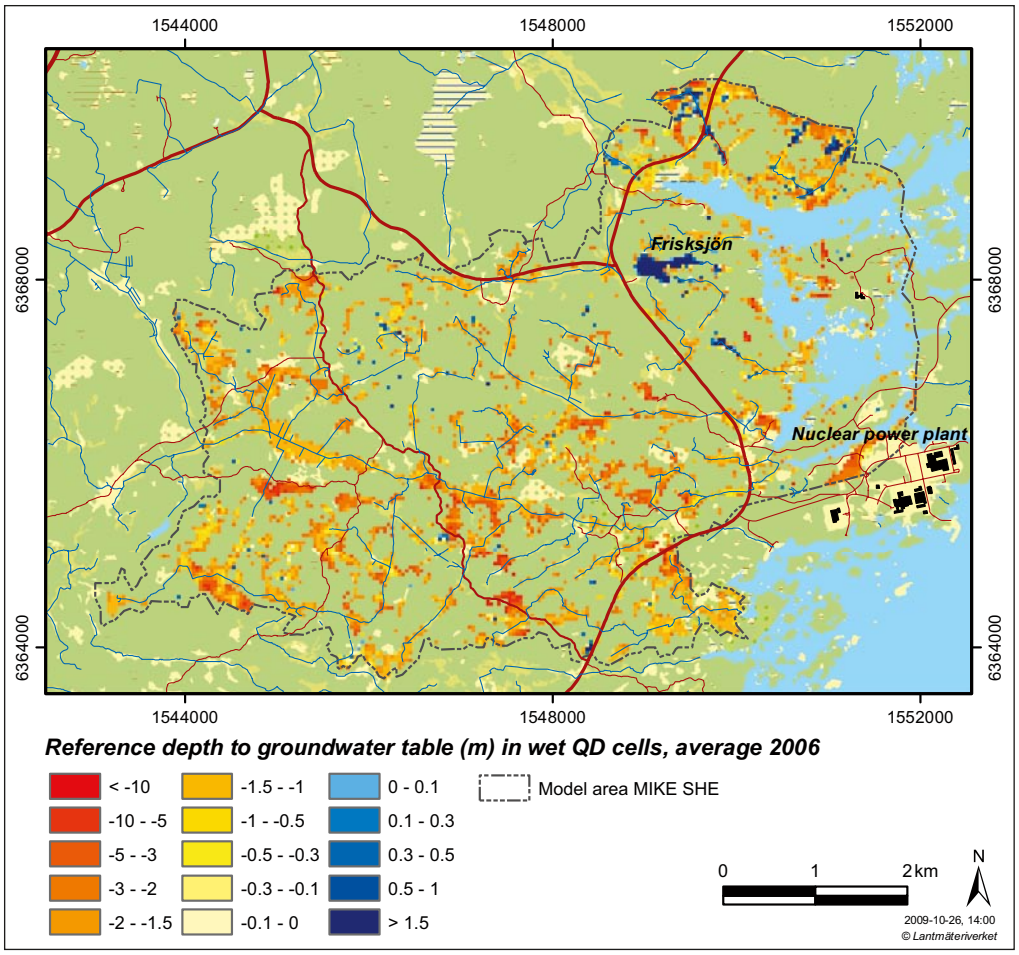

Figure 4-7. *Calculated depth to the groundwater table in "wet" QD cells as an average for 2006, reference simulation. Positive depths (blue colours on land; the depth scale is not applicable in the sea) indicate areas with water above the ground surface.*

Figure 4-8 shows the depth to groundwater during wet spring conditions in April, as calculated for the undisturbed conditions. In this case, the groundwater table has a mean depth of 1.7 m below ground surface (the sea area excluded). The significant difference compared to the average value of 2006 is due to the intense snowmelt in April that year, which drastically decreased the depth to the groundwater table. Areas with a groundwater pressure head above ground surface are no longer concentrated to Lake Frisksjön and the water courses in the north eastern corner of the model area.

Figure 4-9 shows the calculated depth to the groundwater table in the model area during a period of dry conditions in October, as calculated for the undisturbed conditions. October is not only a month with low precipitation itself, but it is also preceded by a number of dry months (June–September). As can be seen in the figure, the groundwater table is deeper and located more than 3.0 m below ground in most of the model area, with a mean depth of 4.8 m below ground surface (the sea area excluded). The areas with overland water are also smaller than those in Figure 4-8.

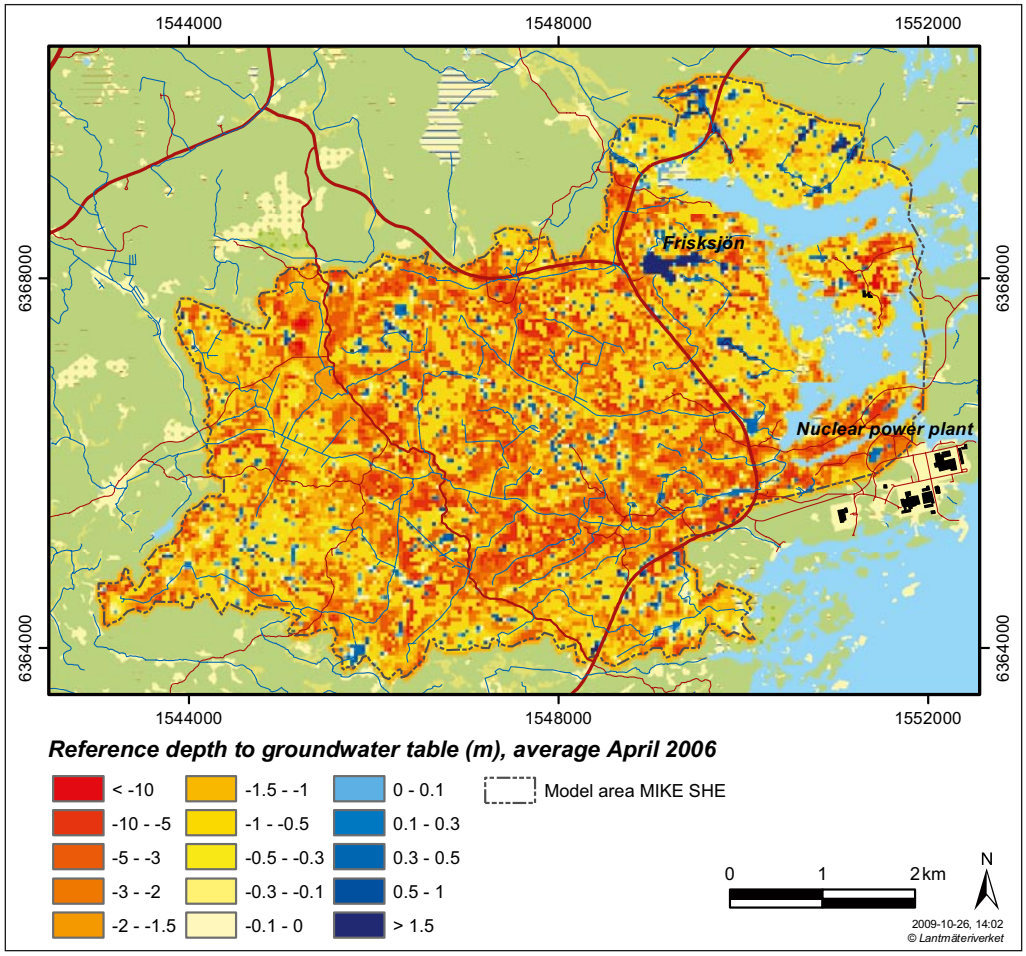

Figure 4-8. *Calculated depth to the groundwater table for a wet period, April 2006, reference simulation. Positive depths (blue colours on land; the depth scale is not applicable in the sea) indicate areas with water above the ground surface.*

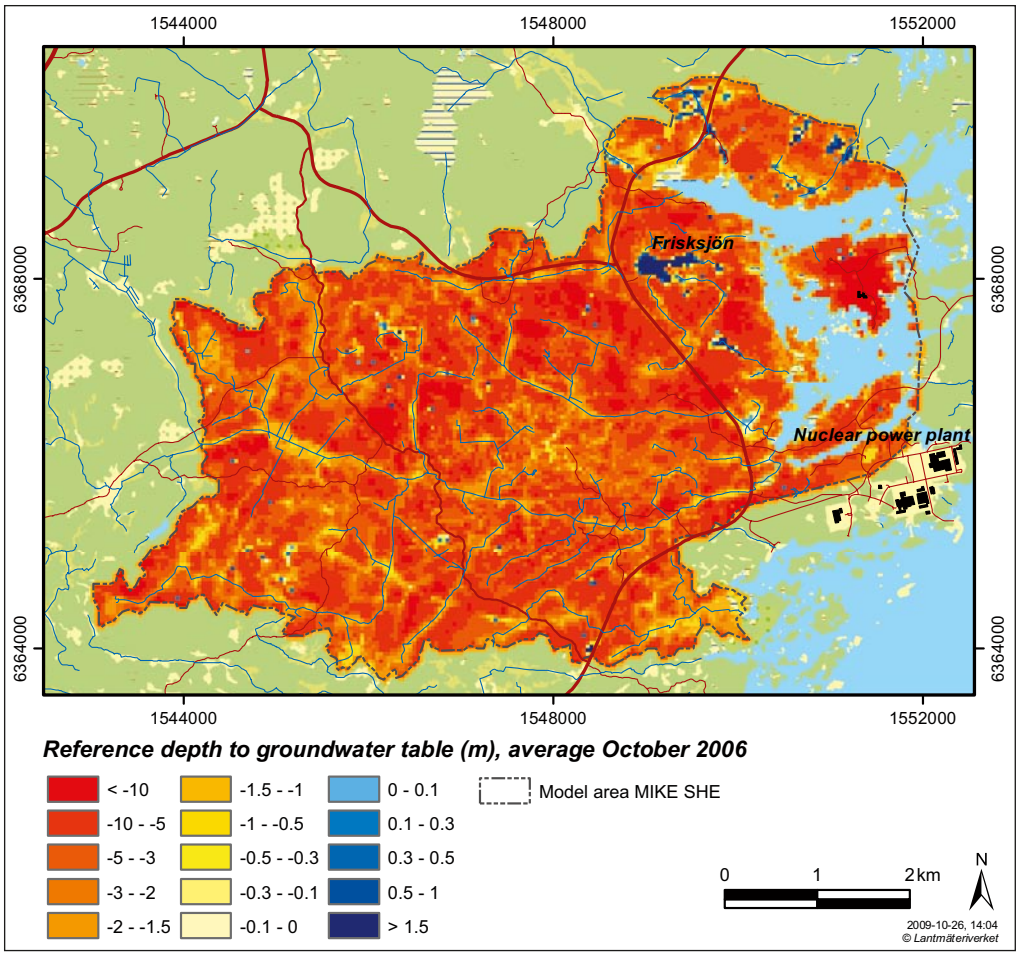

Figure 4-9. *Calculated depth to the groundwater table for a dry period, October 2006, reference simulation. Positive depths (blue colours on land; the depth scale is not applicable in the sea) indicate areas with water above the ground surface.*

5 Results for open repository base case

In this chapter, results of open repository simulations for the full construction, i.e. with all the deposition tunnels open at the same time, are presented. It should be noted that this is a hypothetical worst case that would not occur in reality. In reality, the open repository would be constructed and operated in five phases as described in Section 3.3. Results from simulations for two individual phases with only parts of the repository open are also presented. All results are compared to the reference case without tunnels and shafts, i.e. the results obtained for undisturbed conditions (Chapter 4).

Water balances are presented for the entire model area, as well as for different parts of the model area and detailed results for the saturated zone. Inflows to the tunnels and shafts are presented for each level of grouting for the full construction as well as for the initial construction phase and the second development phase of the construction. The effects of the full construction on the surface water system are evaluated using the water level in Lake Frisksjön and the accumulated discharges at selected discharge stations within the MIKE SHE model area.

The drawdown of the groundwater table is calculated and presented for each level of grouting as well as for the different development phases of the construction. The temporal and spatial variations of the groundwater table and the head drawdown are analysed using horizontal cross sections (for different periods and different depths) and as vertical profiles through the model area and the open repository. The drawdown of the groundwater table is studied in detail for areas with a groundwater table less than 2 m below ground. Finally, the long term development of the groundwater table drawdown is studied.

5.1 Water balance

The inflow of water to the open repository construction affects the total turnover of water in the model area. Table 5-1 shows a summary of the total accumulated water balances for the land part of the model area during 2006 for undisturbed conditions and with the open repository for the three different levels of grouting.

Table 5-1. Total accumulated water balances for 2006 (mm) for the land part of the model area (32 km^2, including the island of Äspö), for the reference simulation without open repository and with open repository for three levels of grouting.

	Reference simulation, without open repository	With open repository, grouting level $K=1\cdot10^{-8}$ m/s	With open repository, grouting level $K=1\cdot10^{-9}$ m/s in deposition tunnels	With open repository, grouting level $K=1\cdot10^{-10}$ m/s in deposition tunnels
Precipitation	591.2	591.2	591.2	591.2
Evapotranspiration	398.3	387.7	388.4	389.7
Canopy storage change	–0.1	–0.1	–0.1	–0.1
Snow storage change	–25.1	–25.1	–25.1	–25.1
Overland storage change	3.6	2.0	1.9	2.3
Subsurface storage change	42.3	19.1	24.9	33.4
Net overland outflow to sea	7.4	8.0	8.0	8.0
Net subsurface outflow to sea	8.8	2.5	5.3	9.0
Drainflow to sea	6.6	6.7	6.7	6.8
Overland flow to river	13.8	12.5	13.0	13.7
Drainflow to river	80.9	66.0	66.7	68.3
Net baseflow to river	37.5	9.1	11.9	16.3
Inflow to the open repository	–	85.9	72.8	53.8
Pumping from Äspö sinks	8.4	8.4	8.4	8.4

For a grouting level of $K=1\cdot10^{-8}$ m/s the total runoff sums up to 105 mm, compared to 156 mm for undisturbed conditions, i.e. a reduction of the total runoff with 50 mm (–32%). The inflow to the repository in this case is 86 mm, which means that the remaining difference in the water balance of 36 mm can be explained by a changed evapotranspiration and changes in overland and subsurface storage. The decrease in evapotranspiration can be explained by less available water, ponded and in the upper QD layers, for evapotranspiration.

The inflow to the open repository in this case (86 mm) is 55% of the total runoff for undisturbed conditions (155 mm) or 82% of the total runoff for disturbed conditions (105 mm). The corresponding relations between inflow to tunnels, with a grouting level of $K=1\cdot10^{-9}$ m/s and $K=1\cdot10^{-10}$ m/s in the deposition tunnels and $K=1\cdot10^{-8}$ m/s in all other tunnels and shafts, and the undisturbed total runoff are 47% and 35%, respectively.

Going further in details, the open repository construction affects the runoff to streams, which is reduced with 44 mm (–33%) from 132 mm to 88 mm in the case with a grouting level of $K=1\cdot10^{-8}$ m/s in the whole repository. Here, the largest effect is found in the drain flow and net base flow to the streams, which is reduced with 15 mm (–18%) and 28 mm (–76%), respectively, in the case with a grouting level of $K=1\cdot10^{-8}$ m/s.

In all cases, undisturbed conditions as well as disturbed conditions with an open repository, there is a net subsurface outflow to the sea, and a net overland outflow to the sea. The net overland outflow to the sea is the same in all of the cases, while the net subsurface outflow to the sea is changed when the open repository is introduced. This runoff component shows a large relative change, with a decrease of 6 mm (–72%) in the case with a grouting level of $K=1\cdot10^{-8}$ m/s.

In Table 5-2 the water balance for the saturated zone is presented layer by layer in the bedrock for the land part of the model area. This water balance shows the amount of water going into and out from the different layers as accumulated annual volumes according to the definitions in Figure 5-1.

As can be seen in Table 5-2, the total horizontal inflow to the bedrock from the sea area increases with 7 mm, from 1 mm to 8 mm, in the case with a grouting level of $K=1\cdot10^{-8}$ m/s. More than two thirds of this change is found in layers 5, 6 and 7, at approximately 30 to 110 m.b.s.l. However, the vertical flow is generally much larger than the horizontal, and is considerably changed when the open repository is introduced. The net vertical inflow from the Quaternary deposits (QD) to the bedrock (layer 3) changes with 55 mm, from 16 mm for undisturbed conditions to 71 mm in the case with a grouting level of $K=1\cdot10^{-8}$ m/s.

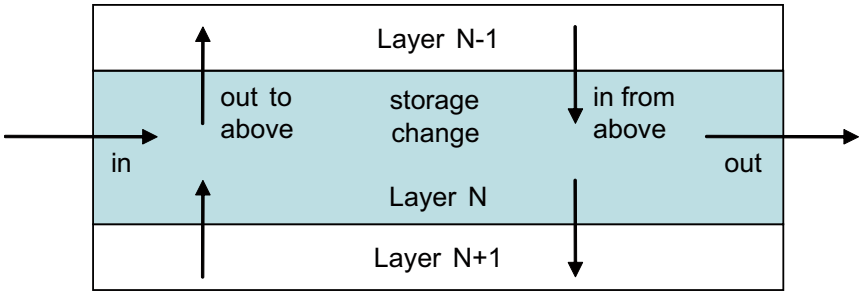

Figure 5-1. *Water balance components for the saturated zone (see Table 5-2). In- and outflow arrows in the figure are labelled for layer N only (because the values for the lower arrows are presented for the layer below in Table 5-2).*

Table 5-2. Water balances for 2006 (mm) in the saturated zone for the land part of the model area, shown for each bedrock calculation layer. Results are presented for undisturbed conditions and with an open repository for the three levels of grouting. The water balance components in the table are defined in Figure 5-1.

		Undisturbed conditions					Grouting $K=1\cdot10^{-8}$ m/s in the whole repository					Grouting $K=1\cdot10^{-9}$ m/s in deposition tunnels					Grouting $K=1\cdot10^{-10}$ m/s in deposition tunnels				
Layer	Lower level [m.b.s.l.]	Net horizontal outflow	Vertical out to above	Vertical in from above	To Äspö wells	To open repository	Net horizontal outflow	Vertical out to above	Vertical in from above	To Äspö wells	To open repository	Net horizontal outflow	Vertical out to above	Vertical in from above	To Äspö wells	To open repository	Net horizontal outflow	Vertical out to above	Vertical in from above	To Äspö wells	To open repository
L3	–10	0.01	28.99	44.98	0.00		0.01	11.70	83.12	0.00	0.00	0.00	12.74	79.17	0.00	0.00	0.00	14.76	72.83	0.00	0.00
L4	–8	0.03	29.63	44.10	0.00		0.02	11.85	82.10	0.00	0.00	0.02	12.89	78.14	0.00	0.00	0.03	14.97	71.92	0.00	0.00
L5	30	0.09	32.55	43.09	0.07		–1.64	13.65	79.49	0.07	0.04	–1.02	14.80	75.75	0.07	0.04	–0.35	17.11	69.89	0.07	0.06
L6	70	–0.05	21.44	29.11	0.08		–1.89	7.96	77.86	0.08	0.10	–1.27	8.97	73.60	0.08	0.14	–0.56	10.53	66.38	0.08	0.22
L7	110	–0.27	14.04	21.52	0.35		–1.50	8.51	84.95	0.35	0.25	–1.08	8.99	80.36	0.35	0.30	–0.61	8.10	65.75	0.35	0.50
L8	150	–0.26	8.30	15.56	0.69		–0.69	10.04	93.51	0.69	0.68	–0.54	8.34	82.95	0.69	0.80	–0.38	5.57	63.06	0.69	1.00
L9	190	–0.19	4.27	10.98	0.30		–0.49	6.16	91.82	0.30	0.71	–0.39	4.89	78.79	0.30	0.98	–0.28	3.21	59.44	0.30	1.45
L10	230	–0.11	2.72	9.24	3.24		–0.32	3.67	89.21	3.23	0.44	–0.25	2.98	76.15	3.24	0.49	–0.17	2.07	56.87	3.23	0.56
L11	270	–0.06	2.72	6.04	0.83		–0.34	3.21	85.61	0.83	0.86	–0.25	2.73	72.56	0.83	1.06	–0.15	2.12	53.32	0.83	1.29
L12	310	–0.11	2.11	4.59	0.75		–0.25	2.57	83.83	0.75	1.22	–0.21	2.12	70.43	0.75	1.35	–0.15	1.61	50.87	0.75	1.50
L13	350	–0.09	1.55	3.32	0.19		–0.21	2.30	82.04	0.19	0.18	–0.17	1.91	68.45	0.19	0.24	–0.13	1.50	48.70	0.19	0.33
L14	390	–0.15	0.97	2.57	0.29		–0.26	1.15	80.92	0.29	0.82	–0.23	0.94	67.36	0.29	0.88	–0.19	0.70	47.54	0.29	0.96
L15	430	–0.09	0.66	2.08	1.14		–0.13	0.99	80.11	1.14	0.26	–0.12	0.77	66.37	1.14	0.28	–0.10	0.54	46.37	1.14	0.30
L16	470	–0.03	0.49	0.82	0.42		–0.06	0.76	78.76	0.42	0.08	–0.05	0.57	64.98	0.42	0.09	–0.04	0.40	44.93	0.42	0.10
L17	510	–0.05	0.64	0.55	0.00		–0.07	0.97	78.65	0.00	60.92	–0.06	0.76	64.79	0.00	47.73	–0.06	0.59	44.68	0.00	29.37
L18	550	–0.03	0.43	0.36	0.00		–0.05	8.00	25.06	0.00	19.32	–0.04	6.89	23.36	0.00	18.38	–0.04	5.42	20.24	0.00	16.12
L19	590	–0.03	0.30	0.24	0.00		–0.03	9.21	7.09	0.00	0.02	–0.03	8.38	6.58	0.00	0.02	–0.03	7.24	6.02	0.00	0.02
L20	630	–0.02	0.20	0.15	0.00		–0.03	5.82	3.82	0.00	0.00	–0.03	5.13	3.43	0.00	0.00	–0.02	4.25	3.09	0.00	0.00
L21	670	–0.01	0.13	0.09	0.00		–0.02	3.72	1.85	0.00	0.00	–0.02	3.23	1.65	0.00	0.00	–0.01	2.55	1.47	0.00	0.00
L22	720	0.00	0.09	0.05	0.00		0.00	2.50	0.74	0.00	0.00	0.00	2.16	0.68	0.00	0.00	0.00	1.65	0.65	0.00	0.00
L23	870	0.00	0.07	0.02	0.00		–0.01	1.91	0.27	0.00	0.00	–0.01	1.63	0.26	0.00	0.00	–0.01	1.18	0.25	0.00	0.00
L24	1,030	0.00	0.03	0.01	0.00		–0.01	1.07	0.05	0.00	0.00	0.00	0.88	0.04	0.00	0.00	0.00	0.60	0.04	0.00	0.00
L25	1,190	0.00	0.01	0.00	0.00		0.00	0.45	0.02	0.00	0.00	0.00	0.37	0.01	0.00	0.00	0.00	0.25	0.02	0.00	0.00
Sum		**–1.40**			**8.36**	**0.00**	**–7.93**			**8.36**	**85.89**	**–5.77**			**8.36**	**72.77**	**–3.24**			**8.36**	**53.80**

Consequently, this means that out of the 86 mm of inflow to the open repository (grouting level of $K=1\cdot10^{-8}$ m/s), 7 mm (8%) can be explained by increased horizontal net inflow from the sea and 55 mm (64%) by increased vertical net inflow from the QD. The remaining 24 mm come from reduced storage in the bedrock because steady state conditions were not reached during the limited simulation period.

Some of the Äspö wells are located under the sea. In order to include all of the sinks/wells representing the Äspö HRL in the water balance, water balances are also made for the whole model area. In Table 5-3, the water balance for the saturated zone is presented layer by layer in the bedrock. The representation is similar to that in Table 5-2, but now concerns the whole model area, i.e. both for the land and the sea part of the model area (consequently covering all of the Äspö sinks). In Table 5-3, however, the average flow during 2006 is expressed in units of L/s, in order to allow a comparison of the contributions to the open repository inflow from different parts of the area, e.g. the land area and the sea area (Table 5-6).

The extraction of water in the Äspö sinks in the land part is 8.6 L/s for all three grouting levels and for undisturbed conditions. The corresponding extraction is 10 L/s when both the land and the sea areas are considered. This shows that out of the specified drainage of 14.2 L/s (85% of the real drainage) c 30% is reduced due to dried out wells in the model.

The calculated changes in the vertical net inflow from the QD over the land part due to the open repository (found in Table 5-2, layer 3, but expressed as average flow changes in L/s) are 57, 52 and 43 L/s for the three grouting levels of $K=1\cdot10^{-8}$ m/s, $1\cdot10^{-9}$ m/s and $K=1\cdot10^{-10}$ m/s, respectively. The corresponding changes in the vertical inflow to the bedrock from both the land and the sea areas (found in Table 5-3, layer 3) are 63, 56 and 45 L/s. The horizontal flow for the whole model area, see Table 5-3, is zero for all layers due to the no-flow boundary conditions described in Section 3.2.1.

The inflows to tunnels and shafts are further discussed in Section 5.2, but are also presented in Table 5-3. The total inflow is 88 L/s with a grouting level of $K=1\cdot10^{-8}$ m/s, 74 L/s with $K=1\cdot10^{-9}$ m/s in the deposition tunnels, and 55 L/s with $K=1\cdot10^{-10}$ m/s in the deposition tunnels.

Considerable changes can be seen in the overall water balances discussed above when introducing the open repository. However, large parts of the model area are not influenced by the groundwater table drawdown (see Chapter 5.4). In order to visualise the magnitude of the open repository influence in areas where the groundwater table is affected, water balances for only these areas has been calculated. Table 5-4 shows a summary of the total accumulated water balances in mm during 2006 for undisturbed and disturbed conditions for those areas where the groundwater table drawdown exceeds 0.3 m with a grouting level of $K=1\cdot10^{-8}$ m/s.

Inside this influence area, the open repository construction causes a major change in the water balance. With a grouting level of $K=1\cdot10^{-8}$ m/s the inflow to the open repository is 159 mm, which is approximately 27% of the precipitation over the area or 97% of the total runoff for undisturbed conditions (164 mm). The change of the evapotranspiration is small. The changes are instead found on the different runoff components. The total runoff decreases with 105 mm, from 165 mm to 60 mm, in the case with a grouting level of $K=1\cdot10^{-8}$ m/s. The largest changes are found in the subsurface outflow, the baseflow to streams and the drainflow to streams components which decrease with 94%, 101% and 36% respectively. For the baseflow to streams component the direction of the flow is even changed from a net outflow to a small net inflow. The rest of the changes are found in subsurface storage changes which are reduced with 96%.

In Table 5-5, the water balance for the saturated zone is presented layer by layer in the bedrock, similarly to Table 5-3, but now only for the influence area (the same area as in Table 5-4). In Table 5-5, however, the unit is average flow in L/s during 2006, to allow a comparison with the water balances for the whole model area in Table 5-3. The Äspö sinks are not included in Table 5-5 as they are not located within the influence area.

Table 5-3. Water balances for 2006 (L/s) in the saturated zone for the whole model area, shown for each bedrock calculation layer. Results are presented for undisturbed conditions and with an open repository for the three levels of grouting. The water balance components in the table are defined in Figure 5-1.

		Undisturbed conditions					Grouting K= $1 \cdot 10^{-8}$ m/s in the whole repository					Grouting K= $1 \cdot 10^{-9}$ m/s in deposition tunnels					Grouting K= $1 \cdot 10^{-10}$ m/s in deposition tunnels				
Layer	Lower level [m.b.s.l.]	Net horizontal outflow	Vertical out to above	Vertical in from above	To Äspö wells	To open repository	Net horizontal outflow	Vertical out to above	Vertical in from above	To Äspö wells	To open repository	Net horizontal outflow	Vertical out to above	Vertical in from above	To Äspö wells	To open repository	Net horizontal outflow	Vertical out to above	Vertical in from above	To Äspö wells	To open repository
L3	–10	0.00	34.12	53.37	0.00		0.00	14.93	97.53	0.00	0.00	0.00	16.15	91.41	0.00	0.00	0.00	18.61	82.75	0.00	0.00
L4	–8	0.00	34.77	52.47	0.00		0.00	15.07	96.48	0.00	0.00	0.00	16.30	90.37	0.00	0.00	0.00	18.82	81.81	0.00	0.00
L5	30	0.00	37.73	51.43	0.08		0.00	16.90	93.81	0.08	0.04	0.00	18.24	87.91	0.08	0.05	0.00	20.98	79.74	0.08	0.06
L6	70	0.00	24.93	35.77	0.08		0.00	10.11	89.49	0.08	0.11	0.00	11.24	83.63	0.08	0.15	0.00	13.08	74.60	0.08	0.23
L7	110	0.00	16.19	26.79	1.56		0.00	9.95	94.09	1.58	0.25	0.00	10.50	88.47	1.58	0.30	0.00	9.71	72.50	1.56	0.51
L8	150	0.00	9.54	18.43	0.90		0.00	11.09	99.66	0.87	0.70	0.00	9.36	88.32	0.87	0.82	0.00	6.55	67.35	0.90	1.03
L9	190	0.00	5.23	13.10	0.30		0.00	7.02	96.97	0.31	0.72	0.00	5.72	83.23	0.31	1.00	0.00	4.01	62.94	0.30	1.48
L10	230	0.00	3.28	10.76	3.31		0.00	4.14	93.45	3.31	0.45	0.00	3.44	79.78	3.31	0.50	0.00	2.50	59.69	3.31	0.57
L11	270	0.00	3.06	7.15	0.85		0.00	3.45	89.23	0.85	0.88	0.00	2.97	75.64	0.85	1.08	0.00	2.36	55.68	0.85	1.32
L12	310	0.00	2.33	5.50	0.77		0.00	2.74	87.00	0.77	1.25	0.00	2.28	73.14	0.77	1.38	0.00	1.77	52.95	0.77	1.54
L13	350	0.00	1.70	4.03	0.20		0.00	2.43	84.88	0.20	0.18	0.00	2.03	70.87	0.20	0.24	0.00	1.62	50.53	0.20	0.34
L14	390	0.00	1.06	3.13	0.29		0.00	1.22	83.48	0.29	0.84	0.00	1.01	69.54	0.29	0.90	0.00	0.77	49.18	0.29	0.99
L15	430	0.00	0.74	2.47	1.16		0.00	1.06	82.38	1.16	0.27	0.00	0.83	68.29	1.16	0.28	0.00	0.60	47.79	1.16	0.30
L16	470	0.00	0.54	1.07	0.43		0.00	0.81	80.86	0.43	0.08	0.00	0.62	66.74	0.43	0.09	0.00	0.44	46.20	0.43	0.10
L17	510	0.00	0.68	0.73	0.00		0.00	1.02	80.67	0.00	62.31	0.00	0.80	66.48	0.00	48.82	0.00	0.63	45.89	0.00	30.04
L18	550	0.00	0.46	0.49	0.00		0.00	8.20	25.79	0.00	19.76	0.00	7.06	24.03	0.00	18.80	0.00	5.57	20.83	0.00	16.49
L19	590	0.00	0.32	0.32	0.00		0.00	9.43	7.35	0.00	0.02	0.00	8.58	6.83	0.00	0.02	0.00	7.42	6.24	0.00	0.02
L20	630	0.00	0.22	0.20	0.00		0.00	5.97	3.97	0.00	0.00	0.00	5.25	3.56	0.00	0.00	0.00	4.36	3.21	0.00	0.00
L21	670	0.00	0.14	0.11	0.00		0.00	3.83	1.93	0.00	0.00	0.00	3.32	1.72	0.00	0.00	0.00	2.62	1.53	0.00	0.00
L22	720	0.00	0.11	0.07	0.00		0.00	2.57	0.77	0.00	0.00	0.00	2.23	0.71	0.00	0.00	0.00	1.71	0.68	0.00	0.00
L23	870	0.00	0.08	0.03	0.00		0.00	1.96	0.29	0.00	0.00	0.00	1.68	0.28	0.00	0.00	0.00	1.22	0.27	0.00	0.00
L24	1,030	0.00	0.04	0.01	0.00		0.00	1.10	0.06	0.00	0.00	0.00	0.91	0.04	0.00	0.00	0.00	0.62	0.04	0.00	0.00
L25	1,190	0.00	0.02	0.00	0.00		0.00	0.47	0.02	0.00	0.00	0.00	0.38	0.02	0.00	0.00	0.00	0.26	0.02	0.00	0.00
Sum		**0.00**			**9.94**		**0.00**			**9.93**	**87.85**	**0.00**			**9.93**	**74.43**	**0.00**			**9.94**	**55.02**

Table 5-4. Total accumulated water balances during 2006 (mm) for the influence area, which here is defined as the area where the groundwater table drawdown exceeds 0.3 m in a simulation with a grouting level of $K=1\cdot10^{-8}$ m/s. Results are presented for undisturbed conditions and for open repository cases with the three studied levels of grouting. Observe that the same area definition, i.e. based on the influence area for a grouting level of $K=1\cdot10^{-8}$ m/s, is applied in all of the four cases below when extracting the water balances.

	Reference simulation, without open repository	With open repository, grouting level $K=1\cdot10^{-8}$ m/s everywhere	With open repository, grouting level $K=1\cdot10^{-9}$ m/s in deposition tunnels	With open repository, grouting level $K=1\cdot10^{-10}$ m/s in deposition tunnels
Precipitation	590.5	590.5	590.5	590.5
Evapotranspiration	394.9	383.7	384.4	385.6
Canopy storage change	–0.1	–0.1	–0.1	–0.1
Snow storage change	–24.9	–24.9	–24.9	–24.9
Overland storage change	1.6	–0.5	–0.8	–0.4
Subsurface storage change	45.3	2.0	12.8	28.0
Net overland outflow	3.4	1.4	1.5	1.8
Net subsurface outflow	27.9	1.7	11.8	23.0
Drain outflow	4.0	3.9	3.9	4.0
Overland flow to river	6.8	5.8	5.9	6.0
Drainflow to river	76.7	48.8	49.6	52.4
Net baseflow to river	46.6	–0.3	2.3	8.1
Inflow to the open repository	–	159.2	134.9	99.9
Pumping from Äspö sinks	0.0	0.0	0.0	0.0

The calculated changes in the vertical net inflows from the QD inside the influence area due to the open repository (found in Table 5-5, layer 3) are 48, 46 and 39 L/s for the three grouting levels of $K=1\cdot10^{-8}$ m/s, $1\cdot10^{-9}$ m/s and $K=1\cdot10^{-10}$ m/s, respectively. The corresponding changes in the vertical inflow to the bedrock from the whole model area (found in Table 5-3, layer 3) are 63, 56 and 45 L/s.

Moreover, according to the results in Table 5-5, the total horizontal outflow in the bedrock from the influence area to neighbouring areas changes from an outflow of 5 L/s to an inflow of 8 L/s in the case with a grouting level of $K=1\cdot10^{-8}$ m/s. The inflow to the open repository is also presented in Table 5-5. The presented inflows are only slightly lower than those in Table 5-3 due to the fact that the entire open repository is located within the influence area (defined as above).

In Table 5-6, a summary is presented of the changes in the vertical net inflow, as well as the changes in the horizontal net inflow from the sea boundary, when the open repository is introduced. The vertical net inflow is divided between the influence area (here defined as the area where the groundwater table drawdown exceeds 0.3 m in a simulation with a grouting level of $K=1\cdot10^{-8}$ m/s), the rest of the land area, and the sea area.

As can be seen from Table 5-6, the changed vertical inflow from the land area contributes to the open repository inflow with 65–80%, depending on the grouting level, with a largest relative contribution for the highest grouting level, $K=1\cdot10^{-10}$ m/s. Approximately 85–90% of the changed vertical inflow from land can be attributed to the influence area. In total, the influence area contributes to the open repository inflow with 55–70%. Storage changes in the bedrock contribute with 15–25% and the changed vertical inflow from the sea together with changed inflow from streams stand for the remaining inflow to the open repository.

Table 5-5. Water balances for 2006 (L/s) in the saturated zone for the influence area (where the groundwater table drawdown exceeds 0.3 m) with a grouting level of K=1·10^{-8} m/s, shown for each bedrock calculation layer. Results are presented for undisturbed conditions and with an open repository for the three levels of grouting. The terms used refer to Figure 5-1.

		Undisturbed conditions				Grouting K= 1·10^{-8} m/s in the whole repository				Grouting K= 1·10^{-9} m/s in deposition tunnels				Grouting K= 1·10^{-10} m/s in deposition tunnels			
Layer	Lower level [m.b.s.l.]	Net horizontal outflow	Vertical out to above	Vertical in from above	To open repository	Net horizontal outflow	Vertical out to above	Vertical in from above	To open repository	Net horizontal outflow	Vertical out to above	Vertical in from above	To open repository	Net horizontal outflow	Vertical out to above	Vertical in from above	To open repository
L3	–10	0.01	14.27	24.57	0.00	0.00	0.13	58.73	0.00	0.00	0.34	56.27	0.00	0.00	1.27	51.07	0.00
L4	–8	0.03	14.80	23.89	0.00	0.00	0.18	57.91	0.00	0.01	0.40	55.45	0.00	0.01	1.38	50.36	0.00
L5	30	1.29	16.36	23.24	0.00	–2.09	0.66	55.71	0.04	–0.90	0.98	53.45	0.04	0.28	2.19	48.73	0.06
L6	70	1.23	11.94	15.84	0.00	–2.03	0.70	61.25	0.10	–0.85	1.15	58.15	0.14	0.36	1.96	51.92	0.22
L7	110	1.04	8.55	11.15	0.00	–1.43	4.47	71.74	0.24	–0.57	4.60	67.95	0.29	0.34	3.25	54.23	0.49
L8	150	0.43	5.54	7.02	0.00	–0.58	7.95	82.48	0.67	–0.23	6.10	72.56	0.79	0.13	3.14	53.44	0.99
L9	190	0.19	2.50	3.48	0.00	–0.29	4.84	82.17	0.70	–0.12	3.48	69.66	0.96	0.06	1.66	50.93	1.43
L10	230	0.14	1.53	2.28	0.00	–0.35	2.79	80.13	0.43	–0.19	2.04	67.56	0.48	0.00	1.03	48.88	0.55
L11	270	0.13	1.18	1.75	0.00	–0.21	1.88	79.39	0.85	–0.09	1.37	66.75	1.05	0.04	0.69	48.06	1.27
L12	310	0.10	0.99	1.40	0.00	–0.14	1.60	78.71	1.20	–0.06	1.12	65.71	1.33	0.02	0.57	46.69	1.48
L13	350	0.06	0.77	1.05	0.00	–0.13	1.62	77.88	0.17	–0.06	1.21	64.68	0.23	0.03	0.78	45.46	0.33
L14	390	0.03	0.51	0.71	0.00	–0.23	0.75	77.18	0.81	–0.15	0.54	63.98	0.87	–0.05	0.28	44.67	0.95
L15	430	0.03	0.34	0.47	0.00	–0.16	0.71	76.76	0.26	–0.12	0.48	63.34	0.27	–0.06	0.24	43.80	0.29
L16	470	0.02	0.23	0.31	0.00	–0.10	0.52	76.64	0.08	–0.08	0.33	63.15	0.09	–0.05	0.15	43.54	0.10
L17	510	0.01	0.17	0.22	0.00	–0.07	0.52	76.79	59.95	0.00	0.31	63.22	46.93	–0.02	0.13	43.52	28.92
L18	550	0.01	0.13	0.16	0.00	–0.05	7.56	24.20	18.77	–0.05	6.47	22.57	17.91	–0.05	5.05	19.60	15.79
L19	590	0.00	0.10	0.11	0.00	–0.04	8.80	6.80	0.02	–0.03	8.00	6.32	0.02	–0.02	6.91	5.77	0.02
L20	630	0.00	0.08	0.07	0.00	0.01	5.54	3.66	0.00	0.01	4.87	3.29	0.00	0.01	4.03	2.95	0.00
L21	670	0.00	0.05	0.04	0.00	–0.01	3.55	1.75	0.00	–0.01	3.07	1.56	0.00	–0.01	2.42	1.39	0.00
L22	720	0.00	0.04	0.02	0.00	0.00	2.37	0.69	0.00	0.00	2.05	0.63	0.00	0.00	1.56	0.61	0.00
L23	870	0.00	0.03	0.01	0.00	0.01	1.81	0.25	0.00	0.01	1.55	0.24	0.00	0.01	1.12	0.23	0.00
L24	1,030	0.00	0.01	0.00	0.00	–0.01	1.03	0.04	0.00	–0.01	0.85	0.03	0.00	0.00	0.58	0.04	0.00
L25	1,190	0.00	0.01	0.00	0.00	–0.01	0.44	0.02	0.00	–0.01	0.36	0.01	0.00	0.00	0.24	0.01	0.00
Sum		**4.73**				**–7.89**			**84.30**	**–3.48**			**71.41**	**1.01**			**52.90**

Table 5-6. Summary water balance for 2006 (L/s) showing the changes in flow components in the bedrock when introducing the open repository, for different levels of grouting.

Changes in flow components due to the open repository:	With open repository, grouting level K=1·10^{-8} m/s everywhere		With open repository, grouting level K=1·10^{-9} m/s in deposition tunnels		With open repository, grouting level K=1·10^{-10} m/s in deposition tunnels	
	(L/s)	relative contribution	(L/s)	relative contribution	(L/s)	relative contribution
Vertical net inflow to bedrock in the influence area	48.30	55%	45.63	61%	39.50	72%
Vertical net inflow to bedrock in the land area, excl influence area	8.46	10%	6.02	8%	3.59	7%
Vertical net inflow to bedrock from the sea area	6.59	7%	4.36	6%	1.80	3%
Horizontal net inflow to bedrock from the sea boundary	0.00	0%	0.00	0%	0.00	0%
Net inflow from river	1.88	2%	1.76	2%	1.51	3%
Storage change in bedrock	–22.60	26%	–16.66	22%	–8.62	16%
Inflow to the open repository	87.85		74.43		55.02	

The relatively large changes in the storage in the bedrock indicate that a new equilibrium has not yet been reached after three simulation years (2004–2006). In Table 5-7, results similar to those in Table 5-6 are presented comparing 2006 (same as the third column in Table 5-6) and the last year in a nine-year simulation where the input data for 2004–2006 were repeated three times, with a grouting level of K=1·10^{-9} m/s in deposition tunnels and K=1·10^{-8} m/s elsewhere. This simulation is further evaluated in Section 5.4.6. After nine years the inflow to the open repository has decreased with c 6% compared to the last year in the first three-year cycle. The relative contribution from changes in bedrock storage decreases from 22% to 8% and increases for all the vertical net inflow components.

Table 5-7. Summary water balances (L/s) for the third years ("2006") in the first and the last three-year simulation cycles ("2004–2006") showing the changes in flow components in the bedrock when introducing the open repository with a grouting level of K=1·10^{-9} m/s in deposition tunnels and K=1·10^{-8} m/s in all other tunnels and shafts.

Changes in flow components due to the open repository:	Third year, first cycle		Third year, third cycle	
	(L/s)	relative contribution	(L/s)	relative contribution
Vertical net inflow to bedrock in the influence area	45.63	61%	45.58	65%
Vertical net inflow to bedrock in the land area, excl influence area	6.02	8%	10.42	15%
Vertical net inflow to bedrock from the sea area	4.36	6%	6.51	9%
Horizontal net inflow to bedrock from the model boundary	0.00	0%	0.00	0%
Net inflow from river	1.76	2%	1.92	3%
Storage change in bedrock	–16.66	22%	–5.41	8%
Inflow to the open repository	74.43		69.85	

5.2 Inflows to tunnels and shafts

The inflow to the tunnels increases with an increased hydraulic conductivity of the grouting in calculation layers 17 and 18 (470 to 550 m.b.s.l.), where the major part of the open repository is located. In all other layers the results are the opposite; the inflows to both tunnels and shafts increase with a decreased grouting conductivity. In the case with the highest grouting conductivity, $K=1\cdot10^{-8}$ m/s, the large drawdown of the groundwater table causes the shafts to dry out and therefore the inflow increases when the grouting conductivity and the drawdown decreases. However, more than 95% of the total inflow to tunnels comes from calculation layers 17 and 18.

A grouting conductivity of $K=1\cdot10^{-8}$ m/s results in a mean inflow over the evaluated simulation period (year 2006) of approximately 85 L/s to tunnels and 2.5 L/s to shafts. With a grouting conductivity of $K=1\cdot10^{-10}$ m/s in the deposition tunnels the lowest inflow of approximately 52 L/s for tunnels and the highest inflow of c 3.3 L/s for shafts is reached. The inflows for the three cases are listed in Table 5-8 for each layer. It should be noted that the inflow to the repository is calculated based on both the grouting conductivity and the conductivities in the surrounding bedrock (see Section 2.3.1 for details). This means that when the bedrock has a lower conductivity than the grouting, the bedrock conductivity controls the inflow, and vice versa.

In Table 5-9 the inflows to the tunnels are presented similarly as in Table 5-8, but now expressed as specific mean inflow (denoted Q_s) in L/s/km tunnel length in each layer. This gives a different picture of the distribution of inflows to the layers. The largest specific inflows are not found in the layers at the repository depth but in the layers between 110 and 390 m.b.s.l. (layers 8–14).

Table 5-8. Calculated mean inflow (L/s) to tunnels and shafts during 2006 for each calculation layer for the three levels of grouting.

Layer	Lower level (m.b.s.l.)	Inflow to tunnels, grouting level $K=1\cdot10^{-8}$ m/s in the whole repository	Inflow to tunnels, grouting level $K=1\cdot10^{-9}$ m/s in deposition tunnels	Inflow to tunnels, grouting level $K=1\cdot10^{-10}$ m/s in deposition tunnels	Inflow to shafts, grouting level $K=1\cdot10^{-8}$ m/s	Inflow to shafts, grouting level $K=1\cdot10^{-9}$ m/s in deposition tunnels	Inflow to shafts, grouting level $K=1\cdot10^{-10}$ m/s in deposition tunnels
L1–L3	–10	0.0	0.0	0.0	0.0	0.0	0.0
L4	–8	0.0	0.0	0.0	0.0	0.0	0.0
L5	30	0.0	0.0	0.0	0.0	0.0	0.1
L6	70	0.0	0.0	0.0	0.1	0.1	0.2
L7	110	0.0	0.0	0.2	0.2	0.3	0.3
L8	150	0.3	0.4	0.5	0.4	0.4	0.5
L9	190	0.5	0.7	1.2	0.3	0.3	0.3
L10	230	0.2	0.3	0.3	0.2	0.2	0.3
L11	270	0.6	0.8	1.0	0.3	0.3	0.4
L12	310	0.8	0.9	1.0	0.3	0.4	0.4
L13	350	1.0	1.0	1.1	0.2	0.3	0.3
L14	390	0.5	0.5	0.6	0.2	0.3	0.3
L15	430	0.0	0.0	0.1	0.2	0.2	0.2
L16	470	0.0	0.0	0.0	0.1	0.1	0.1
L17	510	61.6	48.1	29.2	0.0	0.0	0.0
L18	550	19.8	18.8	16.5	0.0	0.0	0.0
L19	590	0.0	0.0	0.0	0.0	0.0	0.0
L20	630	0.0	0.0	0.0	0.0	0.0	0.0
L21	670	0.0	0.0	0.0	0.0	0.0	0.0
L22	720	0.0	0.0	0.0	0.0	0.0	0.0
L23	870	0.0	0.0	0.0	0.0	0.0	0.0
L24	1,030	0.0	0.0	0.0	0.0	0.0	0.0
L25	1,190	0.0	0.0	0.0	0.0	0.0	0.0
Sum		**85.4**	**71.6**	**51.7**	**2.5**	**2.8**	**3.3**

Table 5-9. Calculated specific mean inflow Q_s (L/s/km tunnel) to the open repository during 2006 for each calculation layer for the three levels of grouting.

Layer	Lower level (m.b.s.l.)	Tunnel length (m)	Qs, grouting level $K=1\cdot10^{-8}$ m/s	Qs, grouting level $K=1\cdot10^{-9}$ m/s in deposition tunnels	Qs, grouting level $K=1\cdot10^{-10}$ m/s in deposition tunnels
L1–L3	–10	31	0.00	0.00	0.00
L4	–8	21	0.10	0.10	0.10
L5	30	460	0.02	0.02	0.02
L6	70	563	0.01	0.01	0.07
L7	110	508	0.03	0.04	0.33
L8	150	413	0.76	0.93	1.27
L9	190	433	1.09	1.69	2.68
L10	230	510	0.49	0.55	0.63
L11	270	489	1.25	1.58	1.96
L12	310	508	1.48	1.68	1.93
L13	350	413	2.43	2.52	2.69
L14	390	433	1.11	1.21	1.34
L15	430	508	0.09	0.09	0.10
L16	470	423	0.07	0.07	0.08
L17	510	71,111	0.87	0.68	0.41
L18	550	35,686	0.55	0.53	0.46
L19	590	121	0.17	0.17	0.19
L20	630		0.00	0.00	0.00
L21	670		0.00	0.00	0.00
L22	720		0.00	0.00	0.00
L23	870		0.00	0.00	0.00
L24	1,030		0.00	0.00	0.00
L25	1,190		0.00	0.00	0.00
Sum		**112,628**	**0.76**	**0.64**	**0.46**

In Figure 5-2 the inflow from layer 17 at repository depth has been resolved in the horizontal plane, by showing the inflow to the repository from each grid cell. The largest inflows are found along the boundaries of the repository, i.e. the outer transport tunnels, especially along the northern and southern boundary. The inflow varies within the area, with a higher inflow in the northern half of the repository.

The temporal variations in the meteorological conditions have only very small effects on the calculated inflows. The inflows are somewhat higher after wet periods, especially after the snowmelt in April, but the variations are small. In Figure 5-3 the relative variations in the inflows from some selected layers are presented together with the total inflow, for the case with a grouting level of $K=1\cdot10^{-9}$ m/s in the deposition tunnels and $K=1\cdot10^{-8}$ m/s elsewhere. The total inflow decreases over the year (2006) from a total inflow of 89 L/s to 83 L/s. This indicates that the drawdown has not yet reached a new equilibrium with the inflow. In layers 13 and 17 the inflow decreases with 7–8% over the year and the influence of the meteorological variations is very small. The relative variation is largest in the upper layers. Below 300 m.b.s.l. the variation is negligible.

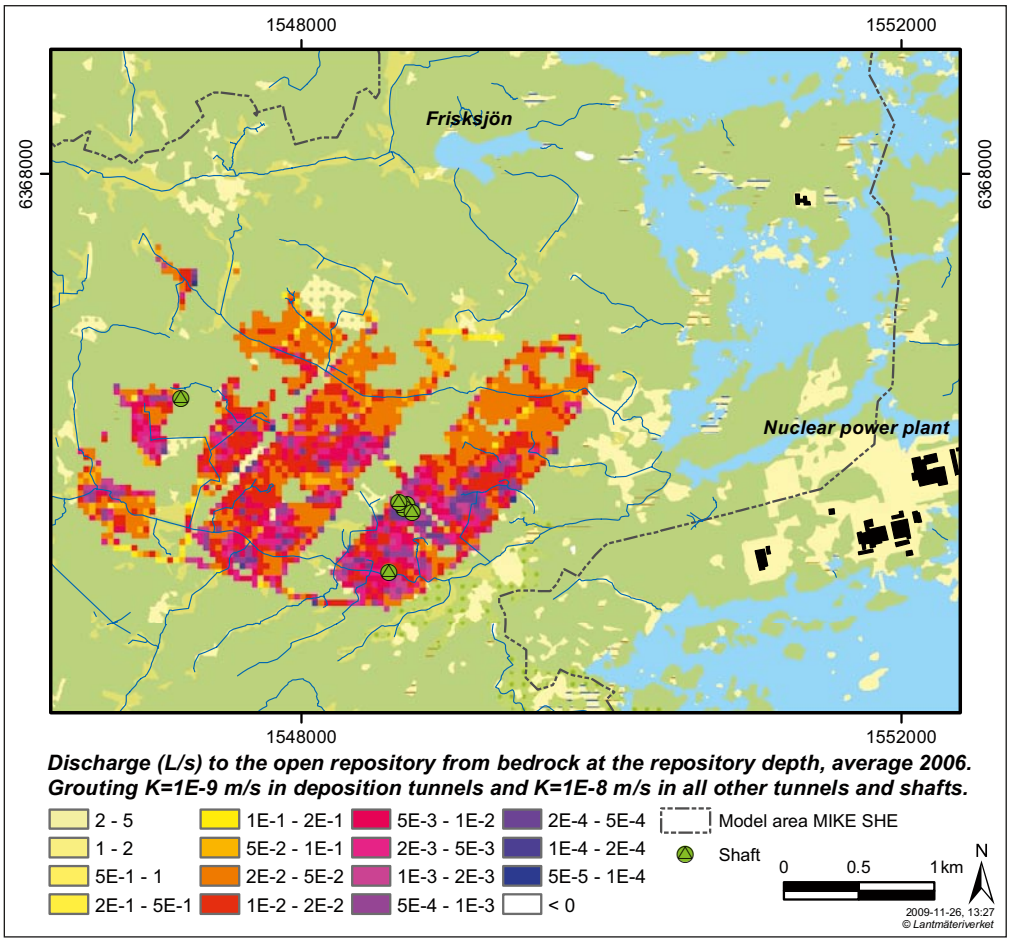

Figure 5-2. *Calculated discharge (L/s) to the open repository from each grid cell in the layer where the repository is located (Layer 17). The discharges are calculated as an average of 2006, with a grouting level of $K=1{\cdot}10^{-9}$ m/s in the deposition tunnels and $K=1{\cdot}10^{-8}$ m/s in all other tunnels and shafts.*

The open repository will be constructed and taken into operation in five different development phases, phases 1–5. In all development phases the transport tunnels will be opened gradually together with the different sections of deposition tunnels. The deposition tunnels will, however, only be open a few sections at a time (see Section 3.3 for details). In Table 5-10, the inflows to tunnels and shafts are presented for the initial construction phase and development phase 2, based on results from simulations with a grouting level of $K=1{\cdot}10^{-9}$ m/s in the deposition tunnels and $K=1{\cdot}10^{-8}$ m/s in all other tunnels and shafts.

Compared to the full open repository construction, the inflows for the different phases are smaller. The initial construction phase has only an inflow of approximately 12% of the inflow to the full construction. The corresponding inflow for development phase 2 is 27% of the inflow for the full construction. The difference is however mainly seen at the repository level. The inflow to the shafts is smaller compared to the full construction, partly because only four out of six shafts are open during the initial construction phase and five out of six shafts in development phase 2.

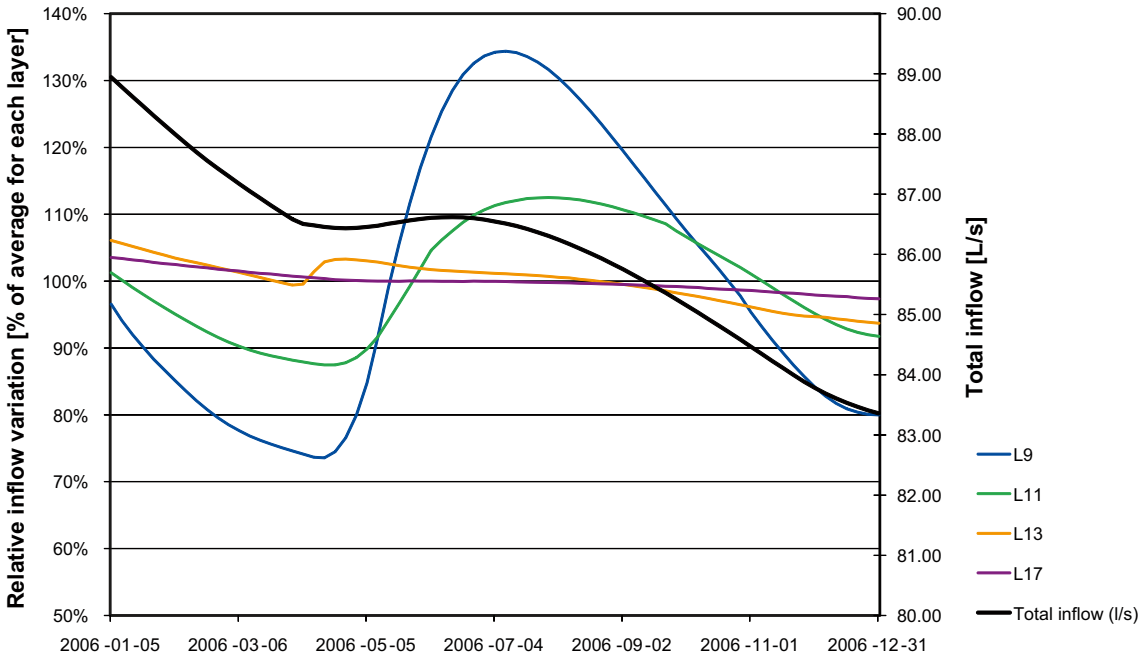

Figure 5-3. Temporal variations in the inflow during 2006 expressed as total inflows (L/s) and relative variations for selected layers, with a grouting level of $K=1\cdot10^{-9}$ m/s in the deposition tunnels and $K=1\cdot10^{-8}$ m/s in all other tunnels and shafts.

Table 5-10. Calculated mean inflow (L/s) to tunnels and shafts during 2006 for each calculation layer and for the initial construction phase and development phase 2. The results are from a simulation with a grouting level of $K=1\cdot10^{-9}$ m/s in the deposition tunnels and $K=1\cdot10^{-8}$ m/s in all other tunnels and shafts.

Layer	Lower level (m.b.s.l.)	Inflow to tunnels, construction phase	Inflow to tunnels, development phase 2	Inflow to shafts, construction phase	Inflow to shafts, development phase 2
L1–L3	–10	0.0	0.0	0.0	0.0
L4	–8	0.0	0.0	0.0	0.0
L5	30	0.0	0.0	0.0	0.0
L6	70	0.2	0.1	0.0	0.1
L7	110	0.5	0.2	0.0	0.2
L8	150	0.7	0.6	0.1	0.3
L9	190	1.7	1.4	0.1	0.3
L10	230	0.4	0.3	0.1	0.3
L11	270	1.1	1.0	0.2	0.4
L12	310	1.1	1.0	0.0	0.2
L13	350	1.2	1.1	0.0	0.0
L14	390	0.6	0.6	0.0	0.0
L15	430	0.1	0.1	0.0	0.0
L16	470	0.0	0.0	0.0	0.0
L17	510	0.9	12.4	0.0	0.0
L18	550	0.1	0.9	0.0	0.0
L19	590	0.0	0.0	0.0	0.0
L20	630	0.0	0.0	0.0	0.0
L21	670	0.0	0.0	0.0	0.0
L22	720	0.0	0.0	0.0	0.0
L23	870	0.0	0.0	0.0	0.0
L24	1,030	0.0	0.0	0.0	0.0
L25	1,190	0.0	0.0	0.0	0.0
Sum		**8.7**	**19.7**	**0.6**	**1.9**

5.3 Surface water levels and discharges

The mean water level in Lake Frisksjön, the only lake within the model area, is affected by the repository and tunnel constructions. Some difference in water level between the different levels of grouting can be noticed, see Figure 5-4, with the largest drawdown of the water level for the highest grouting conductivity ($K=1\cdot10^{-8}$ m/s). For Lake Frisksjön, which is located north of the repository, the average drawdown varies between 0.05 and 0.1 m, depending on the level of grouting, with a maximum drawdown between 0.1 and 0.2 m, see Figure 5-5. The maximum drawdown occurs in the end of October, after a long dry period.

Compared to the natural changes in water level the drawdown due to the open repository is not very drastic, e.g. during spring flood in April the water level rises c 0.6 m for undisturbed conditions compared to the maximum drawdown of 0.2 m in October with a grouting conductivity of $K=1\cdot10^{-8}$ m/s.

The discharges in the water courses are affected by the tunnels and shafts. Table 5-11 shows a comparison of the relative change in average discharge between the natural conditions and the different levels of grouting at the four monitoring stations. Laxemarån is affected the least and Ekerumsbäcken the most. In Ekerumsbäcken the accumulated discharge decreases with 48% and in Laxemarån the decrease is 8% with a grouting level of $K=1\cdot10^{-8}$ m/s. The catchment area of Ekerumsbäcken is underlain by a large part of the repository and therefore the largest decrease of the discharge is observed here.

The facts that the catchment area of Laxemarån is large and only partly underlain by the tunnels and shafts and that approximately 50% of the total flow originates from the inflow across the model boundary (NAM-inflow in MIKE 11) explain why the discharge in this stream is the least affected. During the summer months, between June and October, Ekerumsbäcken completely dries out irrespective of the level of grouting. However, the stream is dry also under undisturbed conditions, but during shorter periods of time (Figure 5-8). Both Laxemarån and Ekerumsbäcken experience high peak flows during the snow melt in April, see Figure 5-6 and Figure 5-8.

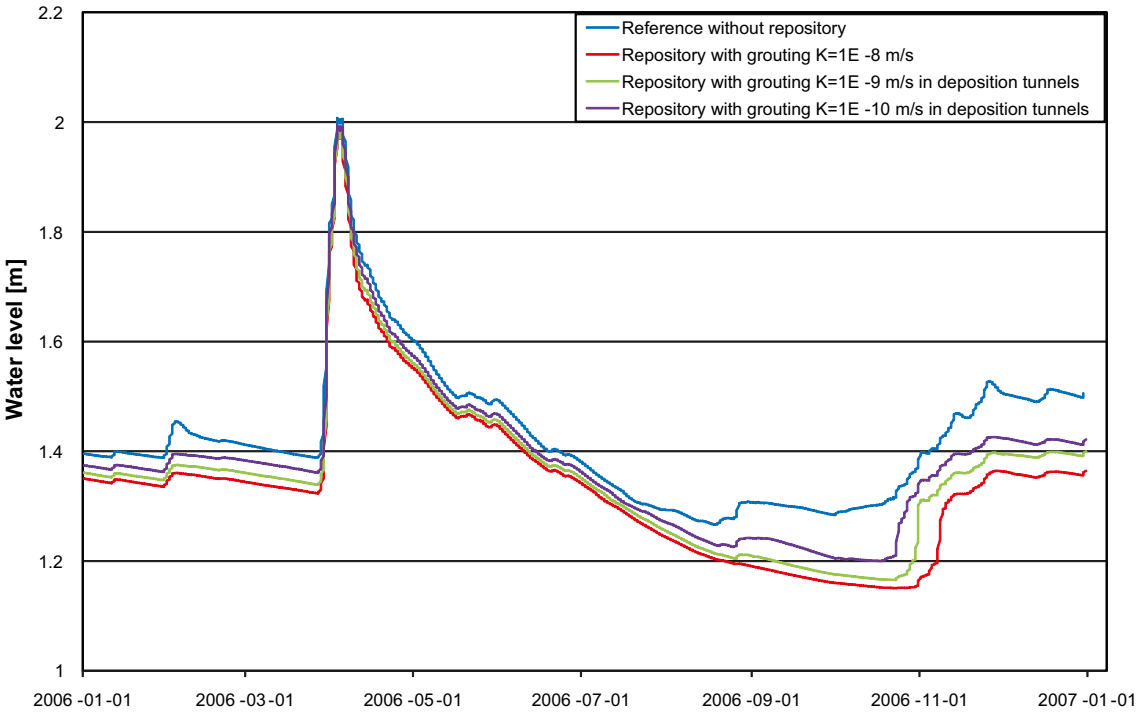

Figure 5-4. *Calculated water levels in Lake Frisksjön for different levels of grouting.*

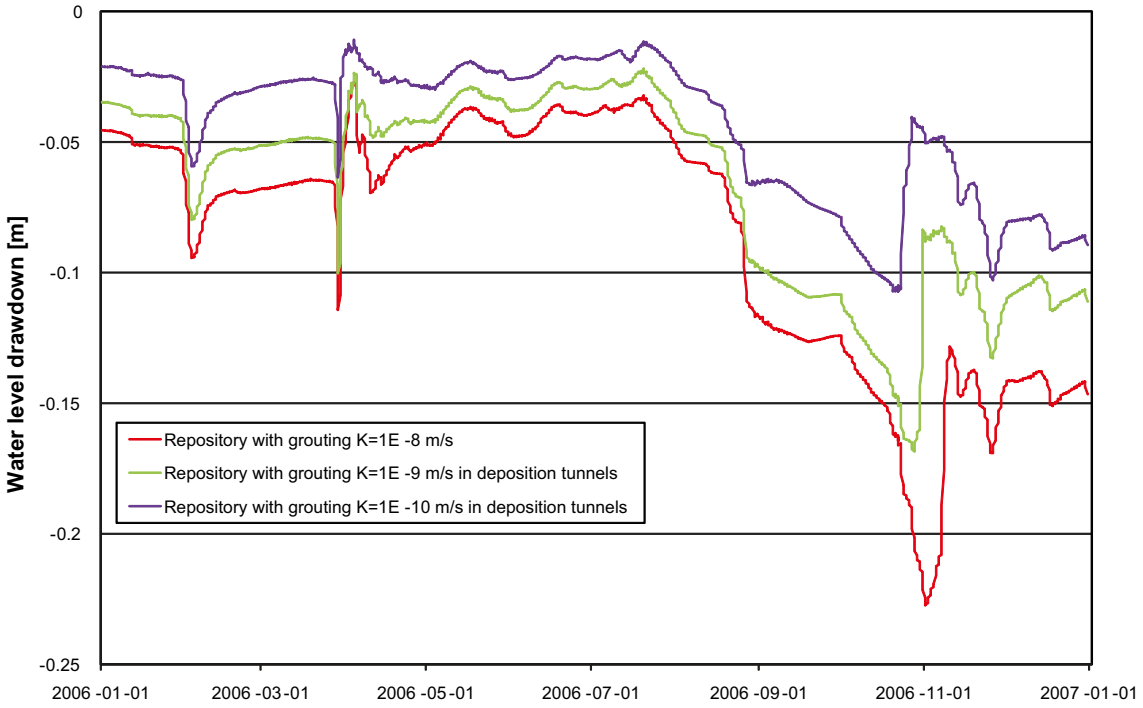

Figure 5-5. *Calculated water level drawdown in Lake Frisksjön for different levels of grouting.*

Table 5-11. Relative changes (decreases) in mean discharges in water courses (during 2006) when introducing an open repository with different levels of grouting.

	$K=1\cdot10^{-8}$ m/s in all tunnels and shafts	$K=1\cdot10^{-9}$ m/s in deposition tunnels	$K=1\cdot10^{-10}$ m/s in deposition tunnels
Laxemarån	8%	7%	6%
Ekerumsbäcken	48%	48%	48%
Kåreviksån, upstream Frisksjön	44%	43%	39%
Kåreviksån, downstream Frisksjön	34%	30%	20%

The calculated accumulated change in discharge in Laxemarån and Ekerumsbäcken are shown in Figure 5-7 and 5-9, respectively. The reduced discharge is a direct consequence of the groundwater table drawdown in the area. For Laxemarån there is a slight difference in the accumulated change in discharge between the different levels of grouting while in Ekerumsbäcken all three levels of grouting causes the same accumulated change.

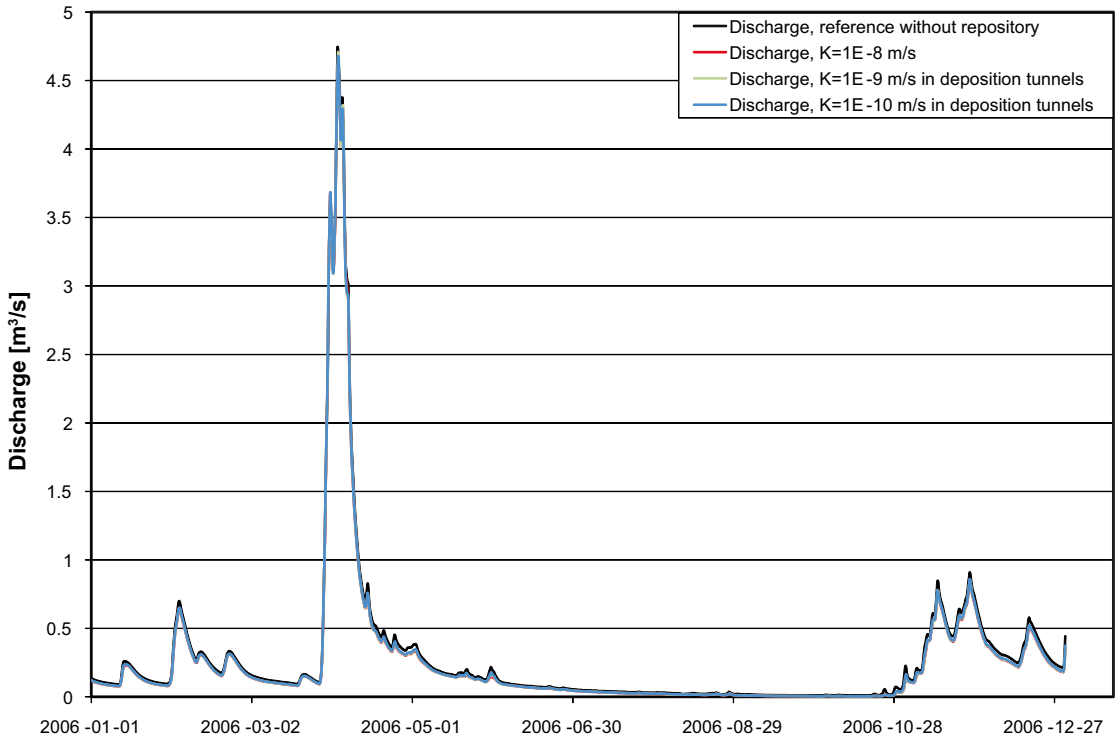

Figure 5-6. *Calculated discharge in Laxemarån for the reference (undisturbed) case and the three different levels of grouting.*

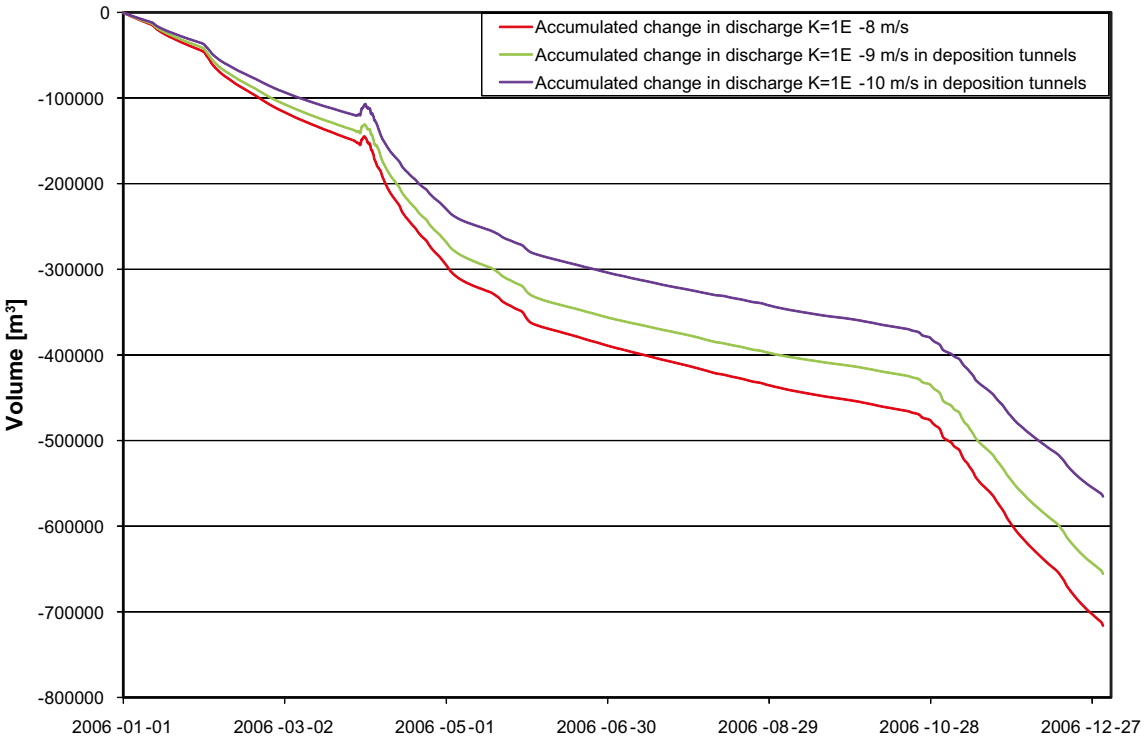

Figure 5-7. *Calculated accumulated change in discharge in Laxemarån compared to the reference (undisturbed) case for the three different levels of grouting.*

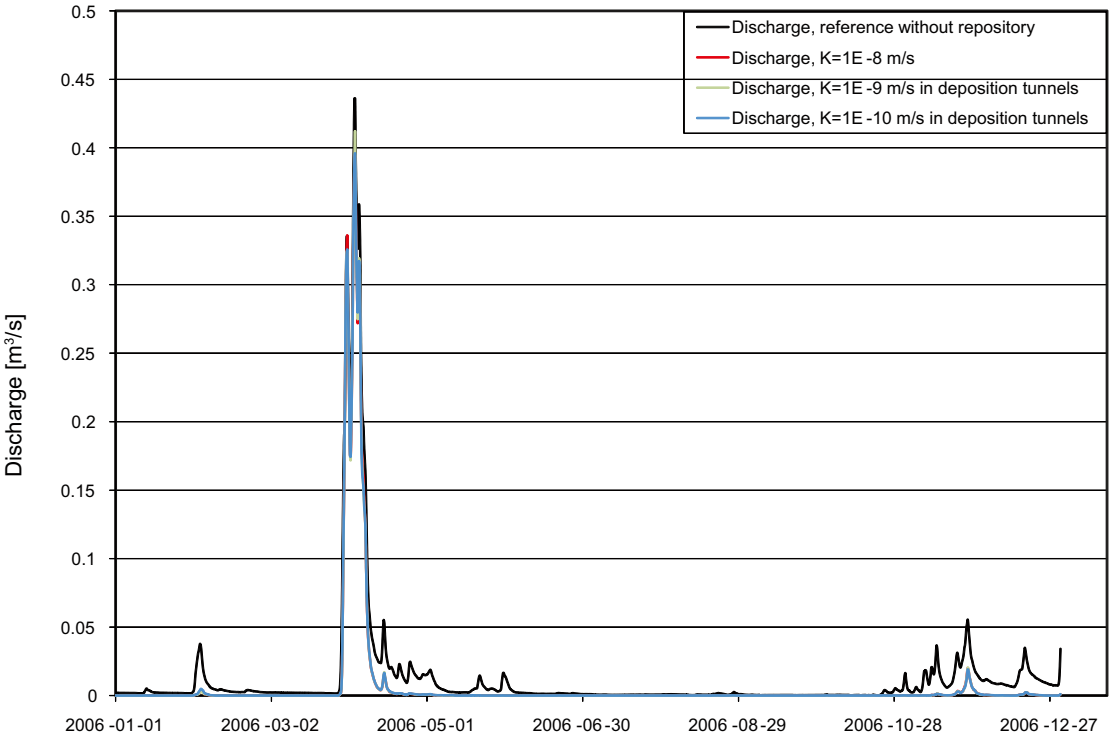

Figure 5-8. *Calculated discharge in Ekerumsbäcken for the reference (undisturbed) case and the three different levels of grouting.*

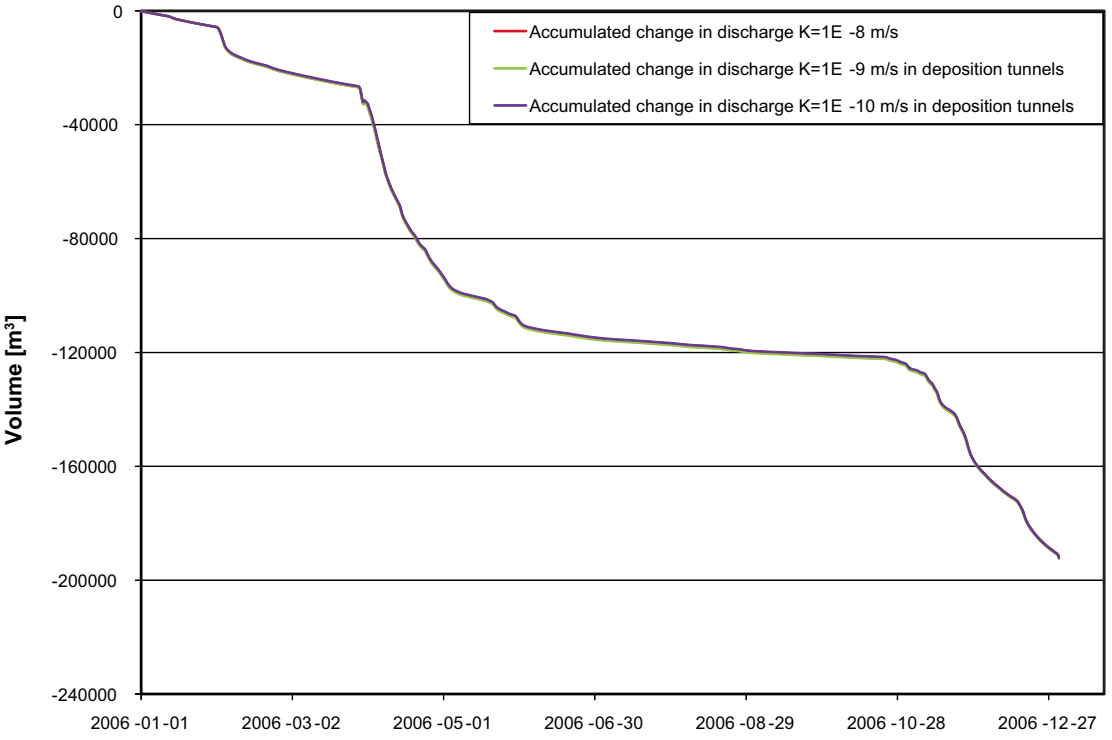

Figure 5-9. *Calculated accumulated change in discharge in Ekerumsbäcken compared to the reference (undisturbed) case for the three different levels of grouting.*

5.4 Groundwater drawdown and head changes

The influence area is here defined as the area where the annual average groundwater table is lowered more than 0.3 m due to the repository. Figure 5-10 shows the drawdown of the groundwater table, as an average for 2006, for a grouting level of $K=1\cdot10^{-9}$ m/s in deposition tunnels and $K=1\cdot10^{-8}$ m/s elsewhere. The influence area, shown in Figure 5-10, covers as much as 45% of the total model area, stretching all the way out to the model boundary in the north and the southwest. The largest drawdown of the groundwater table is found in the area where four of the six shafts are located closely together. The drawdown of the groundwater table is here up to approximately 500 metres, i.e. down to repository depth.

The size and the form of the influence area and the drawdown depend on a number of factors, which are discussed in this chapter. An overview, with references to specific sections, is given below. The influence area and the groundwater head changes increase with depth, and are generally affected by the horizontal and vertical conductivity in the bedrock and the Quaternary deposits. This is further discussed in Section 5.4.1.

The hydraulic conductivity of the grouted zone around tunnels and shafts is also an important factor that influences the size of the groundwater table drawdown and the head changes. This is presented in Section 5.4.2 for the three different levels of grouting.

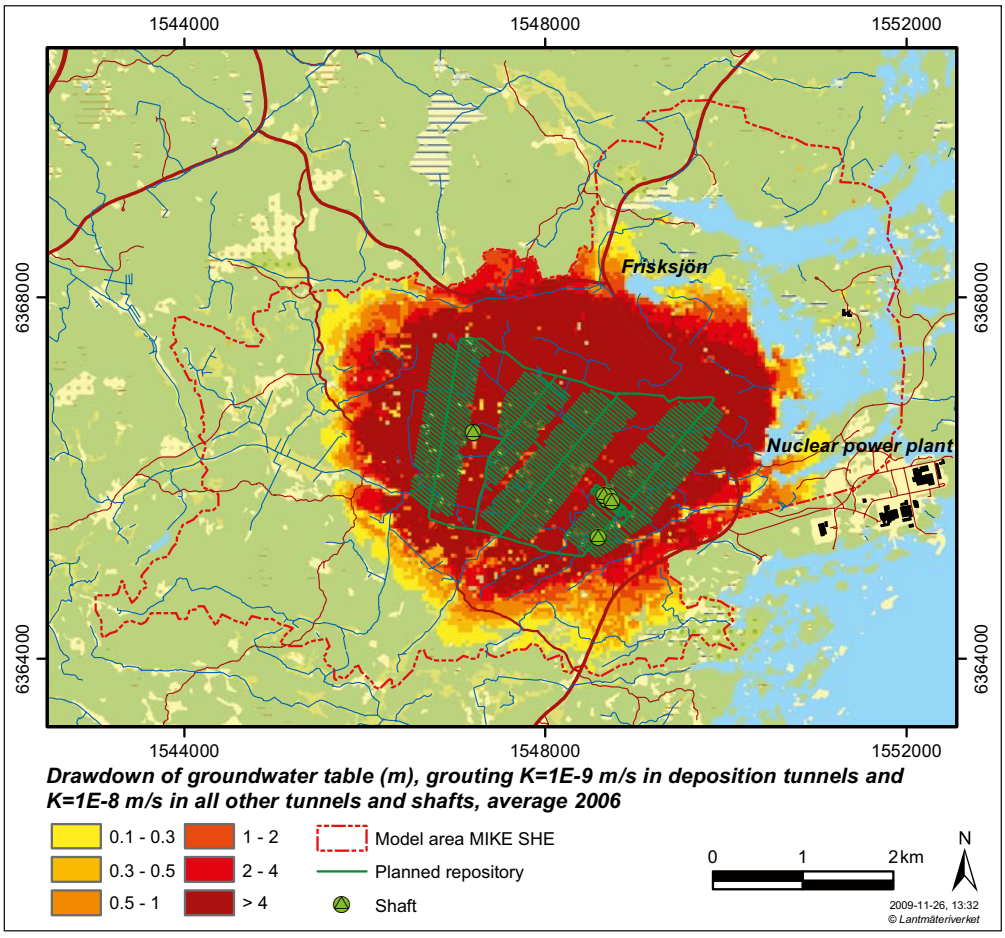

Figure 5-10. *Drawdown of the groundwater table as an average for 2006, with $K=1\cdot10^{-9}$ m/s in deposition tunnels and $K=1\cdot10^{-8}$ m/s elsewhere.*

The groundwater table drawdown for the initial construction phase and for the second of the totally five different development phases of the open repository (with a grouting level of $K=1\cdot10^{-9}$ m/s in deposition tunnels and $K=1\cdot10^{-8}$ m/s in all other tunnels and shafts) are presented in Section 5.4.3. The groundwater table drawdown varies in time due to different meteorological and hydrological conditions, which is illustrated in Section 5.4.5.

In reality, the repository will be open for many decades, and the groundwater table drawdown will have time to be fully developed to new equilibrium conditions (except the influence from temporal variations of the meteorological and hydrological conditions). In practice, it would take to long time to simulate the full period. In order to save simulation time, a rather short simulation period has been applied, only three years, where the first two years are used as an initialisation period. However, the drawback of this approach is that there is a risk that the influence area and the groundwater table drawdown are underestimated. This is further investigated in Section 5.4.6.

5.4.1 Head changes and vertical flow pattern at different depths

The results presented above refer to the drawdown of the groundwater table. The impact of the inflow to the repository on the groundwater table is considerable and the drawdown cone extends to the model boundary, see Figure 5-10. However, there are differences in the head changes of the groundwater when considering different depths in the model. In this section, results of groundwater head changes and vertical flow pattern are shown for different depths in the bedrock, down to 310 m.b.s.l.

In all cases in this section, the level of grouting has been set to $K=1\cdot10^{-9}$ m/s in the deposition tunnels and $K=1\cdot10^{-8}$ m/s in all other tunnels and shafts, and all of the results are either presented as arithmetic averages during 2006 or taken from October 17th 2006 when the groundwater table is at its lowest level during the simulated period. Figures 5-11 and 5-12 show the changes in the groundwater head at different depths in the bedrock (layers 8, 10 and 12) together with the groundwater table drawdown. The head change in the bedrock is considerable and extends all the way to the model boundary. In Figure 5-13, the groundwater head with an open repository is shown at different depths in two profiles through the catchment area and through the centre of the open repository; one from SW to NE and one from NW to SE. In calculation layers 1–6, the groundwater head change is of such magnitude that these calculation layers dry out in some parts of the model area.

As shown in Figures 5-11 and 5-12, the influence areas of the head changes at 150, 230 and 310 m.b.s.l. and that of the groundwater table drawdown reach the model boundary. Due to the no-flow boundary condition in all layers it is not possible for the open repository to draw water from the model boundary. This is, however, further investigated as a sensitivity case in Chapter 7 using a prescribed head boundary condition. The results from the sensitivity analysis show that the inflow to the open repository does not increase with a fixed head boundary and the influence area decreases with approximately 8%.

Table 5-12 shows a summary of the influence areas and head changes at different depths together with the groundwater table drawdown for the case with a grouting level of $K=1\cdot10^{-9}$ m/s in deposition tunnels and $K=1\cdot10^{-8}$ m/s elsewhere. The influence area, defined as the area with a head change larger than 0.3 m, at 310 m.b.s.l. is 6% larger than the corresponding area at 150 m.b.s.l. and 20% larger than the influence area of the groundwater table drawdown.

Table 5-12. Influence area (km²) with different head change at different depths and groundwater table drawdown. The areas are calculated using the average drawdown during 2006.

	Influence area, head change >0.1 m	Influence area, head change >0.3 m	Influence area, head change >1.0 m	Influence area, head change >4.0 m	Influence area, head change >10.0 m
Groundwater table drawdown	17.5	15.7	13.5	10.3	8.1
150 m.b.s.l.	19.7	17.9	15.4	12.2	9.7
230 m.b.s.l.	20.2	18.4	15.8	12.5	10.0
310 m.b.s.l.	20.6	18.9	16.2	12.9	10.4

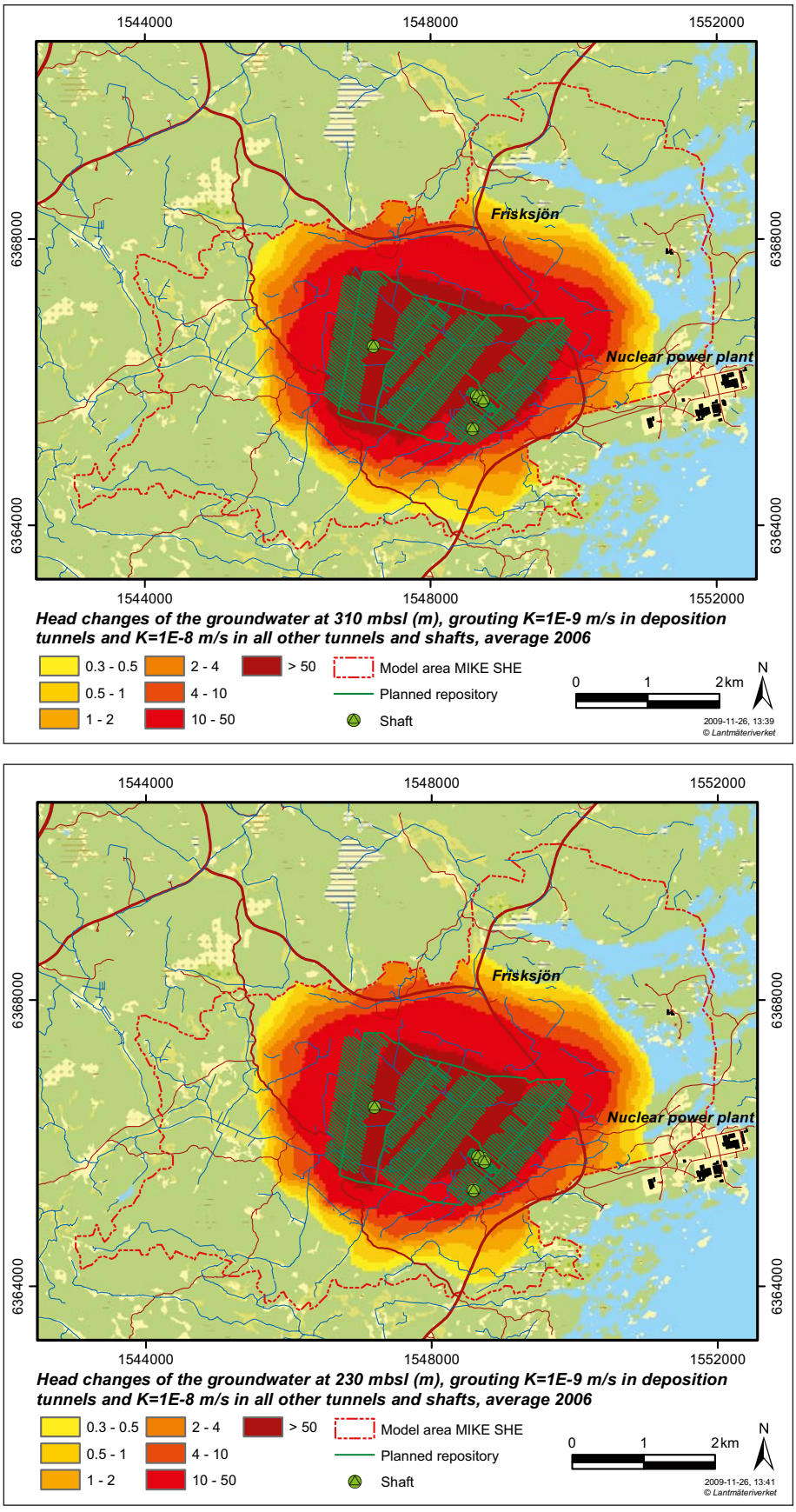

Figure 5-11. *Groundwater head changes at 310 m.b.s.l. (layer 12, upper graph) and 230 m.b.s.l. (layer 10, lower graph), averages for 2006 for a grouting level of $K=1\cdot10^{-9}$ m/s in the deposition tunnels and $K=1\cdot10^{-8}$ m/s in all other tunnels and shafts.*

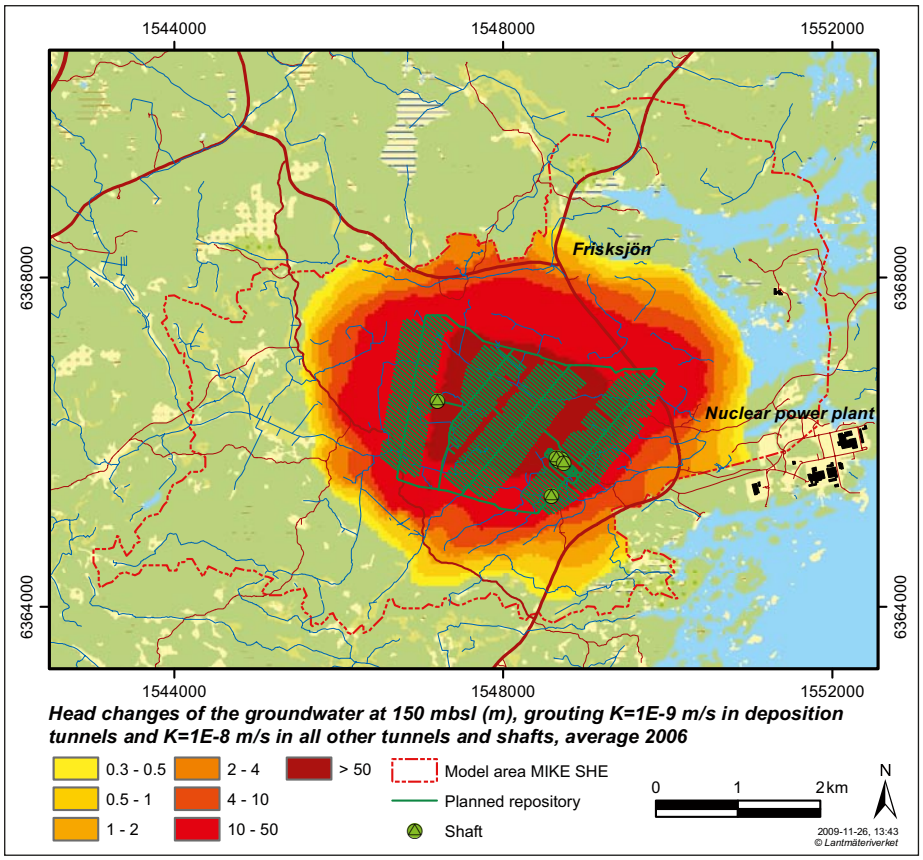

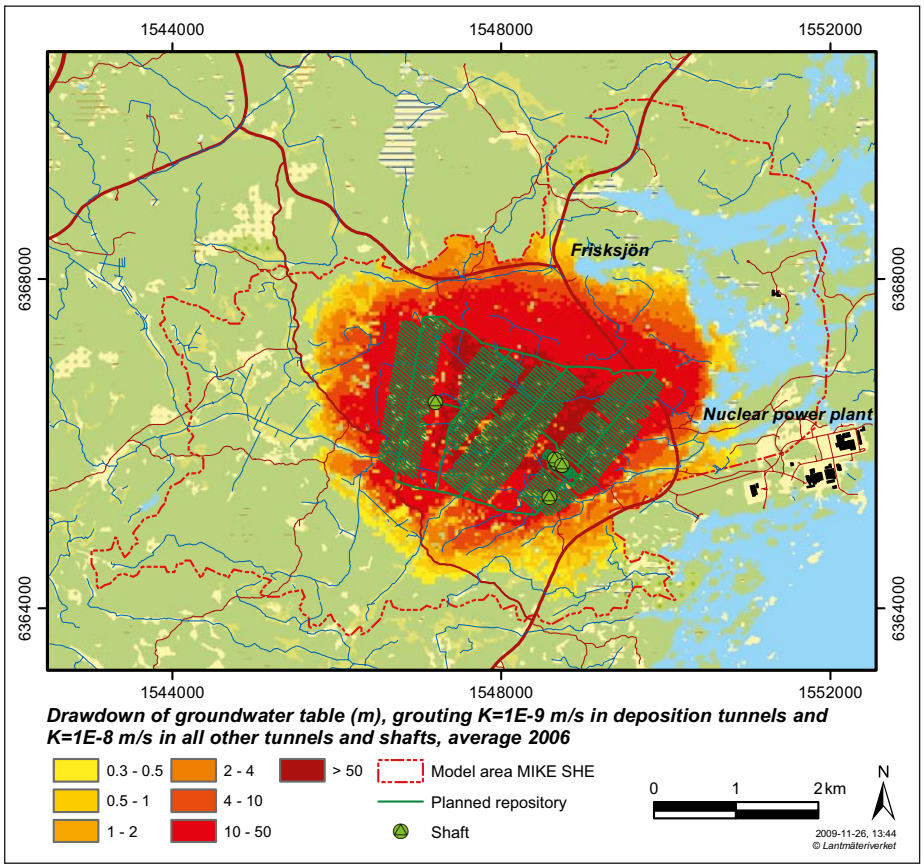

Figure 5-12. *Groundwater head changes at 150 m.b.s.l. (layer 8, upper graph) and groundwater table drawdown (lower graph), averages for 2006 for a grouting level of $K=1\cdot10^{-9}$ m/s in the deposition tunnels and $K=1\cdot10^{-8}$ m/s in all other tunnels and shafts.*

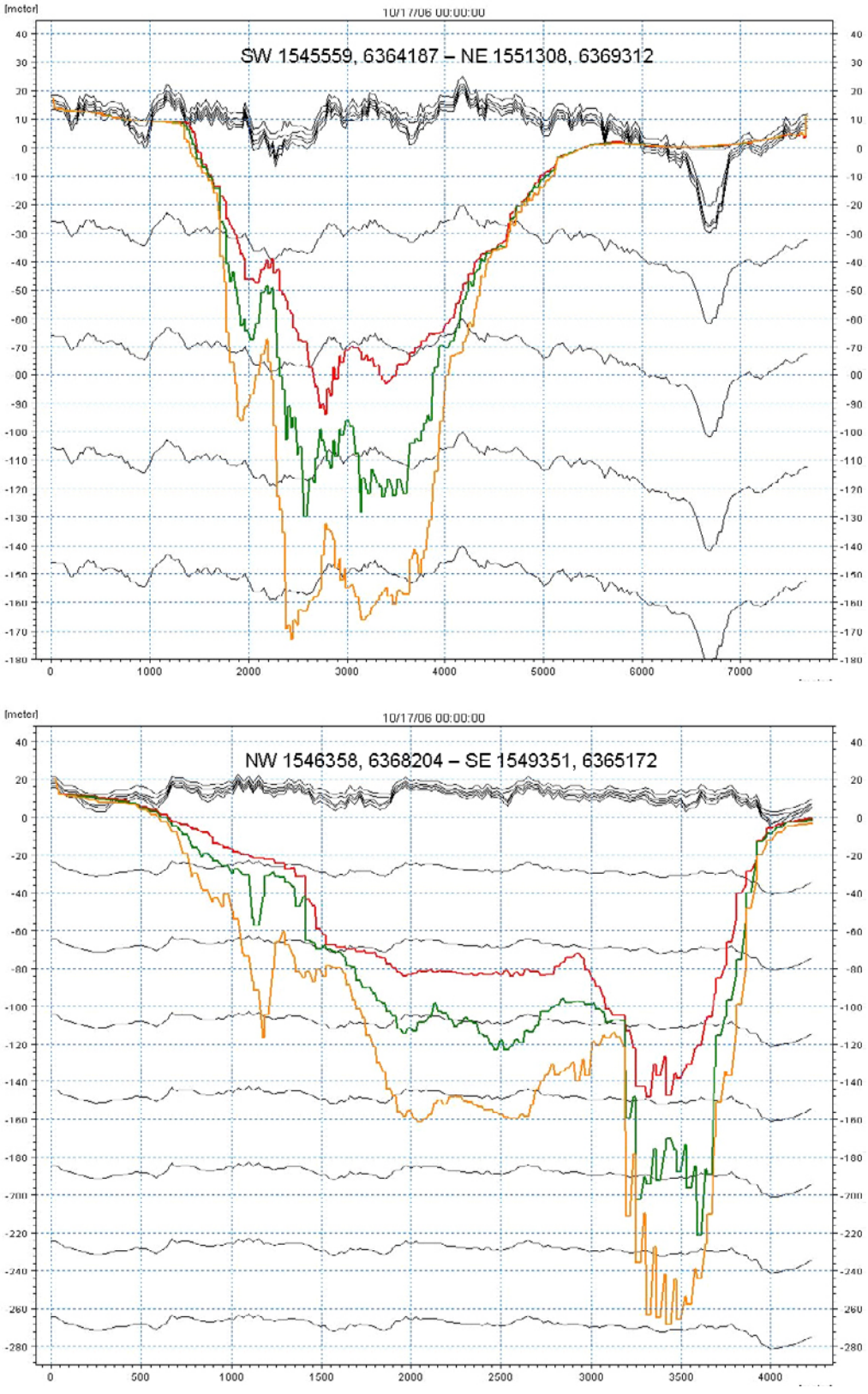

Figure 5-13. *Groundwater head elevations for different layers (coloured thick lines) in two profiles, one SW-NE profile (upper graph) and one NW-SE profile (lower graph) through the model area and the repository, based on an open repository with a grouting level of $K=1{\cdot}10^{-9}$ m/s in the deposition tunnels and $K=1{\cdot}10^{-8}$ m/s in all other tunnels and shafts;. The black lines show the lower level of each calculation layer. The head elevations are from October 17th 2006. The red line shows the head elevation in layer 8 (bedrock at 150 m.b.s.l.), the green line the head elevation in layer 10 (bedrock at 230 m.b.s.l.), and the orange line for head elevation in layer 12 (bedrock at 310 m.b.s.l.).*

Figures 5-14 and 5-15 present the horizontal and vertical hydraulic conductivities in a SW-NE profile through the area, corresponding to the upper profile in Figure 5-13. Vertical fracture zones (red areas) are present at approximately 4,000 m and 6,500 m along the x-axis in Figures 5-14 and 5-15. These zones are highly permeable both horizontally and vertically and extend down to 300 m.b.s.l. The conductivities in the fracture zones are approximately 10^{-5}–10^{-4} m/s, as compared to the surrounding bedrock (yellow areas) that has a conductivity of 10^{-8}–10^{-7} m/s.

Comparing Figures 5-14 and 5-15, it is evident that the differences between the vertical and horizontal conductivity are relatively small, i.e. the bedrock is rather isotropic. This is also illustrated in Figure 5-16, where the horizontal and vertical conductivities are shown for layer 6 at 70 m.b.s.l. The fact that the bedrock is rather permeable and also isotropic explains the magnitude of the drawdown and the "homogeneity" of the influence area seen in Figures 5-11 and 5-12.

In Figure 5-17, the vertical groundwater flow at 70 m.b.s.l. is shown for the reference simulation without a repository (upper graph) and with the open repository present (lower graph). In large parts of the areas that are discharge areas (upward flow) in the reference simulation, the direction of the flow is changed when the open repository is included.

5.4.2 Drawdown for different levels of grouting

The hydraulic conductivity of the grouted zone around the tunnels affects the drawdown of the groundwater table. Figures 5-18 to 5-20 show the arithmetic average drawdown of the groundwater table during 2006 for the three levels of grouting that have been studied: $K=1\cdot10^{-8}$ m/s in all tunnels, $K=1\cdot10^{-9}$ m/s or $K=1\cdot10^{-10}$ m/s in deposition tunnels combined with $K=1\cdot10^{-8}$ m/s in all other tunnels and shafts. The overall pattern of the influence area is the same for all three grouting levels. A grouting level of $K=1\cdot10^{-8}$ m/s obviously gives the largest influence areas and drawdowns around the repository and also the highest inflow to the tunnels (Section 5.2). For all levels of grouting, the drawdown reaches the model boundary. Due to the no-flow boundary condition it is not possible for the repository to draw any water from the boundary. The effect of changed boundary conditions is tested in Section 7.2.3.

Table 5-13 shows a summary of the influence areas and drawdowns for the different levels of grouting. A grouting level of $K=1\cdot10^{-8}$ m/s gives an influence area, with a drawdown larger than 0.3 m, that is 20% larger than that for a grouting level of $K=1\cdot10^{-10}$ m/s in the deposition tunnels and $K=1\cdot10^{-8}$ m/s in all other tunnels and shafts. The corresponding increase of the influence area for a grouting level of $K=1\cdot10^{-9}$ m/s in the deposition tunnels is 13% compared to that for a grouting level of $K=1\cdot10^{-10}$ m/s. The influence areas for the three levels of grouting are shown together in Figure 5-21. The figure shows that there are small differences in influence areas between the three grouting cases. This implies that properties other than the level of grouting determine the size of the drawdown. This is further evaluated in the sensitivity analysis in Section 7.2.

Table 5-13. Influence areas (km²) for different drawdowns for different levels of grouting of the full open repository. The areas are taken from the average drawdown during 2006.

Case	Maximum lowering of the water table, (m)	Influence area, drawdown >0.1 m	Influence area, drawdown >0.3 m	Influence area, drawdown >1.0 m	Influence area, drawdown >4.0 m	Influence area, drawdown >10.0 m
$K=1\cdot10^{-8}$ m/s in the whole repository	370	18.3	16.7	14.5	11.7	9.2
$K=1\cdot10^{-9}$ m/s in deposition tunnels	370	17.5	15.7	13.5	10.3	8.1
$K=1\cdot10^{-10}$ m/s in deposition tunnels	369	15.9	13.9	11.6	8.3	5.7

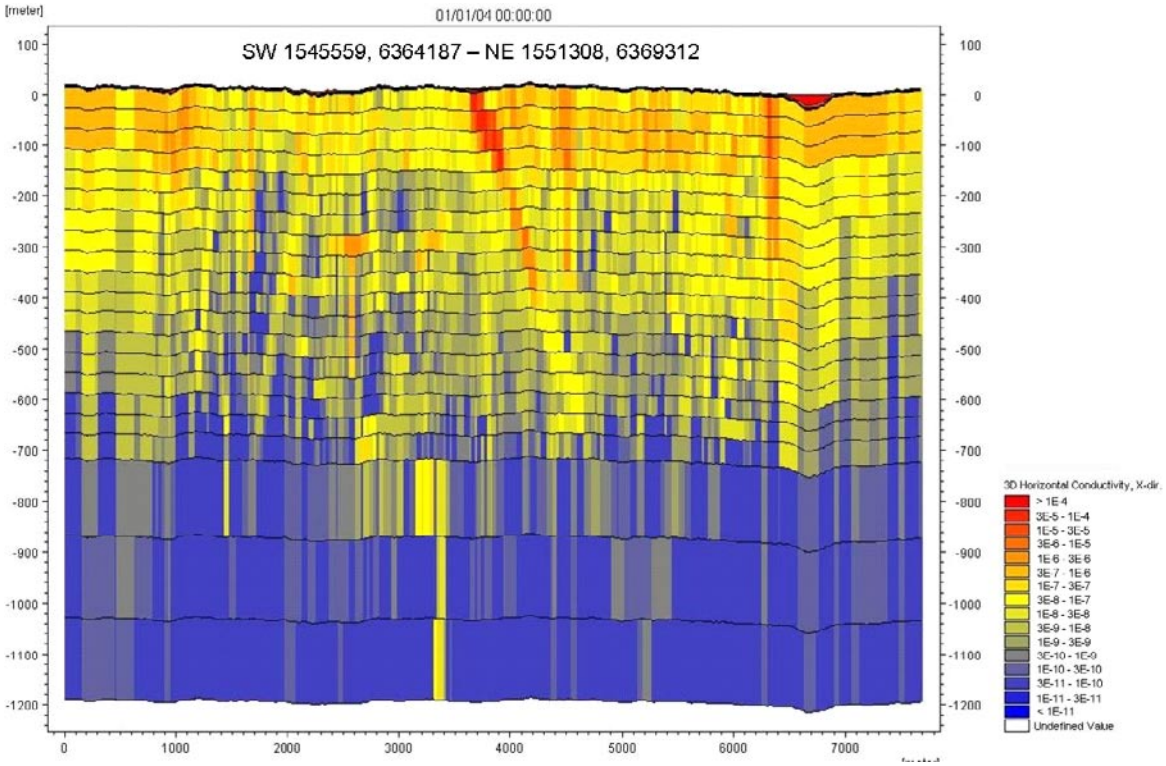

Figure 5-14. *Horizontal hydraulic conductivities (m/s) in a SW-NE section through the planned repository. Red colours represent high-permeable cells.*

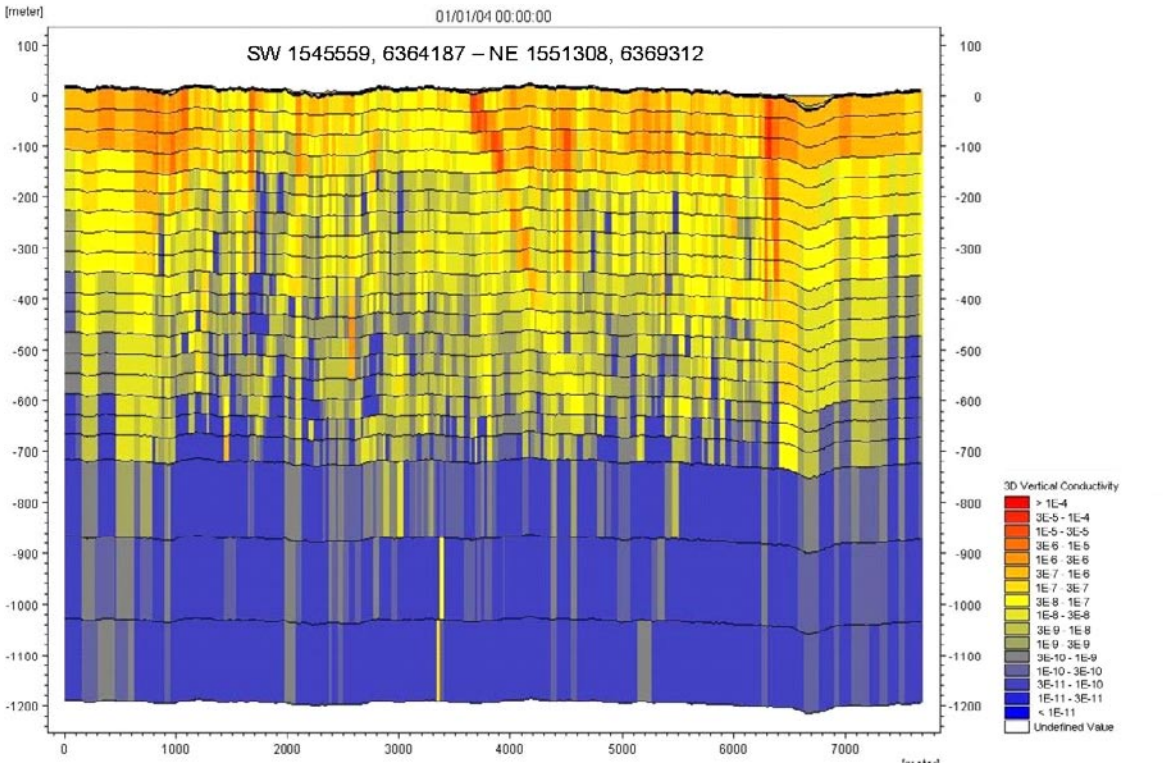

Figure 5-15. *Vertical hydraulic conductivities (m/s) in a SW-NE section through the planned repository. Red colours represent high-permeable cells.*

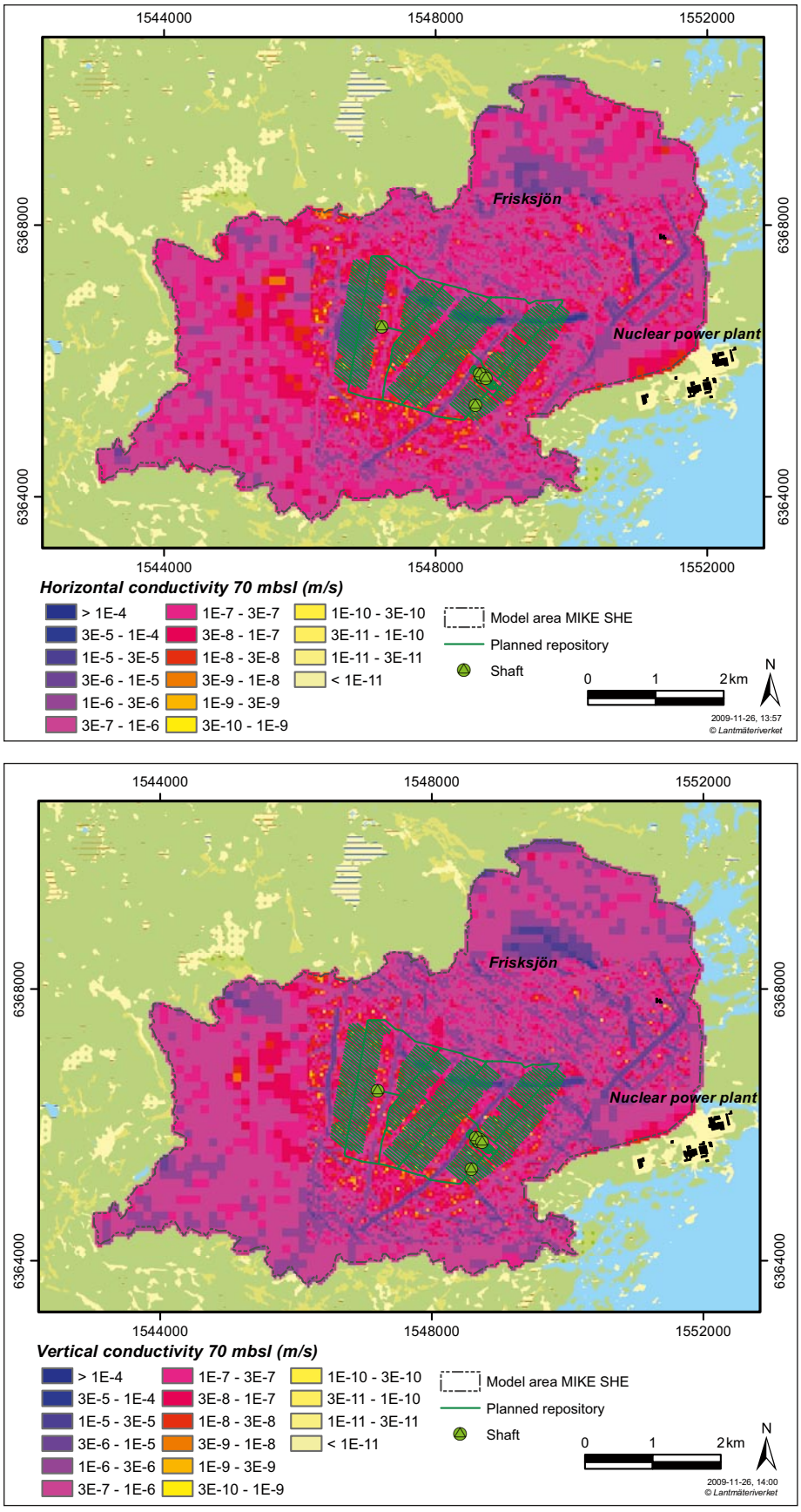

Figure 5-16. *Horizontal (upper map) and vertical (lower map) hydraulic conductivities (m/s) in the bedrock, calculation layer 6 (70 m.b.s.l.). Blue and purple colours represent high-permeable zones.*

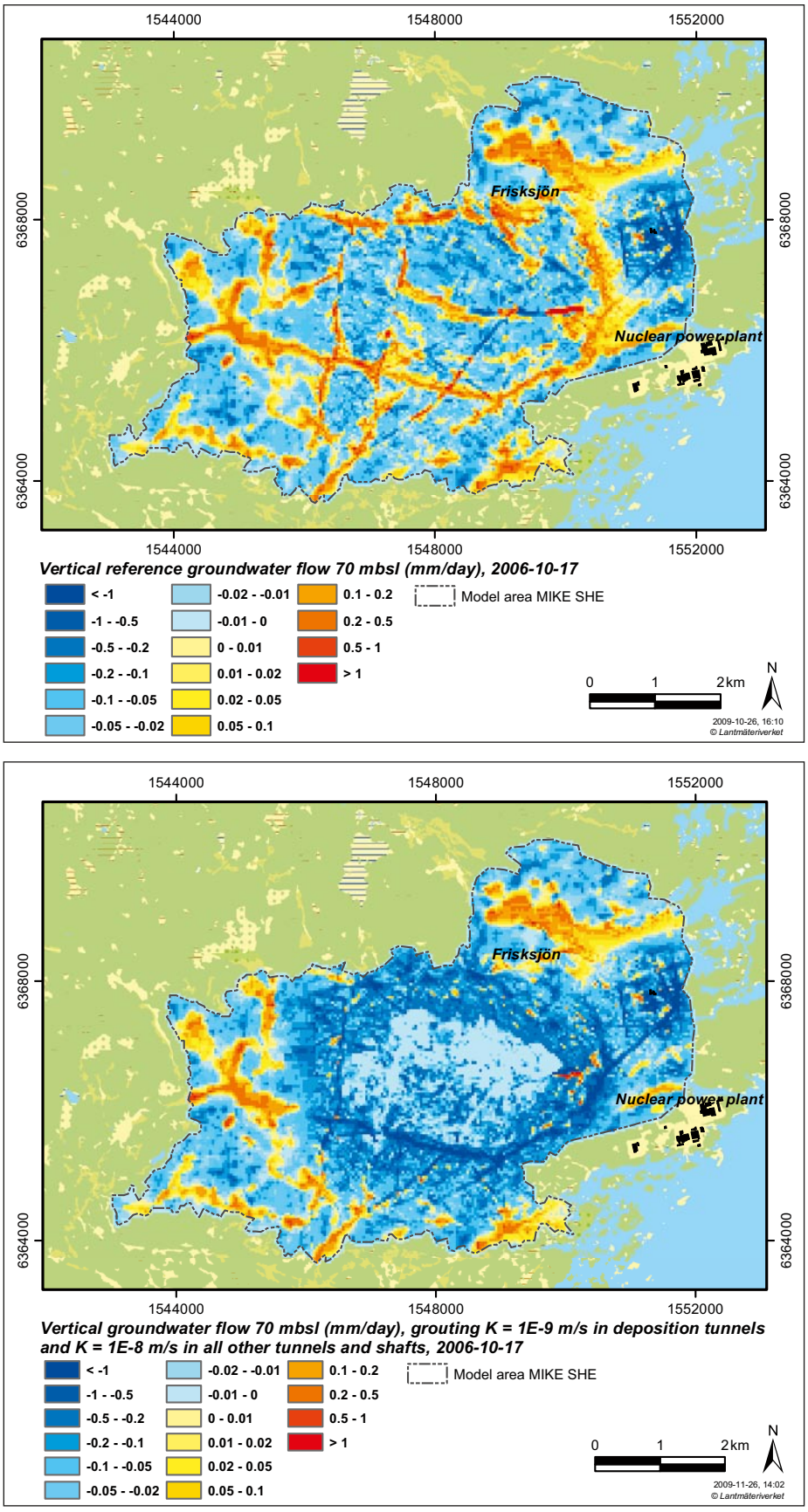

Figure 5-17. *Vertical groundwater flow (mm/day) in calculation layer 6 (70 m.b.s.l.), October 17th 2006, in the reference simulation without the repository (upper map) and with an open repository (lower map) with a grouting level of $K=1\cdot10^{-9}$ m/s in the deposition tunnels and $K=1\cdot10^{-8}$ m/s in all other tunnels and shafts. Blue colours denote downward flow and yellow/red colours upward flow.*

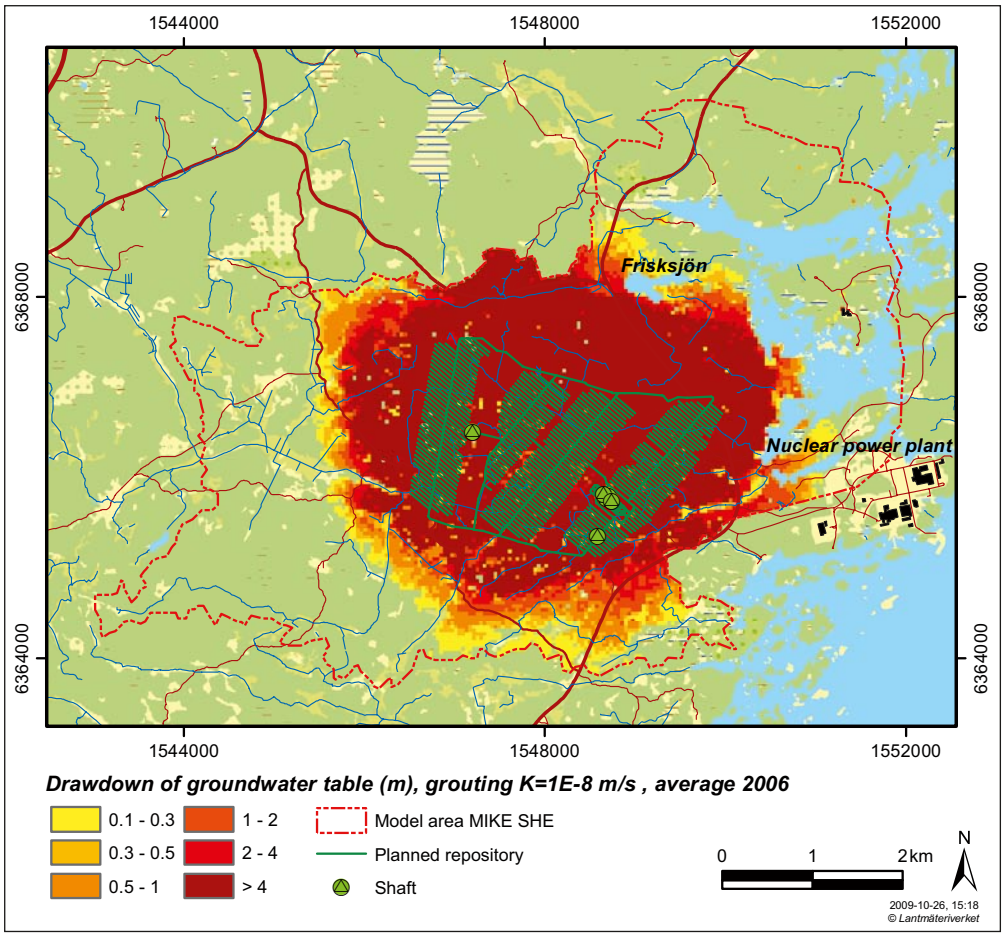

Figure 5-18. *Drawdown of the groundwater table as an average for 2006, with a grouting level of* $K=1\cdot10^{-8}$ *m/s.*

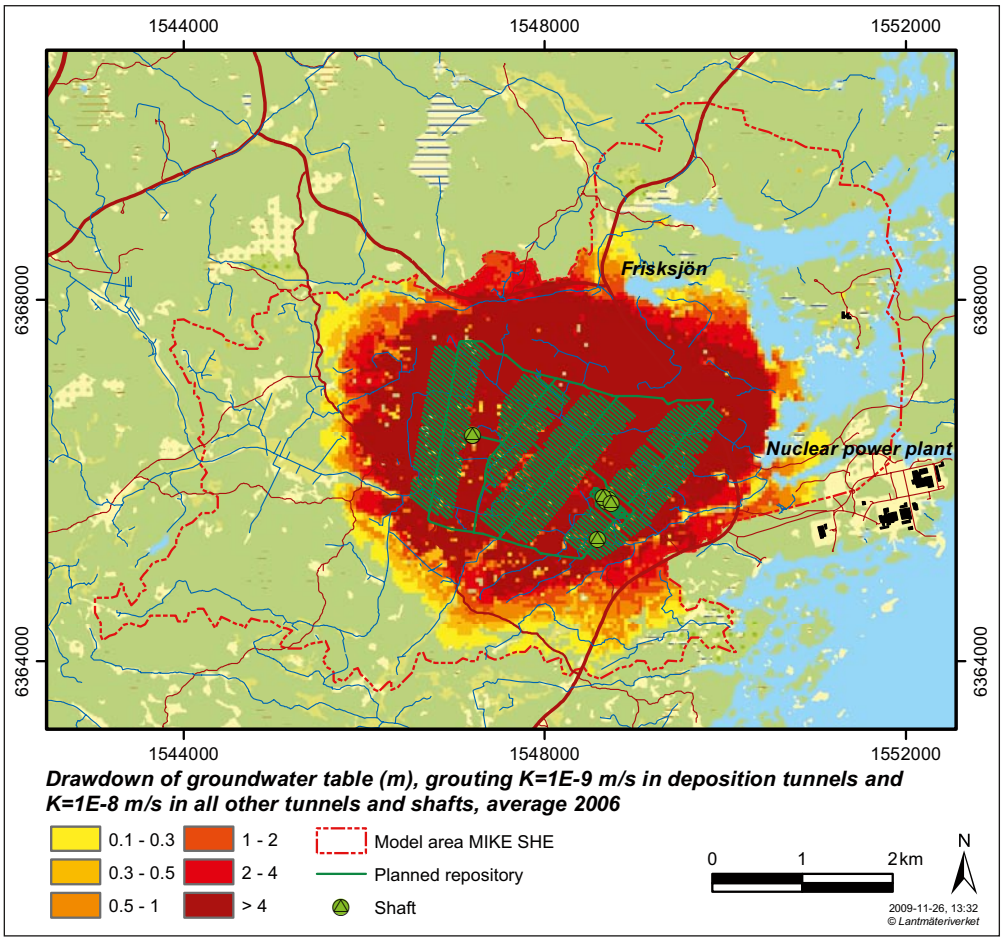

Figure 5-19. *Drawdown of the groundwater table as an average for 2006, with a grouting level of $K=1\cdot10^{-9}$ m/s in deposition tunnels and $K=1\cdot10^{-8}$ m/s elsewhere.*

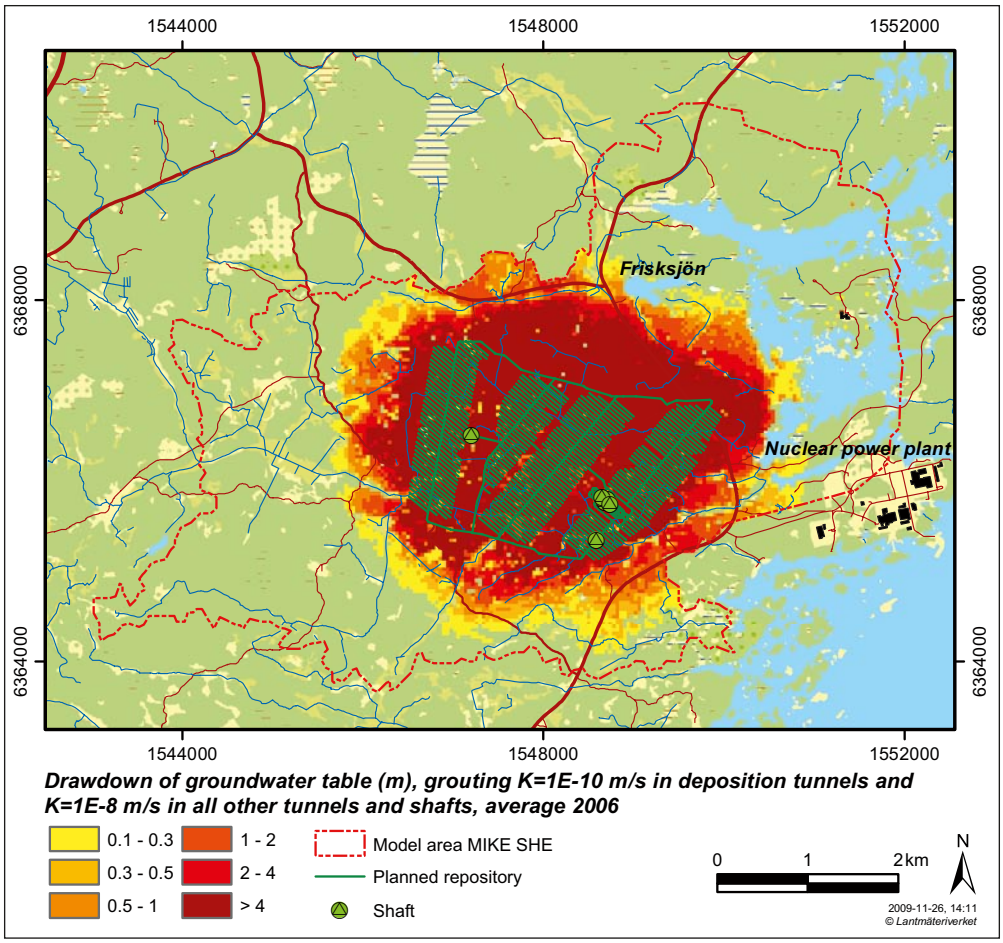

Figure 5-20. *Drawdown of the groundwater table as an average for 2006, with a grouting level of $K=1\cdot10^{-10}$ m/s in deposition tunnels and $K=1\cdot10^{-8}$ m/s in all other tunnels and shafts.*

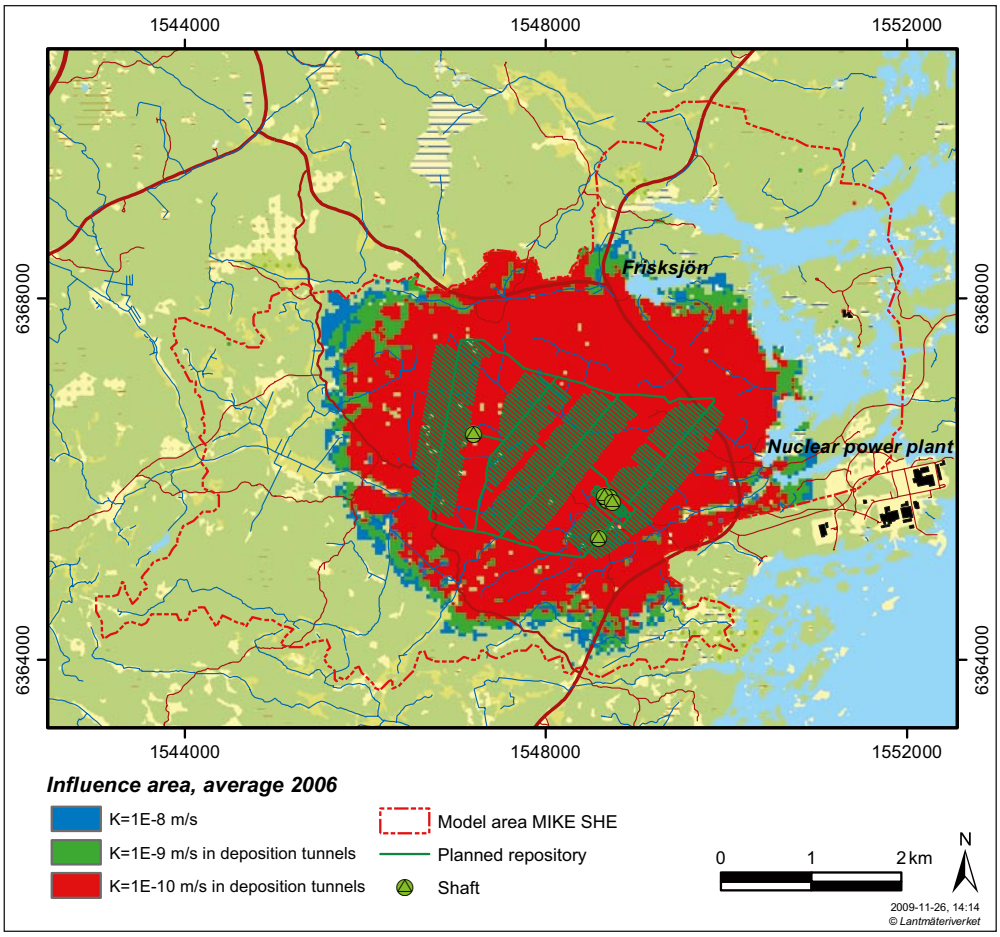

Figure 5-21. *Influence areas for an average groundwater table drawdown larger than 0.3 m during 2006 for the three grouting levels with $K=1\cdot10^{-8}$ m/s (blue, red and green areas), $1\cdot10^{-9}$ m/s (red and green areas) and $1\cdot10^{-10}$ m/s (red areas only) in the deposition tunnels and $K=1\cdot10^{-8}$ m/s in all other tunnels and shafts in all cases.*

5.4.3 Groundwater table drawdown for different development phases

The whole open repository will not be constructed and taken in operation at once; the operation phase is divided into five development phases (phases 1–5). In all development phases, the transport tunnels will be opened gradually together with the different sections of deposition tunnels. The deposition tunnels will, however, only be open a few sections at a time (see Section 3.3 for details).

The drawdown of the groundwater table varies with the different phases of the repository development. Figure 5-22 shows the average drawdown of the groundwater table during 2006 for the initial construction phase ("phase 0") and Figure 5-23 for the second development phase (phase 2), in both cases with a grouting level of $K=1\cdot10^{-9}$ m/s in deposition tunnels and $K=1\cdot10^{-8}$ m/s in all other tunnels and shafts. As can be seen in these figures, the influence area is concentrated to areas in the vicinity of the parts of the repository that are open during each specific phase.

Table 5-14 shows a summary of the influence areas and the maximum groundwater table drawdowns for the initial construction phase and development phase 2 compared to those of the full repository construction. For obvious reasons, the largest impact is obtained if the whole repository is open at the same time, which is a hypothetical case that will not occur in reality. Development phase 2 gives an influence area for a drawdown larger than 0.3 m that is approximately 42% of that obtained for the full construction. The corresponding result for the construction phase is 20%.

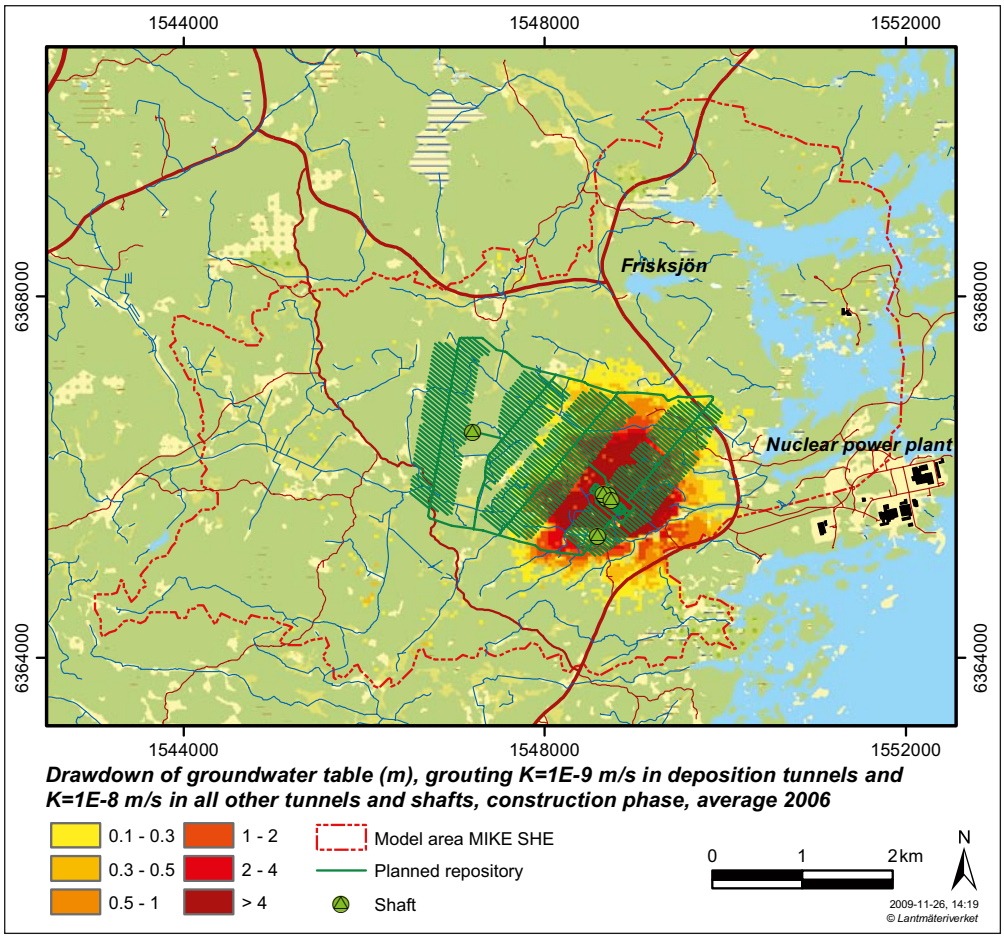

Figure 5-22. *Drawdown of the groundwater table during the initial construction phase, average for 2006, with a grouting level of K=1·10^{-9} m/s in deposition tunnels and K=1·10^{-8} m/s in all other tunnels and shafts.*

Table 5-14. Influence areas (km²) with different drawdowns of the groundwater table for different development phases and for a grouting level of K=1·10^{-9} m/s in the deposition tunnels and K=1·10^{-8} m/s in all other tunnels and shafts. The areas are calculated from the average drawdowns during 2006.

Case	Maximum lowering of the water table, (m)	Influence area, drawdown >0.1 m	Influence area, drawdown >0.3 m	Influence area, drawdown >1.0 m	Influence area, drawdown >4.0 m	Influence area, drawdown >10.0 m
Initial construction phase	369	4.5	3.1	1.7	0.9	0.6
Development phase 2	369	8.8	6.6	4.2	2.2	1.4
Full construction (hypothetical case)	370	17.5	15.7	13.5	10.3	8.1

5.4.4 Changes in the degree of saturation

The degree of saturation in the upper QD layers is an important measure from an ecological point of view. For typical Swedish soil conditions, the upper 2 m of the soil can be divided into three general classes depending on the depth to the groundwater table; <0.05 m, between 0.05 and 1 m and between 1 and 2 m (Ulrika Hamrén, Ekologigruppen AB, personal communication). These classes can be used as a general tool to define the degree of saturation. In Table 5-15, areas for the different saturation classes are presented for undisturbed and disturbed conditions with a grouting level of K=1·10^{-9} m/s in deposition tunnels and K=1·10^{-8} m/s in all other tunnels and shafts, as average values for the entire year of 2006 and for the vegetation period. The vegetation period is here defined as the period from the first of April to the end of October.

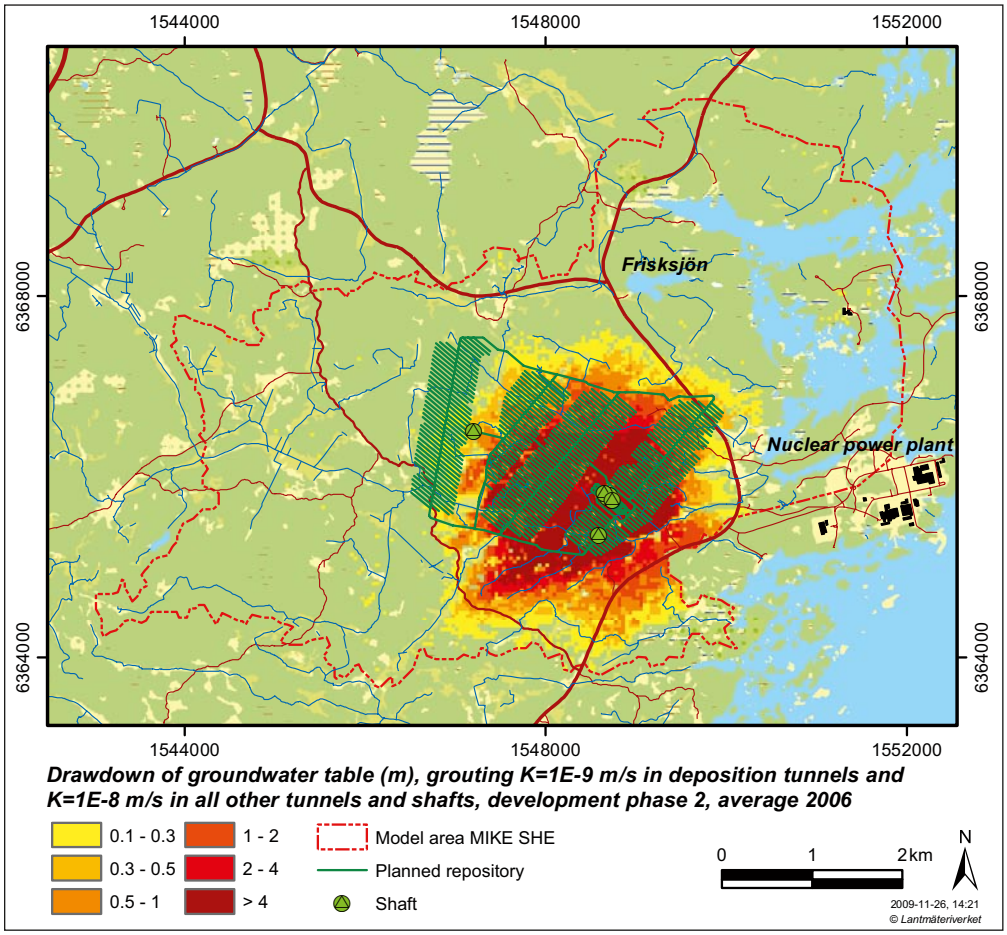

Figure 5-23. *Drawdown of the groundwater table during development phase 2, average for 2006, with a grouting level of K=1·10^{-9} m/s in deposition tunnels and K=1·10^{-8} m/s in all other tunnels and shafts.*

Table 5-15. Areas (km²) for different degrees of saturation (i.e. depths to the groundwater table). Areas are presented for undisturbed and disturbed conditions, with a grouting level of K=1·10^{-9} m/s in deposition tunnels and K=1·10^{-8} m/s in all other tunnels and shafts. Results are given as average values for the whole year of 2006 and for the vegetation period, April–October 2006.

Depth to groundwater table (m)	Undisturbed conditions, year of 2006	With open repository, year of 2006	Undisturbed conditions, Apr–Oct 2006	With open repository, Apr–Oct 2006
<0.05	0.53	0.47	0.59	0.52
0.05–1	1.49	1.21	1.38	1.16
1–2	5.85	3.75	6.50	4.28
Sum	**7.87**	**5.43**	**8.47**	**5.96**

The largest relative and absolute change between undisturbed and disturbed conditions is found in areas with a groundwater table depth of 1–2 m. The extent of these areas decrease with 36% and 34% for the whole year of 2006 and the vegetation period, respectively.

Areas with a groundwater table depth less than 2 m below the ground surface are here defined as wet and areas with deeper groundwater table are defined as dry. The drawdown causes approximately one third of the wet areas in the reference simulation to turn dry when the open repository is introduced. In Figure 5-24 wet and dry areas for 2006 are shown together. It should be pointed out that for undisturbed conditions during 2006 the wet areas constitute only approximately 25% of the land area. For disturbed conditions, with a grouting level of K=1·10^{-9} m/s in deposition tunnels and K=1·10^{-8} m/s elsewhere, these areas decrease and constitute c 17% of the land area.

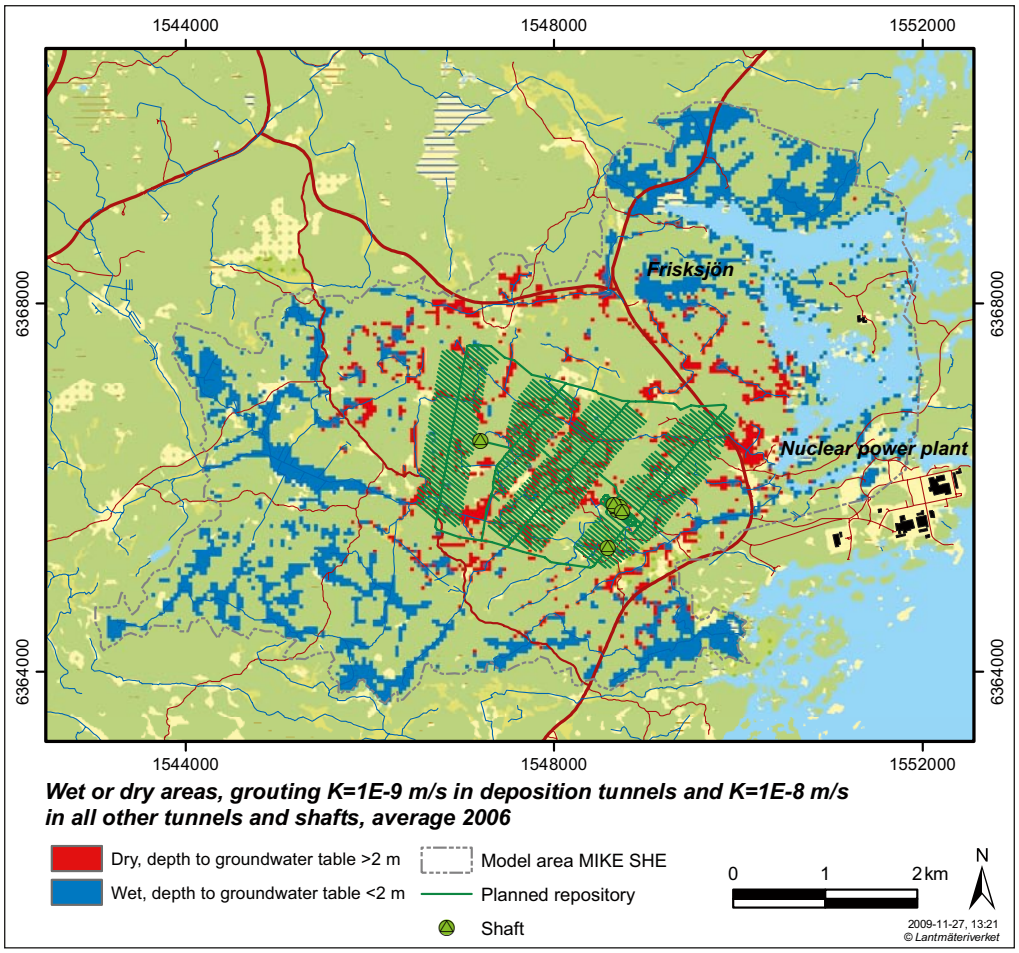

Figure 5-24. *Wet areas (blue colour) with a depth to groundwater table <2 m and dry areas (red colour) with a depth to groundwater table >2 m as an average for 2006, with K=1·10^{-9} m/s in deposition tunnels and K=1·10^{-8} m/s in all other tunnels and shafts. Red and blue areas are both wet for undisturbed conditions.*

Figure 5-25 shows the areas within the influence area (here defined as the area where the groundwater table drawdown exceeds 0.3 m for a grouting level of K=1·10^{-8} m/s) where the groundwater table is located in the QD layers (red and blue areas) for undisturbed conditions. Also, areas where the drawdown lowers the groundwater table from the QD to the bedrock (red areas) when the open repository is included, with a grouting level of K=1·10^{-9} m/s in deposition tunnels and K=1·10^{-8} m/s elsewhere, are shown in Figure 5-25.

5.4.5 Temporal variation of groundwater table drawdown

In Table 5-16, the influence areas for different drawdown limits for the groundwater table are presented as average values for each month during 2006. The results are based on a grouting level of K=1·10^{-9} m/s in deposition tunnels and K=1·10^{-8} m/s in all other tunnels and shafts. The results show that the size of the influence area is affected by the hydrometeorological conditions during the year.

In Figures 5-26 and 5-27, the drawdown of the groundwater table for two types of conditions are presented; a relatively wet period with high groundwater table represented by April 2006, shown in Figure 5-26, and a dry period with low groundwater table represented by October 2006, shown in Figure 5-27. These two months appear as extremes in Table 5-16, due to the large difference in groundwater head elevation.

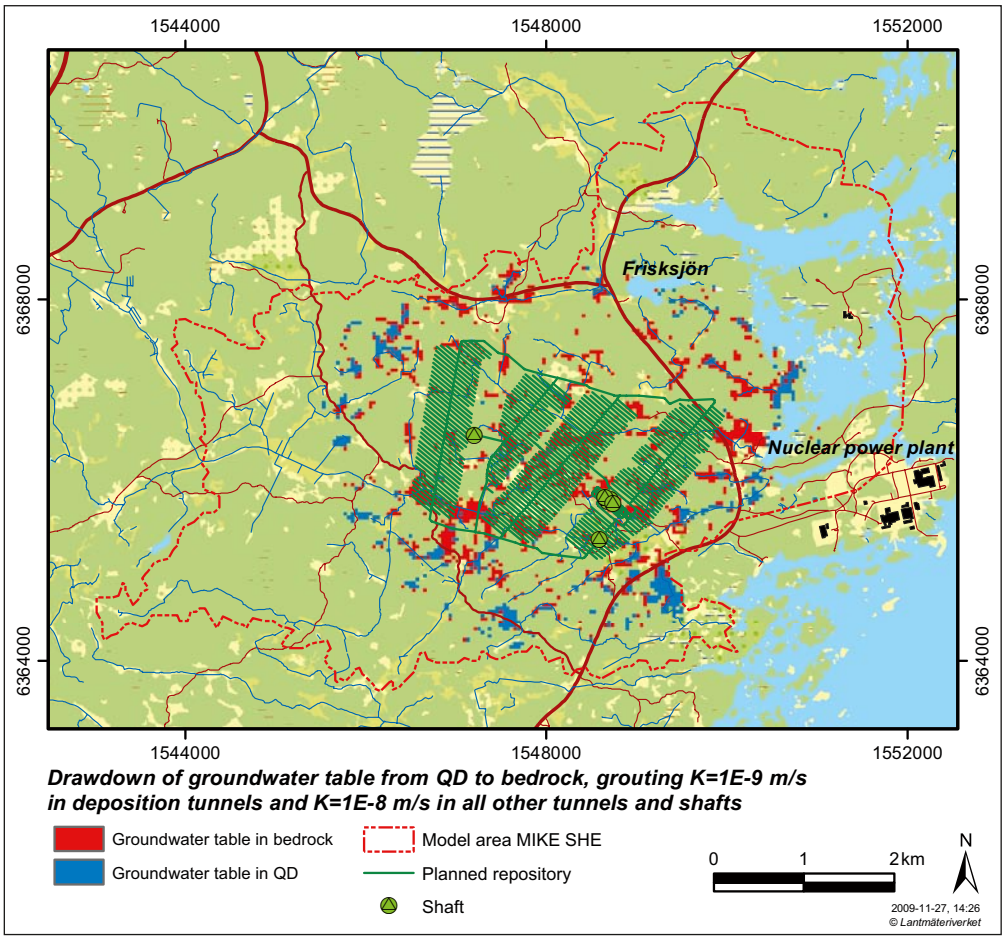

Figure 5-25. Location of the groundwater table within the influence area (drawdown >0.3 m with a grouting level of $K=1{\cdot}10^{-8}$ m/s) in Quaternary deposits (blue areas) and bedrock (red areas), with $K=1{\cdot}10^{-9}$ m/s in deposition tunnels and $K=1{\cdot}10^{-8}$ m/s elsewhere. For undisturbed conditions the groundwater table is located in Quaternary deposits in both red and blue areas.

Table 5-16. Average influence areas (km²) each month during 2006, with a grouting level of $K=1{\cdot}10^{-9}$ m/s in deposition tunnels and $K=1{\cdot}10^{-8}$ m/s in all other tunnels and shafts.

Month 2006	Maximum lowering of the water table, (m)	Influence area, drawdown >0.1 m	Influence area, drawdown >0.3 m	Influence area, drawdown >1.0 m	Influence area, drawdown >4.0 m	Influence area, drawdown >10.0 m
January	538	18.0	15.9	13.5	10.4	8.4
February	536	17.9	15.5	13.1	9.6	7.2
March	462	16.6	14.9	12.8	9.6	7.6
April	215	10.8	9.0	7.3	4.9	3.7
May	214	15.6	13.6	11.3	7.5	5.8
June	210	16.4	14.6	12.3	8.5	6.8
July	232	16.8	15.1	12.9	9.3	7.5
August	538	17.2	15.5	13.3	10.0	8.1
September	538	17.5	16.0	13.8	10.6	8.5
October	538	18.0	16.3	14.2	11.2	8.9
November	536	18.0	16.2	13.9	10.9	8.4
December	536	13.7	12.0	10.1	7.6	5.9
Average 2006	**370**	**17.5**	**15.7**	**13.5**	**10.3**	**8.1**

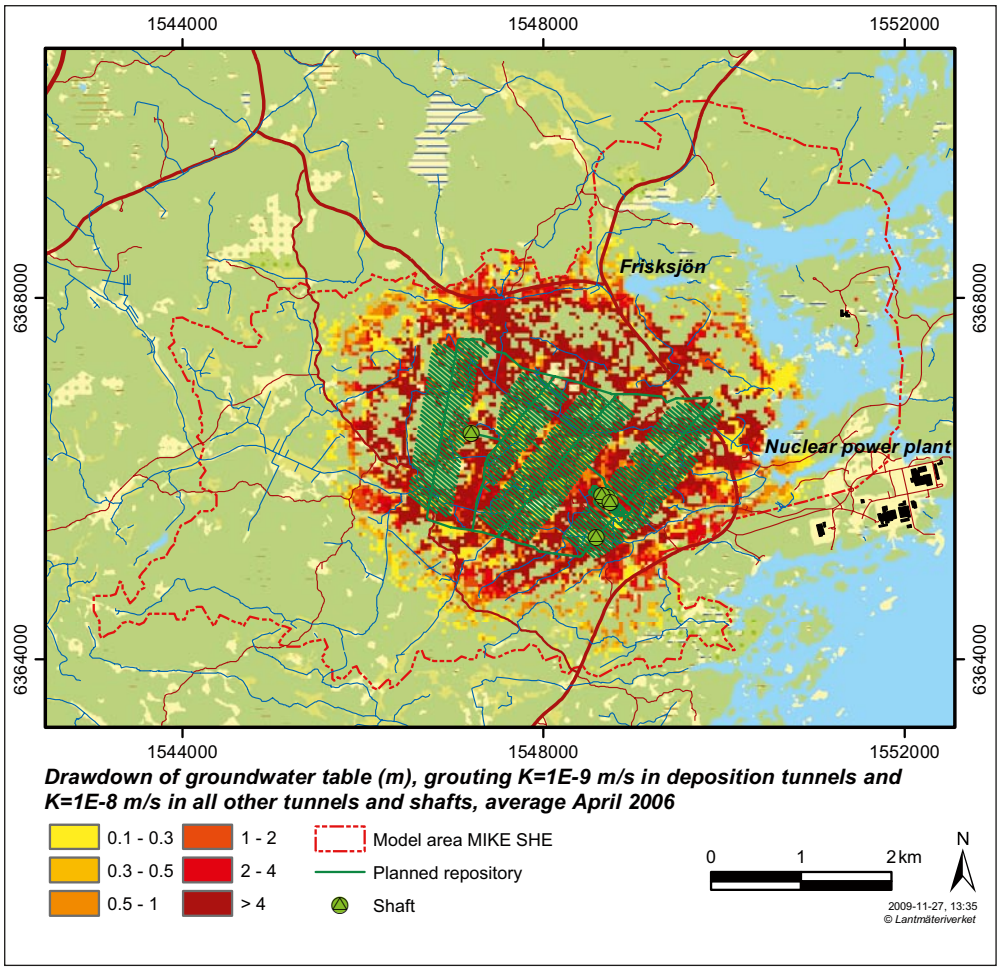

Figure 5-26. *Drawdown of the groundwater table under wet conditions (April 2006), with a grouting level of $K=1{\cdot}10^{-9}$ m/s in deposition tunnels and $K=1{\cdot}10^{-8}$ m/s in all other tunnels and shafts.*

The gradient between the groundwater table and the groundwater head deeper in the bedrock, which governs the downward flow and thereby the drawdown, is constantly high. This means that even if the groundwater table is recharged the gradient will not be affected and the downward flow will remain the same. As a consequence, the temporal variation of the groundwater table drawdown is small during the whole year. The influence area is, however, smaller during wet periods as in April and December. This is explained by the fact that during wet periods, with lots of precipitation or snowmelt, the groundwater table is recharged to an extent that exceeds the increase of the downward flow.

The maximum drawdown of the groundwater table exceeds 500 m in all but five months during 2006. However, this large drawdown only occurs in a limited area, approximately 3,000 m^2. Within the influence area, with a drawdown larger than 0.3 m, the average drawdown is 25 m in October, when the maximum drawdown is at its highest, and 20 m in June when the maximum drawdown is at its lowest.

The maximum influence area in Table 5-16 is found in October and the minimum influence area in April. The influence areas for these two months, with groundwater table drawdown larger than 0.3 m, are presented in Figure 5-26 (April) and Figure 5-27 (October) and also together in Figure 5-28. The influence area in October covers an area approximately 80% larger than the corresponding area in April. The minimum influence area is scattered while the area in October has a more homogenous pattern.

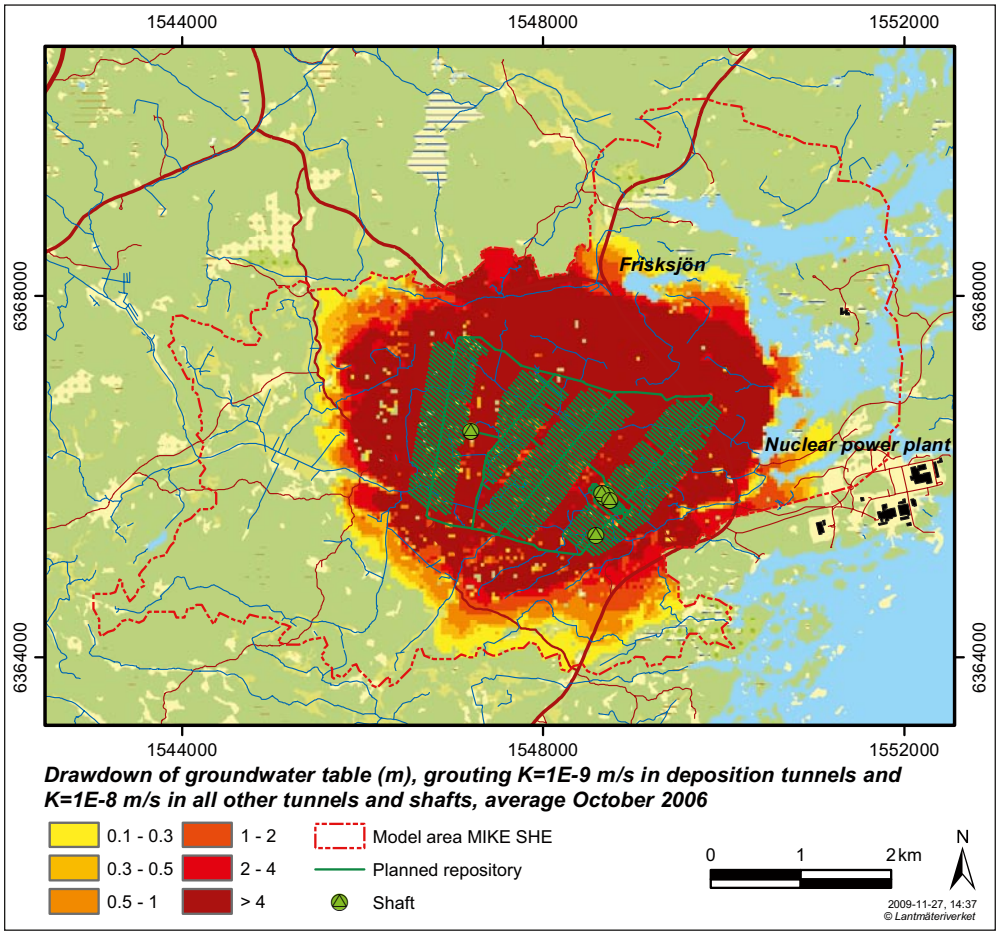

Figure 5-27. *Drawdown of the groundwater table under dry conditions (October 2006) with a grouting level of K=1·10^{-9} m/s in deposition tunnels and K=1·10^{-8} m/s in all other tunnels and shafts.*

5.4.6 Effects of extended simulation periods on influence areas

The results presented in the previous sections are all based on a simulation period of three years, 2004–2006, where the years of 2004 and 2005 have been used as an initialisation period. However, in reality the repository would be open for many decades, and the drawdown would have time to adjust to the influence of the repository and reach new equilibrium conditions. Clearly, the establishment of equilibrium conditions is also affected by other transients in the system, but in the present analysis the effects of seasonal variations and differences induced by the successive development of the repository are disregarded.

In practice, it would take too long time to simulate the whole open repository period using the present model. In order to save simulation time, as mentioned above a rather short simulation period has been applied, only three years, where the first two years are considered an initialisation period. However, the drawback of this approach is a risk that the influence areas and the drawdowns are underestimated.

In order to investigate this, simulations have been performed for a 9-year period with the whole repository open and for a grouting level of K= 1·10^{-9} m/s in the deposition tunnels and K= 1·10^{-8} m/s in all other tunnels and shafts. The input data for this simulation is a periodic cycling of the input data for 2004, 2005 and 2006, i.e. this three-year sequence is repeated three times. All results presented are derived based on input data from the year 2006, i.e. the third year in each three-year cycle, to make them comparable to the results presented in earlier sections. The results are summarised in Table 5-17.

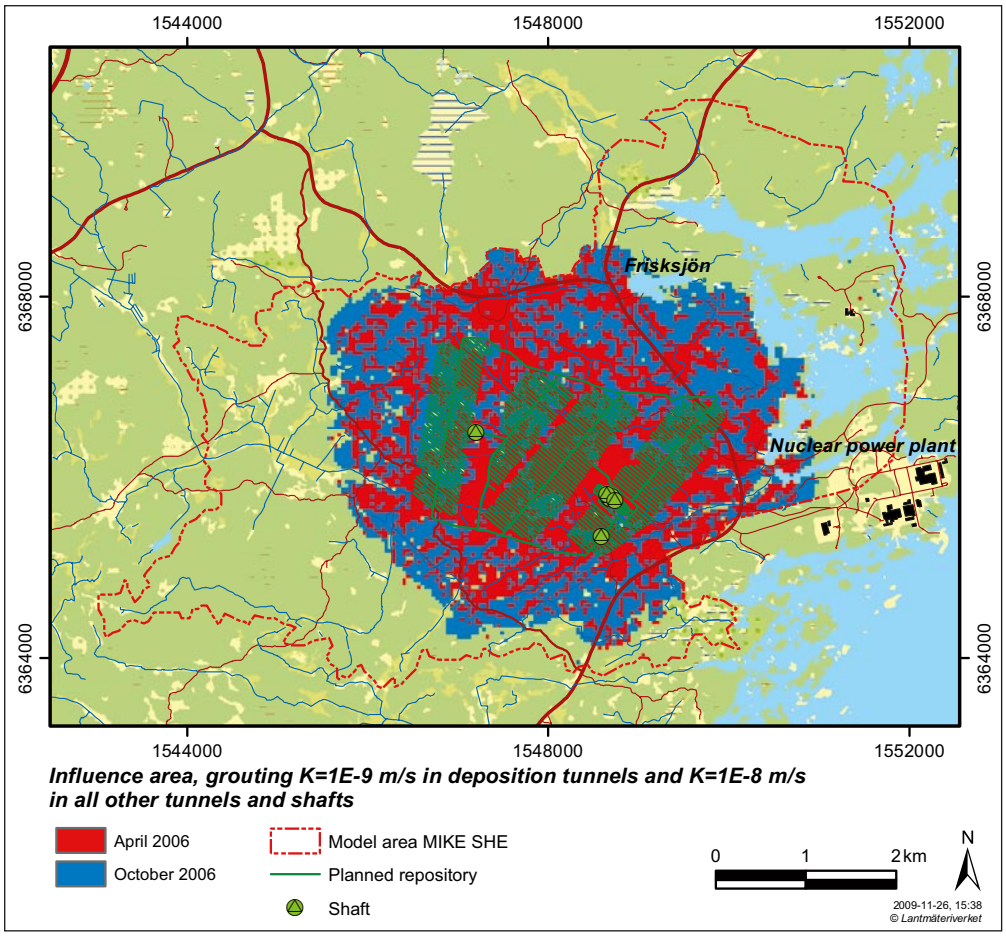

Figure 5-28. *Influence areas (with groundwater table drawdown larger than 0.3 m) in October (red and blue areas) and April (red areas only), representing the maximum and minimum during 2006, with a grouting level of $K=1{\cdot}10^{-9}$ m/s in deposition tunnels and $K=1{\cdot}10^{-8}$ m/s in all other tunnels and shafts.*

Table 5-17. Influence area (km²) after different lengths of simulation periods with a grouting level of K= $1{\cdot}10^{-9}$ m/s in deposition tunnels and K= $1{\cdot}10^{-8}$ m/s in all other tunnels and shafts. The results are taken from the mean drawdown for the third year in each three-year cycle (corresponding to 2006 in the first cycle).

	Influence area, drawdown >0.1 m	Influence area, drawdown >0.3 m	Influence area, drawdown >1.0 m	Influence area, drawdown >4.0 m	Influence area, drawdown >10.0 m
Average for the third year, first cycle	17.5	15.7	13.5	10.3	8.1
Average for the third year, second cycle	18.7	17.0	14.6	11.8	9.3
Average for the third year, third cycle	18.9	17.3	14.9	12.1	9.8

The results in the first row in Table 5-17, referred to as the “first cycle”, correspond to the results presented in the previous sections. The second row in the table shows the result after another three-year cycle. The influence area for the third year of the second cycle is somewhat larger; approximately 8% larger for a drawdown >0.3 m. After the second cycle, the drawdown of the groundwater table is more or less in equilibrium with the inflow, as indicated by the small difference in drawdown between the second and third cycles. The influence area after the third cycle is approximately 9% larger than after the first cycle. In Figure 5-29 the influence area based on the first cycle is compared with that from the third cycle. The two results show the same overall pattern, only the size differs, meaning that no new drawdown areas are developed during the third cycle compared to the first.

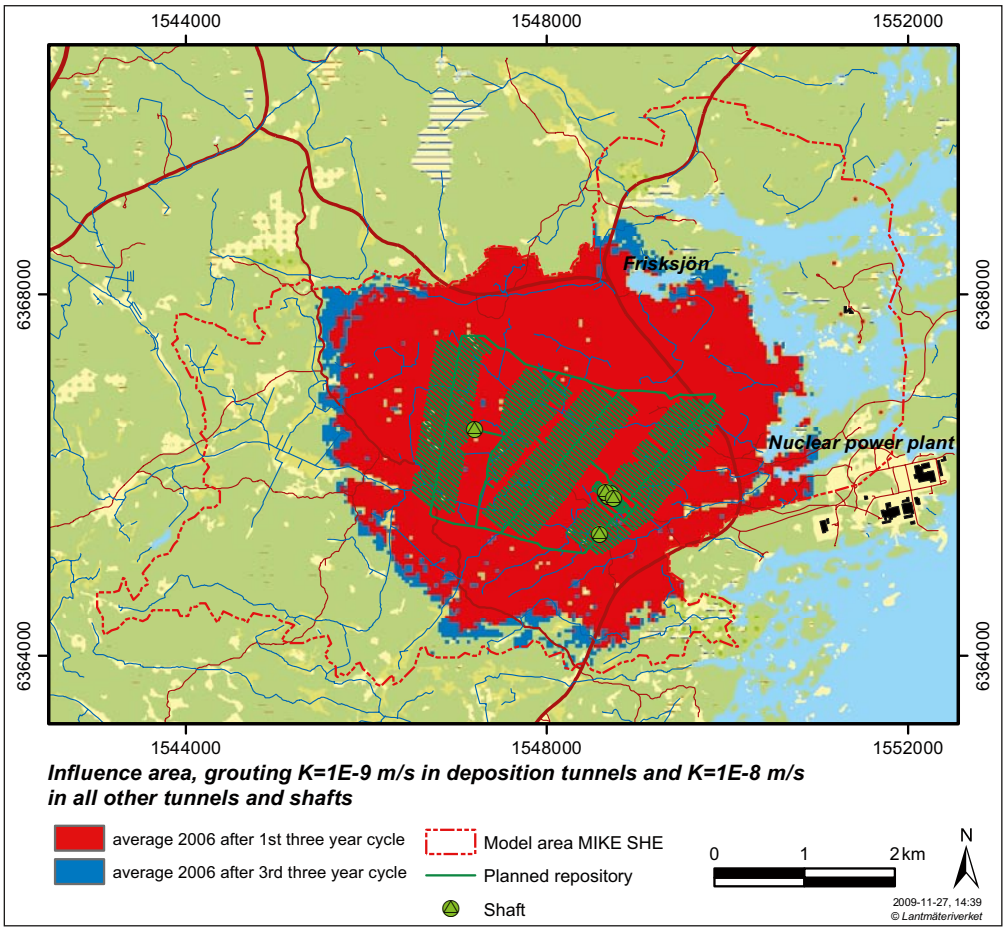

Figure 5-29. *Influence areas (with average groundwater table drawdown larger than 0.3 m during 2006) for the third year of the first three-year cycle (red area) and the third year of the third cycle (red and blue areas), with a grouting level of $K=1{\cdot}10^{-9}$ m/s in deposition tunnels and $K=1{\cdot}10^{-8}$ m/s in all other tunnels and shafts.*

The temporal variations caused by the short term meteorological variations during a year are however much larger than the effect from the development of the drawdown over several years. This is clearly seen in Table 5-18, where the minimum, maximum and average influence areas for different drawdown limits are presented. The maximum influence area is almost twice as large as the minimum influence area, irrespective of which drawdown limit that is studied.

Table 5-18. Minimum, maximum and average influence areas (km²) during the third year of the first cycle (2006), with a grouting level of K= $1{\cdot}10^{-9}$ m/s in deposition tunnels and K= $1{\cdot}10^{-8}$ m/s in all other tunnels and shafts.

	Influence area, drawdown >0.3 m	Influence area, drawdown >1.0 m	Influence area, drawdown >4.0 m	Influence area, drawdown >10.0 m
Average 2006 (1st cycle)	15.7	13.5	10.3	8.1
Maximum 2006 (1st cycle)	16.3	14.2	11.2	8.9
Minimum 2006 (1st cycle)	9.0	7.3	4.9	3.7

5.4.7 Recovery of the groundwater table after repository closure

When the operational phase of the open repository is finished, the pumping from the repository will cease and the repository will be closed. In order to evaluate how fast the groundwater table will recover, i.e. return to its normal undisturbed level, a simulation was done without tunnels and shafts, but initialised from the conditions with an open repository. This means that the open repository simply is replaced with the original bedrock, and that the initial conditions are given by the open repository simulation.

The initial conditions were taken from simulations with a grouting level of $K=1\cdot10^{-9}$ m/s in the deposition tunnels and $K=1\cdot10^{-8}$ m/s in all other tunnels and shafts, after the third three-year cycle according to Section 5.4.6. The simulation was done for a nine-year period (using data from 2004–2006), and the results were compared with a parallel reference simulation of undisturbed conditions, for calculating the drawdown of the groundwater table (see also Section 3.3, where all simulation cases are described).

In Table 5-19, the influence areas for a drawdown larger than 0.3 m are presented as average values for every sixth month after repository closure. The results show that the size of the influence area decreases slowly during the first two years. After two and a half years, the influence area is approximately half of the size compared to the same month of the last year in the nine-year simulation with an open repository (columns 1 and 2 in the table). Six years after repository closure, the influence area is reduced to less than 1% of the influence area with an open repository.

Observe that the results above show how fast the drawdown of the groundwater table will recover, i.e. how long it will take for the groundwater table to return to its normal undisturbed elevation. The results do not show how long time it takes to recover the groundwater head in the bedrock at the repository depth, neither how long it will take until the head inside the tunnels is the same as in the surrounding bedrock. The recovery of heads in the repository takes longer time than the time required for recovery of the groundwater table. Detailed modelling of the groundwater head recovery is performed by SKB using the DarcyTools code. The results will be presented as a part of the SR-Site safety assessment.

Table 5-19. Influence areas (km²) for every sixth months after closure of the repository, starting from conditions with a grouting level of $K= 1\cdot10^{-9}$ m/s in deposition tunnels and $K= 1\cdot10^{-8}$ m/s in all other tunnels and shafts (right side), compared to the influence area for an open repository (same grouting level), for corresponding months in the last year of the nine-year simulation (left columns).

Simulation with an open repository		Simulation of recovery after closure		
Months from last year in nine-year simulation	Influence area, drawdown >0.3 m	Months after closure, January 2004	Influence area, drawdown >0.3 m	
July	16.5	6	16.1	(98%)
January	18.0	12	10.2	(57%)
July	16.5	18	11.2	(68%)
January	18.0	24	11.7	(65%)
July	16.5	30	7.31	(44%)
January	18.0	36	3.49	(19%)
July	16.5	42	1.27	(8%)
January	18.0	48	0.43	(2%)
July	16.5	54	0.23	(1%)
January	18.0	60	0.31	(2%)
July	16.5	66	0.14	(1%)
January	18.0	72	0.11	(<1%)

6 Sensitivity to meteorological conditions

The simulations presented in the previous chapters use precipitation data for the time period 2004–2006. To investigate the influence of the precipitation on the effects of the open repository, three different meteorological scenarios were simulated, representing normal, dry and wet conditions. In the following sections, the input data and the meteorological influence on the groundwater table drawdown, the inflow to the open repository and the surface water levels and discharges are presented for the different simulation cases studied.

6.1 Precipitation input and simulation cases

Average monthly sums of the precipitation were calculated from data for the reference normal period 1961–1990. In the observation data from the SKB meteorological stations at Plittorp and Äspö a time period with matching annual average precipitation, compared to the long term annual average precipitation for the reference normal period, was chosen. The chosen period, August 2004–July 2005, only differ 1 mm/year at Äspö and 10 mm/year at Plittorp compared to the reference normal period (Tables 6-1 and 6-2). August 2004–July 2005 was therefore considered to represent a year with "normal" precipitation.

The precipitation in 2006, the year from which previous results in this report have been evaluated for, is almost identical to the long term annual average precipitation for the reference normal period; see Table 6-1 and 6-2.

Through statistical analysis of precipitation data, sums on a monthly and yearly basis for different return periods (5, 10, 20, 50 and 100 years) were calculated /Johansson 2008, Appendix 1/. A "wet" and a "dry" year, i.e. a year with either high or low precipitation, were defined as a year with an annual precipitation corresponding to a return period of 100 years. Thus, based on the normal year, August 2004–July 2005, two time series with an annual precipitation corresponding to a return period of 100 years for either wet or dry conditions were created. This was done by simply replacing the monthly sums with the highest precipitation, in the normal year, with monthly sums with a return period of 10–50 years for either high or low precipitation volumes. In this way, two time series with the most extreme meteorological conditions were obtained.

Table 6-1. Monthly sums (mm) for the reference normal period 1961–1990, the year 2006, the observed normal year 2004–2005, and for dry and wet years at Plittorp. Months with corrected precipitation are highlighted.

Month	Average monthly sums, 1961–1990	Observed precipitation, 2006	Observed normal precipitation, Aug. 2004–July 2005	Corrected sums for a dry year	Corrected sums for a wet year
January	54	33	54	54	141
February	39	55	70	70	87
March	36	61	32	32	32
April	43	54	5	5	5
May	45	64	35	35	35
June	51	16	93	16	157
July	73	23	47	47	47
August	61	107	71	71	161
September	64	9	16	16	16
October	51	67	90	21	164
November	56	90	84	25	144
December	56	23	22	22	22
Sum	**629**	**602**	**619**	**415**	**1,011**
100 years return period				420	1,017

Table 6-2. Monthly sums (mm) for the reference normal period 1961–1990, the year 2006, the observed normal year 2004–2005, and for dry and wet years at Äspö. Months with corrected precipitation are highlighted.

Month	Average monthly sums, 1961–1990	Observed precipitation, 2006	Observed normal precipitation, Aug. 2004–July 2005	Corrected sums for a dry year	Corrected sums for a wet year
January	49	29	44	44	126
February	35	59	46	46	76
March	32	64	32	32	32
April	38	54	4	4	4
May	39	52	34	34	34
June	44	21	72	14	137
July	64	12	48	48	48
August	53	78	66	66	140
September	55	10	14	14	14
October	45	79	81	19	145
November	49	107	87	22	130
December	50	25	22	22	22
Sum	**553**	**590**	**552**	**366**	**909**
100 years return period				365	900

In Tables 6-1 and 6-2 the average monthly sums for the reference normal period 1961–1990, the year 2006, the normal year (August 2004–July 2005), and for "constructed" wet and dry years are presented for the monitoring SKB meteorological stations at Plittorp and Äspö. The corrected months during the wet and dry years are marked in yellow.

From Table 6-1 it can be seen that the precipitation at Plittorp is 33% (204 mm) lower during the dry year and 63% (392 mm) higher during the wet year, compared to the observed normal year (August 2004–July 2005). The relative differences are approximately the same at the Äspö meteorological station, but the accumulated precipitation is a bit lower than at Plittorp. It should also be noted that the total precipitation in 2006 differs only slightly compared to the observed normal year, –17 mm at Plittorp and +38 mm at Äspö. However, the monthly sums vary to a larger extent between the years.

Six different simulation cases were defined according to the different meteorological conditions, see Table 6-3. Each case with a different precipitation input was simulated for undisturbed conditions and with the open repository. All cases with the open repository were based on a grouting level of $K=1\cdot10^{-9}$ m/s in the deposition tunnels and $K=1\cdot10^{-8}$ m/s in all other tunnels and shafts.

Table 6-3. Summary of the different simulation cases. Results are evaluated from the highlighted years.

Case	Type of simulation	Meteorological conditions				Initial conditions
1	Undisturbed conditions	Normal, 1st year	Normal, 2nd year	Normal, 3rd year		Same as in previous simulations
2	With open repository	Normal, 1st year	Normal, 2nd year	Normal, 3rd year		Same as in previous simulations
3	Undisturbed conditions			Dry, 1st year	Dry, 2nd year	After two years according to case 1
4	With open repository			Dry, 1st year	Dry, 2nd year	After two years according to case 2
5	Undisturbed conditions			Wet, 1st year	Wet, 2nd year	After two years according to case 1
6	With open repository			Wet, 1st year	Wet, 2nd year	After two years according to case 2

In cases 1 and 2 the observed normal year, August 2004–July 2005, was repeated three times where the first two years were used as an initialisation period. In the simulations with wet or dry conditions, cases 3–6, the meteorological input was repeated twice and the conditions after two years according to simulation case 1 or 2, depending on whether the open repository was included or not, was used as initial conditions.

6.2 Inflow to tunnels and shafts

In Table 6-4, the total inflow to the repository is presented as a mean value for the different meteorological cases. The results are based on a grouting level of $K=1\cdot10^{-9}$ m/s in deposition tunnels and $K=1\cdot10^{-8}$ m/s in all other tunnels and shafts. The results show that the inflow to the repository decreases under dry conditions; –9% for the second dry year compared to the year with normal precipitation. For wet conditions the results are the opposite, the inflow to tunnels and shafts increases with 5% for the second wet year compared to the year with normal precipitation.

Comparing the changes in inflow with the changes in influence areas in Section 6.3, the difference between the different "meteorological years" is more substantial for the influence areas. The hydraulic gradient controlling the downward flow is reasonably constant even under extreme weather conditions, with high or low precipitation, which explains why the inflow is influenced to such a small extent.

6.3 Groundwater table drawdown

In Table 6-5 the depth to the groundwater table for undisturbed conditions as well as influence areas for different levels of drawdown are presented as an average value for the different meteorological cases. The results are based on a grouting level of $K=1\cdot10^{-9}$ m/s in deposition tunnels and $K=1\cdot10^{-8}$ m/s in all other tunnels and shafts. The results show that the size of the influence area is affected by the amount of precipitation.

The reference depth to the groundwater table shows great variation depending on the meteorological conditions. The difference in groundwater table depth is approximately –1.5 m between the second dry year and the normal year. The corresponding difference for the second wet year is +0.8 m. The normal year has a somewhat higher groundwater table, +0.2 m, and a slightly smaller influence area compared to 2006. This is explained by the very dry summer and early autumn of 2006, see Table 6-1 and Table 6-2, as well as by the dry year of 2005 that preceded 2006.

In Figure 6-1 the drawdown of the groundwater table for a year with normal precipitation is shown. The corresponding drawdowns for years with dry or wet conditions are shown in Figures 6-2 and 6-3, respectively. As expected, the influence area increases for dry conditions and decreases for wet conditions. The influence area (drawdown >0.3 m) increases with 10% for the first dry year compared to the year with normal precipitation. For the first wet year the corresponding decrease is 11%.

Table 6-4. Calculated mean inflow (L/s) to tunnels and shafts for different meteorological conditions, with a grouting level of $K=1\cdot10^{-9}$ m/s in deposition tunnels and $K=1\cdot10^{-8}$ m/s in all other tunnels and shafts.

Year	Total inflow to tunnels and shafts (L/s)
2006	74.4
Normal year	75.5
Dry year, 1st	74.2
Dry year, 2nd	68.9
Wet year, 1st	78.0
Wet year, 2nd	79.4

Table 6-5. Average depth to groundwater table (m) for undisturbed conditions and average influence areas (km²) for different meteorological conditions, with a grouting level of K=1·10⁻⁹ m/s in deposition tunnels and K=1·10⁻⁸ m/s in all other tunnels and shafts.

Year	Depth to groundwater table, undisturbed conditions	Influence area, drawdown >0.1 m	Influence area, drawdown >0.3 m	Influence area, drawdown >1.0 m	Influence area, drawdown >4.0 m	Influence area, drawdown >10.0 m
2006	3.40	17.5	15.7	13.5	10.3	8.1
Normal year	3.19	16.6	14.9	12.4	9.2	7.1
Dry year, 1st	4.15	18.1	16.4	14.2	11.0	8.8
Dry year, 2nd	4.66	20.5	19.0	16.9	13.7	11.4
Wet year, 1st	2.53	15.5	13.3	10.8	7.7	5.1
Wet year, 2nd	2.35	14.5	12.3	9.8	6.7	4.0

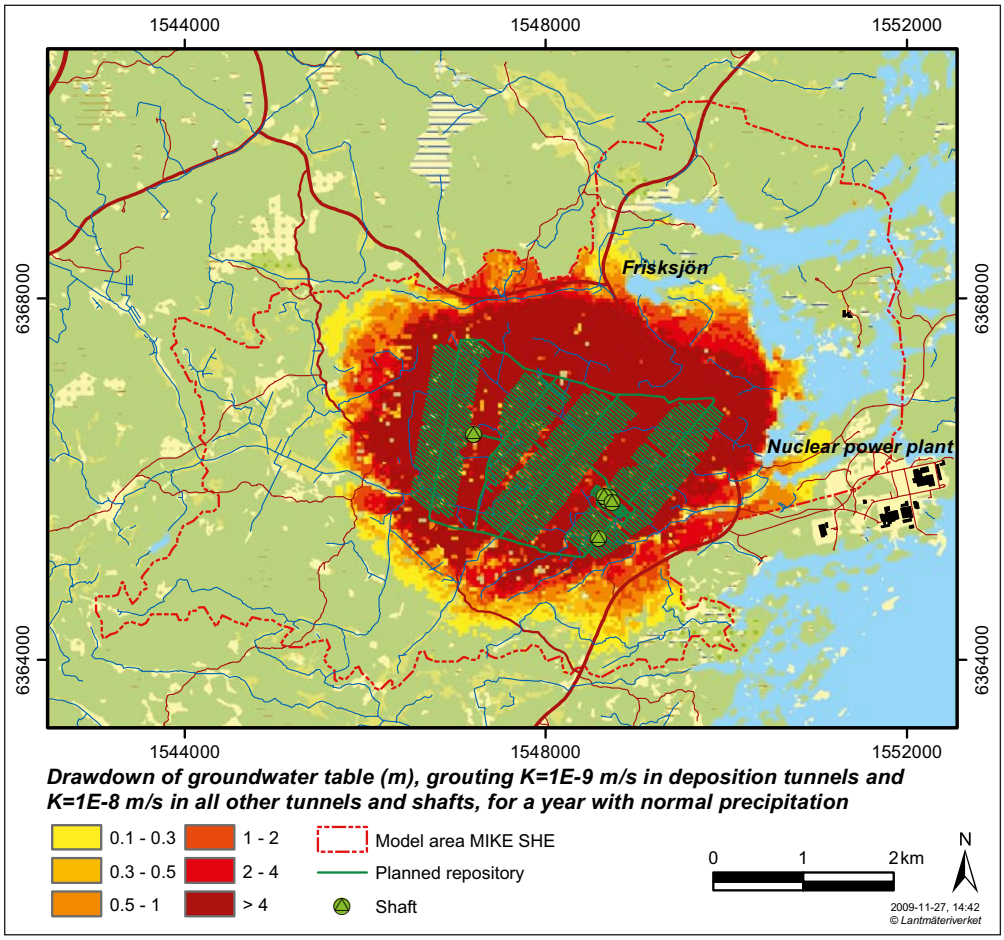

Figure 6-1. Drawdown of the groundwater table as an average for a year with normal precipitation, for the case with K=1·10⁻⁹ m/s in deposition tunnels and K=1·10⁻⁸ m/s in all other tunnels and shafts.

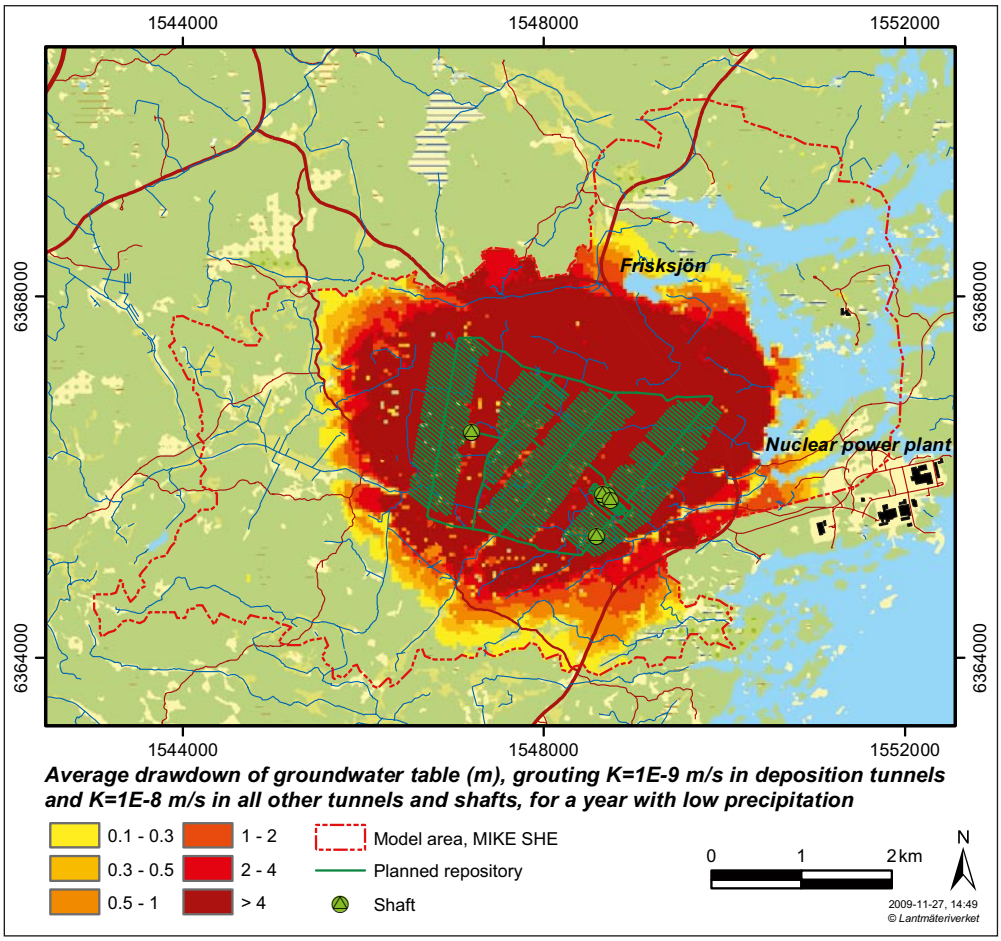

Figure 6-2. *Drawdown of the groundwater table as an average for a year with low precipitation, for the case with $K=1\cdot10^{-9}$ m/s in deposition tunnels and $K=1\cdot10^{-8}$ m/s in all other tunnels and shafts.*

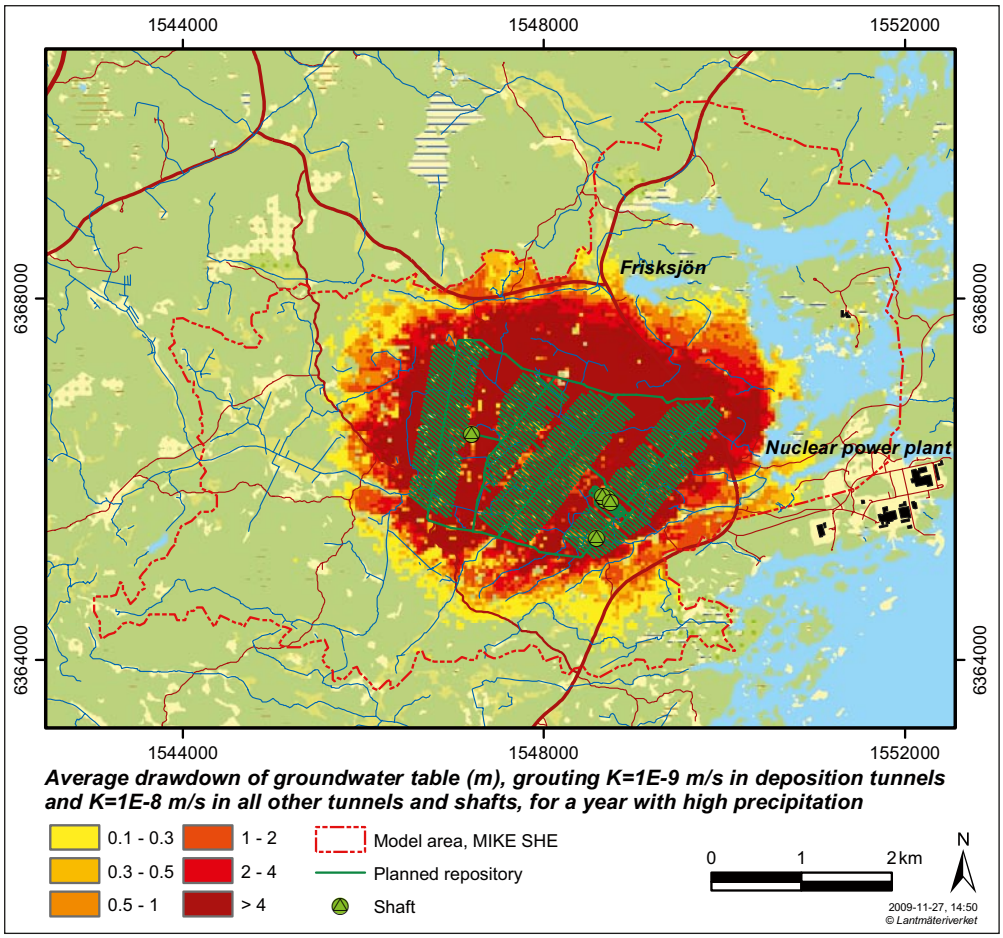

Figure 6-3. *Drawdown of the groundwater table as an average for a year with high precipitation, for the case with $K=1\cdot10^{-9}$ m/s in deposition tunnels and $K=1\cdot10^{-8}$ m/s in all other tunnels and shafts.*

Figures 6-4 and 6-5 show the groundwater table drawdown for the second of two consecutive years with dry or wet conditions. During this year the meteorological influence is strengthened and the influence area increases with 28% (dry year) and decreases with –17% (wet year) compared to the normal year. The meteorological influence on the groundwater table drawdown is substantial, e.g. the area where the drawdown exceeds 4 m for the second dry year is more than twice as large as the corresponding area for the second wet year. However, it is very unlikely with two consecutive years, each with a return period of 100 years, to occur. The influence areas for the second wet and dry years with a groundwater table drawdown larger than 0.3 m are presented together in Figure 6-6.

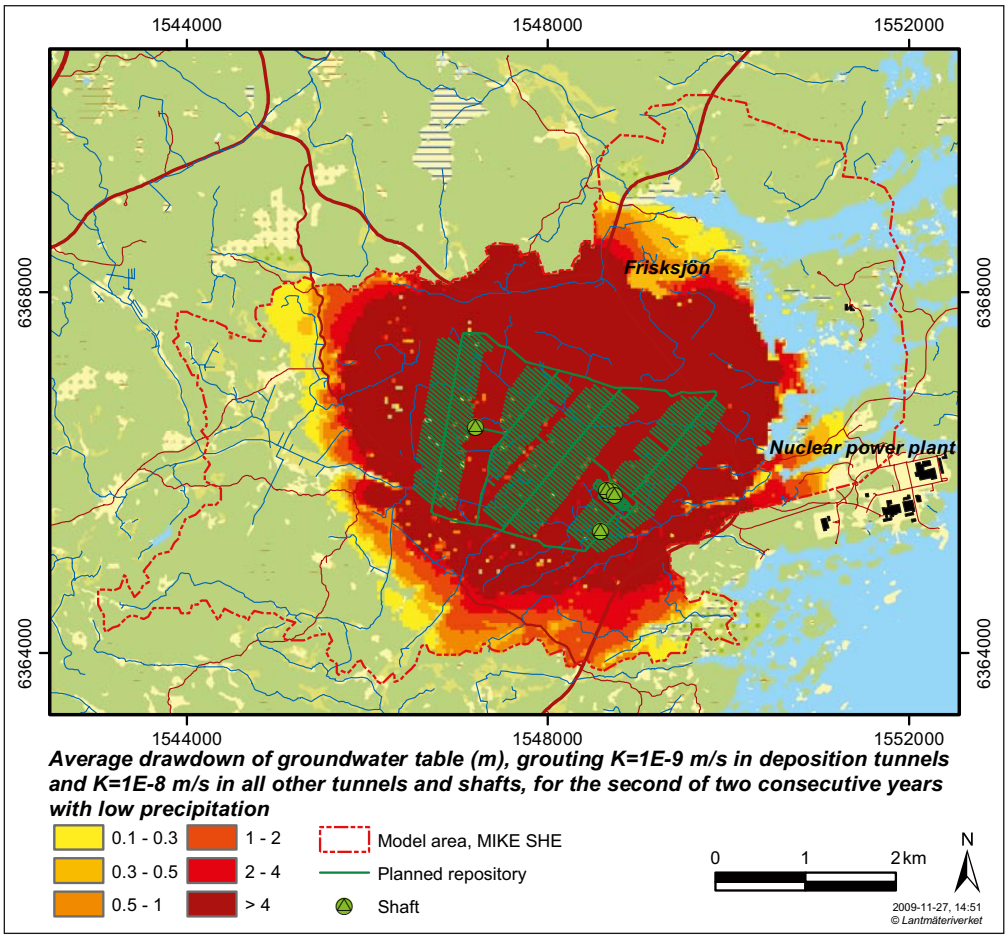

Figure 6-4. *Drawdown of the groundwater table as an average for the second of two consecutive years with low precipitation, for the case with $K=1\cdot10^{-9}$ m/s in deposition tunnels and $K=1\cdot10^{-8}$ m/s in all other tunnels and shafts.*

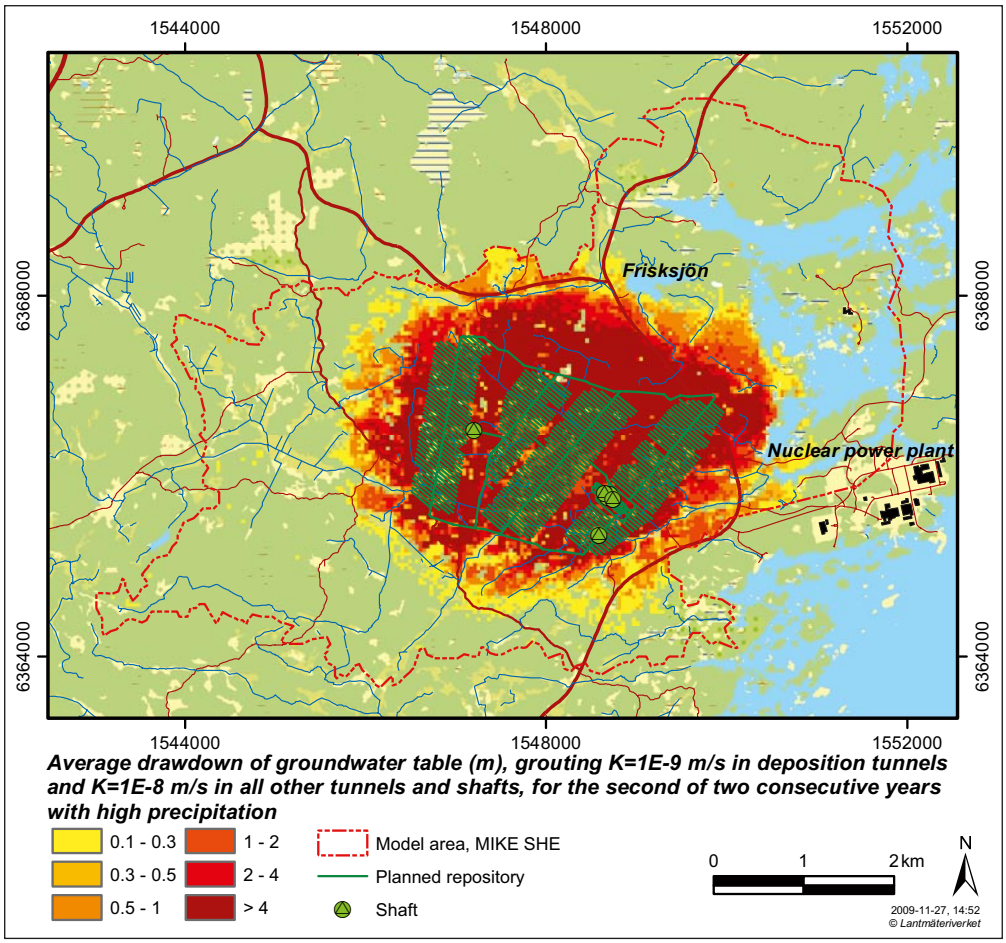

Figure 6-5. *Drawdown of the groundwater table as an average for the second of two consecutive years with high precipitation, for the case with $K=1\cdot10^{-9}$ m/s in deposition tunnels and $K=1\cdot10^{-8}$ m/s in all other tunnels and shafts.*

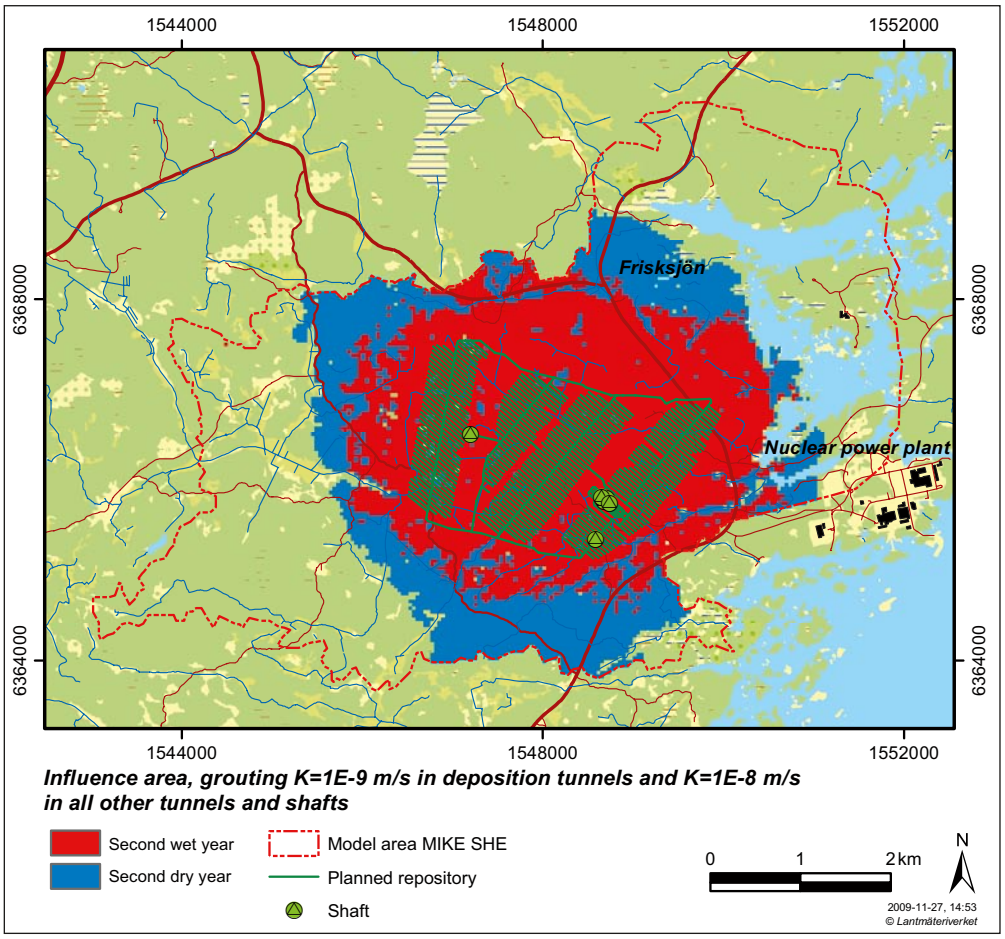

Figure 6-6. *Influence area for the second consecutive wet year (red areas only) and second consecutive dry year (red and blue areas), for a case with a grouting level of $K=1\cdot10^{-9}$ m/s in deposition tunnels and $K=1\cdot10^{-8}$ m/s in all other tunnels and shafts.*

6.4 Surface water levels and surface water discharge

In Table 6-6 the mean water level and the water-level drawdown in Lake Frisksjön are presented for the different meteorological cases. For undisturbed conditions, the mean water level is approximately the same for 2006 and the year with normal precipitation. Moreover, for the second dry year the mean water level is 0.17 m lower compared to the normal year, and 0.17 m higher for the second wet year. For disturbed conditions, the lake-level drawdown varies between 0.04 and 0.05 m (compared to undisturbed conditions) for all years except the second dry year where the lake-water level drawdown is 0.35 m. This can also be seen in Figure 6-4, where the lake-level drawdown in Lake Frisksjön exceeds 0.3 m.

In order to investigate the reason for the large drawdown in Lake Frisksjön during the second dry year, separate water balances were calculated for Lake Frisksjön for both the normal and the second dry year. Figure 6-7 explains the different water balance components presented in Table 6-7. The effect of the open repository on the overall water balance is small for the year with normal precipitation. For the second dry year, both the groundwater inflow and the flow of water from the saturated zone to Lake Frisksjön decrease with approximately 60% compared to the normal year for undisturbed conditions. With the open repository, the direction of the flow is changed for the second dry year; the vertical flow from the saturated zone to overland flow changes from 572 mm/year to 264 mm/year in the opposite direction. This together with the decrease in inflow of overland water explains the change in overland storage and the large drawdown of Lake Frisksjön during the second dry year according to Table 6-6 and Figure 6-4.

In Figure 6-8, the water level for undisturbed conditions in the stream Laxemarån, at the location of the monitoring station PSM000364, is shown for 2006. The water level for the normal year is shown together with the first wet and dry years in Figure 6-9 and together with those for the second wet and dry years in Figure 6-10. Note that the evaluated time periods differ between 2006 (January–December) and the years with different meteorological conditions (August–July).

Table 6-6. Mean water level for undisturbed conditions and drawdown for Lake Frisksjön for different meteorological conditions, with a grouting level of $K=1\cdot10^{-9}$ m/s in deposition tunnels and $K=1\cdot10^{-8}$ m/s in all other tunnels and shafts.

Year	Mean water level, undisturbed conditions (m)	Drawdown (m)
2006	1.50	0.05
Normal year	1.51	0.05
Dry year, 1st	1.40	0.05
Dry year, 2nd	1.34	0.35
Wet year, 1st	1.64	0.04
Wet year, 2nd	1.68	0.04

Table 6-7. Water balance (mm/year) for Lake Frisksjön, undisturbed and disturbed conditions, with a grouting level of $K=1\cdot10^{-9}$ m/s in deposition tunnels and $K=1\cdot10^{-8}$ m/s in all other tunnels and shafts, for the normal year and the second dry year.

	Reference (undisturbed), normal year	With open repository, normal year	Reference (undisturbed), 2nd dry year	With open repository, 2nd dry year
Net precipitation	167	167	–13	–6
Infiltration	128	125	90	82
Evapotranspiration of soil water	89	88	85	102
Overland storage change	–10	–22	–25	–340
Overland inflow	–1,366	–1,305	–494	0
Vertical flow OL–>SZ	–1,316	–1,241	–572	264
Groundwater outflow	–1,130	–1,069	–468	86
Vertical flow QD–>bedrock	–145	–131	–77	180
Storage change SZ in QD	–1	–2	–2	–20

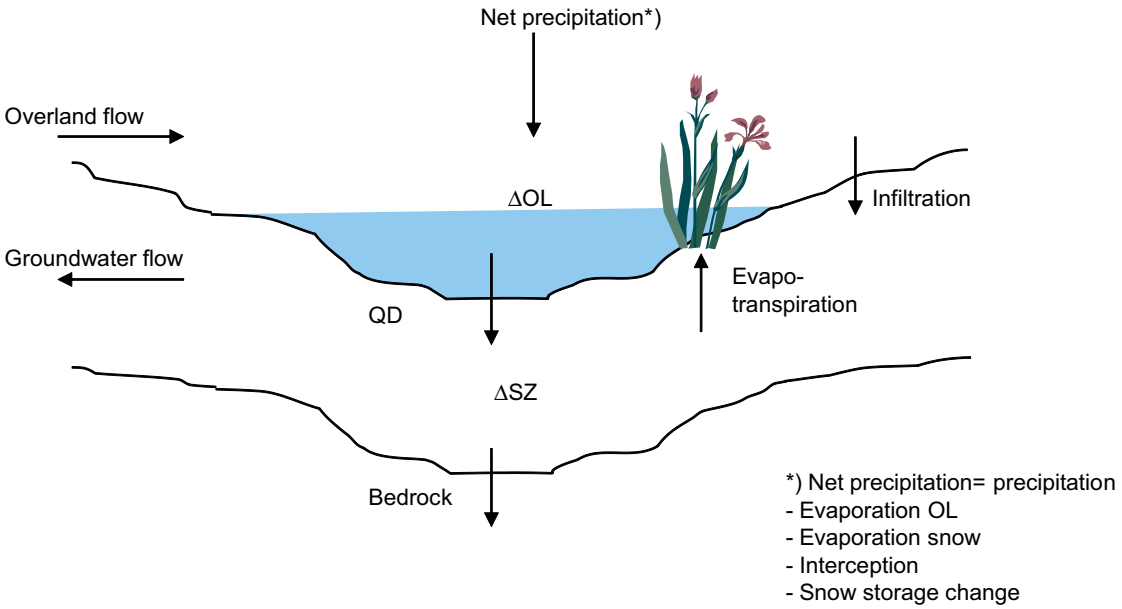

Figure 6-7. *Water balance components for Lake Frisksjön (see Table 6-7).*

In Figure 6-8, the dry summer and autumn in 2006 is seen as a constantly decreasing water level between June and October. The difference between the extreme water levels in 2006 is large due to the intense snowmelt in April. During the normal year, the natural fluctuations in water level are less than during 2006 and vary the most during winter and spring (November–April), see Figure 6-9.

A large part of the catchment area of Laxemarån is located outside the MIKE SHE model area. Therefore, the flow across the model boundary in MIKE 11 has been recalculated for wet and dry conditions using the corrected precipitation data for both the extreme (wet and dry) meteorological conditions.

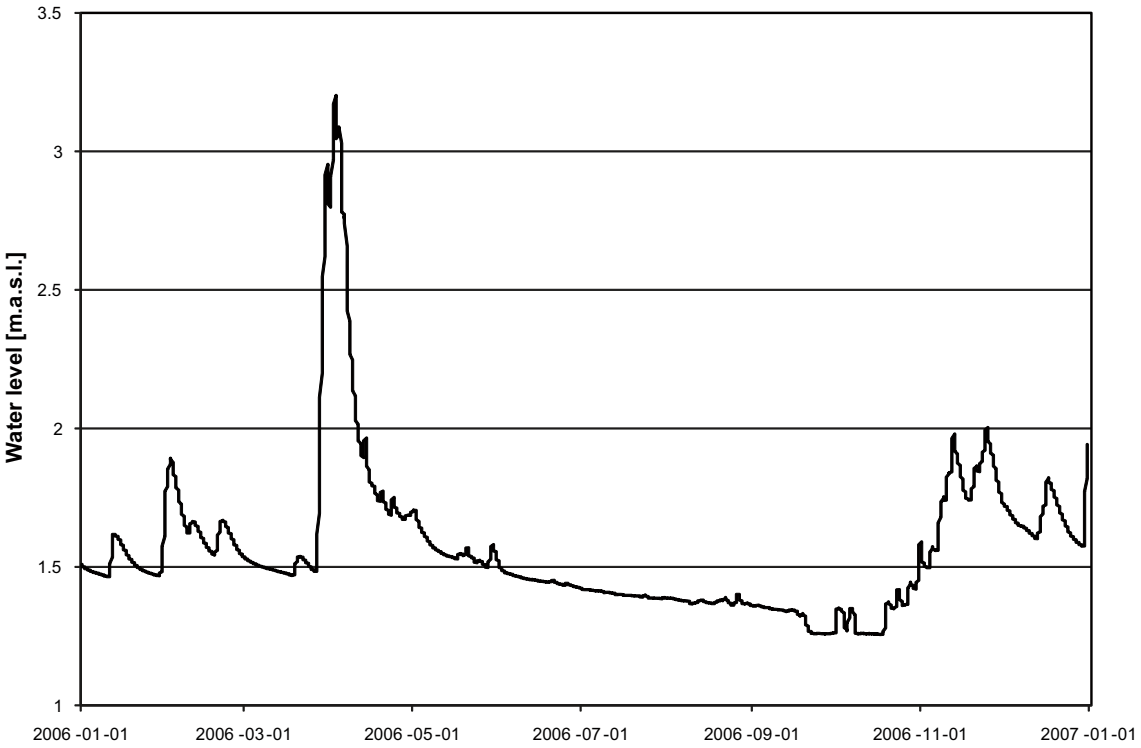

Figure 6-8. *Calculated water level (m.a.s.l.) 2006 for undisturbed conditions in Laxemarån at monitoring station PSM000364.*

The meteorological influence on the water level during wet and dry conditions is clearly seen in Figures 6-9 and 6-10. The highest water levels for the wet years are observed in the end of the year, October–December, and during the snowmelt in April. Peak elevations can also be observed in June, which is one of the months for which the precipitation has been corrected, see Section 6.1. During the dry years, the water level is constantly low except in April, even though the precipitation is extremely low during that specific month. This shows that the discharge and the water elevation are also affected by the temperature, which causes the snowmelt in April. The water levels do not differ considerably between the first and second dry years and between the first and second wet years.

Maximum and minimum water levels and mean discharges have been calculated for both undisturbed and disturbed conditions, with a grouting level of $K=1\cdot10^{-9}$ m/s in deposition tunnels and $K=1\cdot10^{-8}$ m/s in all other tunnels and shafts, as well as the mean flow at three different locations in Laxemarån. The results are presented in Table 6-8. Besides the monitoring station at Ström (PSM000364), one observation point is located downstream PSM000364 at Ekhyddan and one is located upstream at Åby, see Figure 6-11. The difference in mean flow between the different observation points is negligible and can only be observed for wet conditions where the mean flow increases slightly downstream.

The mean flow for undisturbed conditions is almost seven times larger during the first wet year than during the first dry year and almost three times larger than during the normal year. The influence of the open repository on the mean flow is rather small; the largest difference between undisturbed and disturbed conditions, 12%, is seen during the normal year.

In Table 6-8 it can also be seen that the drawdown due to the open repository for both minimum and maximum elevations varies between 0.01 m and 0.1 m. The largest drawdown is observed for dry conditions. The drawdown for H_{min} is larger than for H_{max} during the dry years, whereas the opposite effect is observed during the wet years.

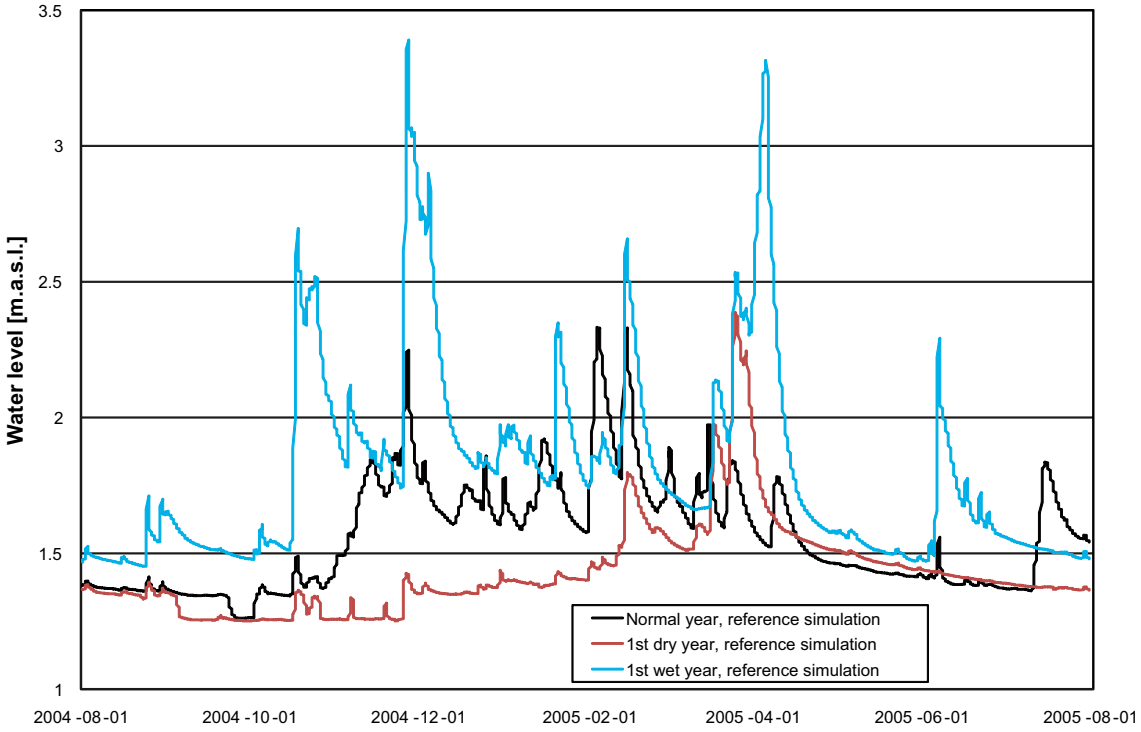

Figure 6-9. *Calculated water level (m.a.s.l.) for undisturbed conditions in Laxemarån at the location of the monitoring station PSM000364, for the normal year (August 2004–July 2005) and the first wet and dry years.*

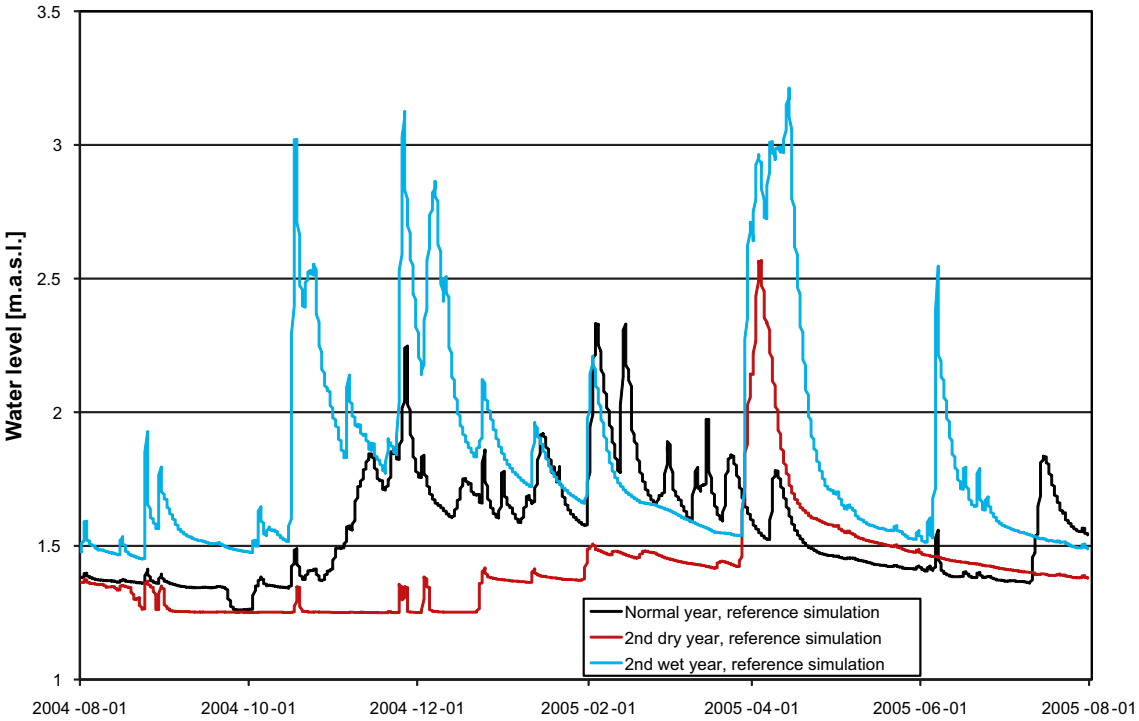

Figure 6-10. *Calculated water level (m.a.s.l.) for undisturbed conditions in Laxemarån at the location of the monitoring station PSM000364, for the normal year (August 2004–July 2005) and the second wet and dry years.*

Table 6-8. Maximum (H_{max}) and minimum (H_{min}) water level (m.a.s.l.) and mean discharge (Q_{mean}, m^3/s) at three different locations in Laxemarån. Results are presented for undisturbed and disturbed conditions, with a grouting level of $K=1\cdot10^{-9}$ m/s in deposition tunnels and $K=1\cdot10^{-8}$ m/s in all other tunnels and shafts, for different meteorological conditions.

Year	Simulation	Ekhyddan			Ström			Åby		
		H_{min}	H_{max}	Q_{mean}	H_{min}	H_{max}	Q_{mean}	H_{min}	H_{max}	Q_{mean}
2006	Undisturbed conditions	0.03	1.75	0.28	1.25	3.20	0.28	2.08	4.24	0.28
	With open repository	–0.05	1.71	0.26	1.24	3.15	0.26	2.00	4.19	0.26
Normal year	Undisturbed conditions	0.03	1.23	0.25	1.26	2.34	0.25	2.08	3.42	0.24
	With open repository	–0.03	1.22	0.22	1.25	2.30	0.22	2.02	3.40	0.22
Dry year, 1st	Undisturbed conditions	0.01	1.14	0.11	1.25	2.38	0.11	2.05	3.47	0.11
	With open repository	–0.07	1.13	0.10	1.24	2.37	0.10	1.97	3.46	0.10
Dry year, 2nd	Undisturbed conditions	0.00	1.28	0.11	1.25	2.56	0.11	2.00	3.65	0.11
	With open repository	–0.10	1.26	0.09	1.24	2.54	0.10	1.92	2.63	0.10
Wet year, 1st	Undisturbed conditions	0.31	1.96	0.68	1.45	3.39	0.67	2.34	4.40	0.66
	With open repository	0.29	1.94	0.64	1.44	3.35	0.63	2.32	4.37	0.63
Wet year, 2nd	Undisturbed conditions	0.31	1.78	0.71	1.45	3.21	0.70	2.34	4.26	0.69
	With open repository	0.28	1.76	0.67	1.44	3.19	0.67	2.32	4.24	0.66

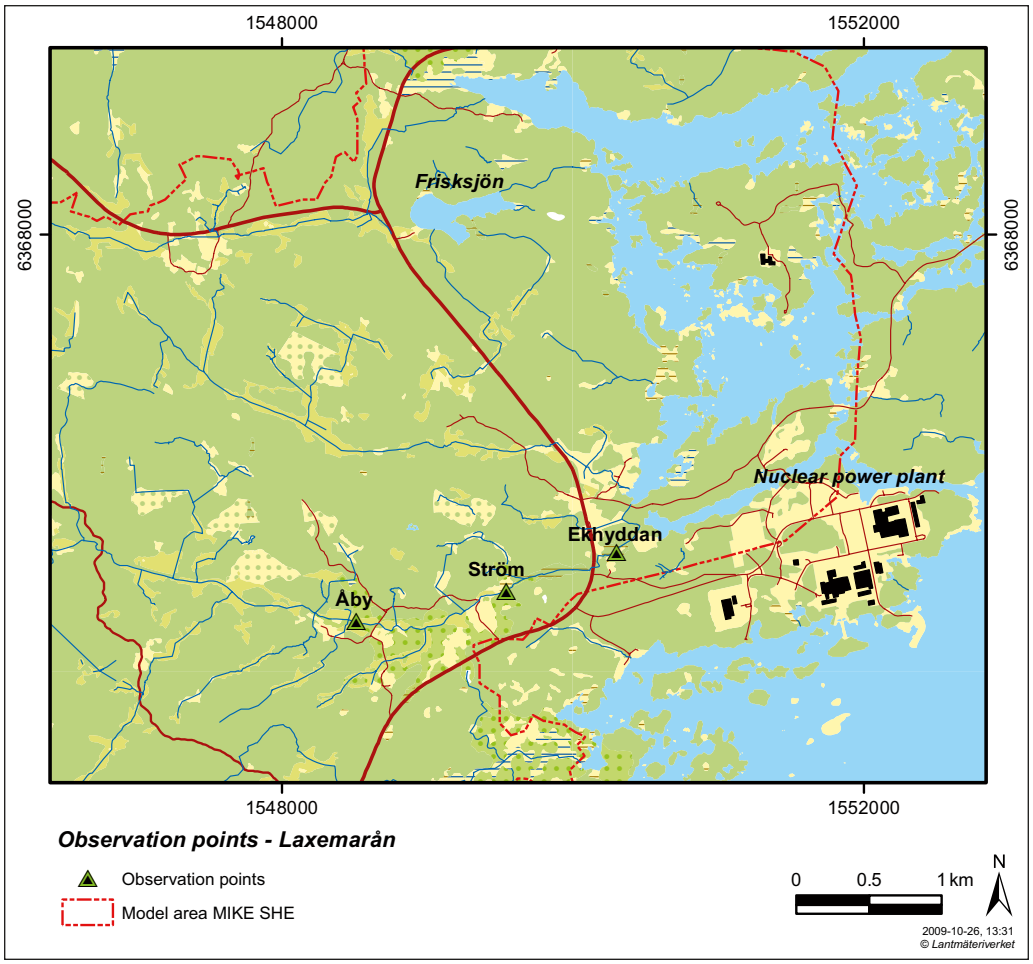

Figure 6-11. *Observation points in Laxemarån, located at Åby, Ström (PSM000364) and Ekhyddan.*

7 Sensitivity to hydraulic properties

The third and final step in the modelling process was to analyse the sensitivity of the model to the hydrogeological properties of the bedrock and the Quaternary deposits (QD), with respect to the impact from an open repository. Also, the importance of the sediments under the sea as well as the sensitivity to changed boundary conditions were analysed in terms of the effects of an open repository.

7.1 Definition of simulation cases

Nine different sensitivity cases have been studied with respect to open repository conditions compared with undisturbed conditions. The sensitivity cases are all based on changes of the hydraulic properties of the bedrock, the properties of the QD layers or the boundary conditions. The nine cases are summarised in Table 7-1. The reference model is the updated version of the SDM-Site Laxemar MIKE SHE model (Chapter 3).

There are of course some uncertainties regarding the parameterisation of the bedrock properties and during the calibration of the SDM-Site Laxemar MIKE SHE model the conductivities seemed to be overestimated. Although a new bedrock model was delivered from the ConnectFlow (CF) modelling and used in this report (see Section 3.1 for further details), it is of interest to test the sensitivity of the modelling results to the hydraulic conductivity of the bedrock. This interest motivates the first three sensitivity cases shown in Table 7-1.

The hydraulic conductivities of the bedrock are decreased with a factor of 10 in three different ways: only the vertical conductivity (*BR-V-low)*, only the horizontal conductivity (*BR-H-low)* or both (*BR-HV-low)*. In order to investigate the opposite situation, i.e. an increased conductivity in the bedrock, both the horizontal and the vertical conductivity are increased with a factor of 3 in the bedrock below 150 m.b.s.l. in sensitivity case *BR-HV-high*. In this case the boundary condition in all layers is changed from a no-flow to a fixed head condition; see sensitivity case *BR-boundary* for further details.

Table 7-1. Definition of simulation cases in the sensitivity analysis. Changes are compared to the reference model (i.e. the updated version of the SDM-Site Laxemar MIKE SHE model).

Name of the simulation case	Short description	Changes in conductivity in layers Z3 and Z5	Changes in horizontal conductivity in the bedrock	Changes in vertical conductivity in the bedrock
BR-V-low	Decreased vertical conductivity in bedrock	–	–	Kv / 10
BR-H-low	Decreased horizontal conductivity in bedrock	–	Kh / 10	–
BR-HV-low	Decreased horizontal and vertical conductivity in bedrock	–	Kh / 10	Kv / 10
BR-HV-high	Increased horizontal and vertical conductivity in bedrock, fixed head boundary	–	Kh×3 (below 150 m.b.s.l.)	Kv×3 (below 150 m.b.s.l.)
BR-wall	Dolerite dykes	–	–	–
S0	No sediments under the sea	–	–	–
Z3Z5-HV-low	Decreased horizontal and vertical conductivity in layer Z3 and Z5	K / 100	–	–
Z5-lens	Extra clay lens extending layer Z5	–	–	–
BR-boundary	Fixed head boundary	–	–	–

Some deformation zones crossing the model area contain dolerite; these zones are called dolerite dykes. The dolerite dykes are assumed to have a tight core, representing the dolerite, but to be permeable outside the dolerite. Since the horizontal conductivity in MIKE SHE only can be given as a mean of K_x and K_y (K_h) the anisotropy of K_x and K_y due to the dolerite is not properly described in the MIKE SHE model. To handle this, the dolerite dykes are described by activating the "sheet piling module" in sensitivity case *BR-wall*. This was also tested as a sensitivity case in /Bosson et al. 2009/. By introducing a flow resistance in the east-west direction, this module enables groundwater to flow easily in the north-south direction but not in the east-west direction. The east-west flow resistance is given as a small leakage coefficient, set to $1 \cdot 10^{-12}$ s^{-1}. In the MIKE SHE model, the dolerite dykes extend through the entire bedrock (down to 1,190 m.b.s.l.). The locations of the dykes are shown in Figure 7-1.

The low-permeable sediment layers (glacial clay) at the bottom of the sea in the model are assumed to have a strong influence on the inflow to the repository and the drawdown. It is therefore of interest to evaluate whether the above-mentioned assumption is correct or not. In sensitivity case *S0* the sediments under the sea are simply removed from the model and replaced by the underlying geological layers (glacial till or bedrock).

In sensitivity cases *Z3Z5-HV-low* and *Z5-lens* the sensitivity to changes in the clay QD layers Z3 (postglacial clay) and Z5 (glacial clay) are tested. In the first case (*Z3Z5-HV-low*), the horizontal and the vertical hydraulic conductivity are decreased with a factor of 100 in both layer Z3 and layer Z5. In the second case (*Z5-lens*), a clay lens with $K=1 \cdot 10^{-9}$ m/s is added to the model. This lens extends layer Z5 with 1.7 m in the vertical direction. The effect on the vertical conductivity is illustrated in Figure 7-2 as the ratio between the reference case and *Z5-lens* in computational layer 1 and 2. In some areas the vertical hydraulic conductivity is reduced with more than a factor of 10^5 in both layers.

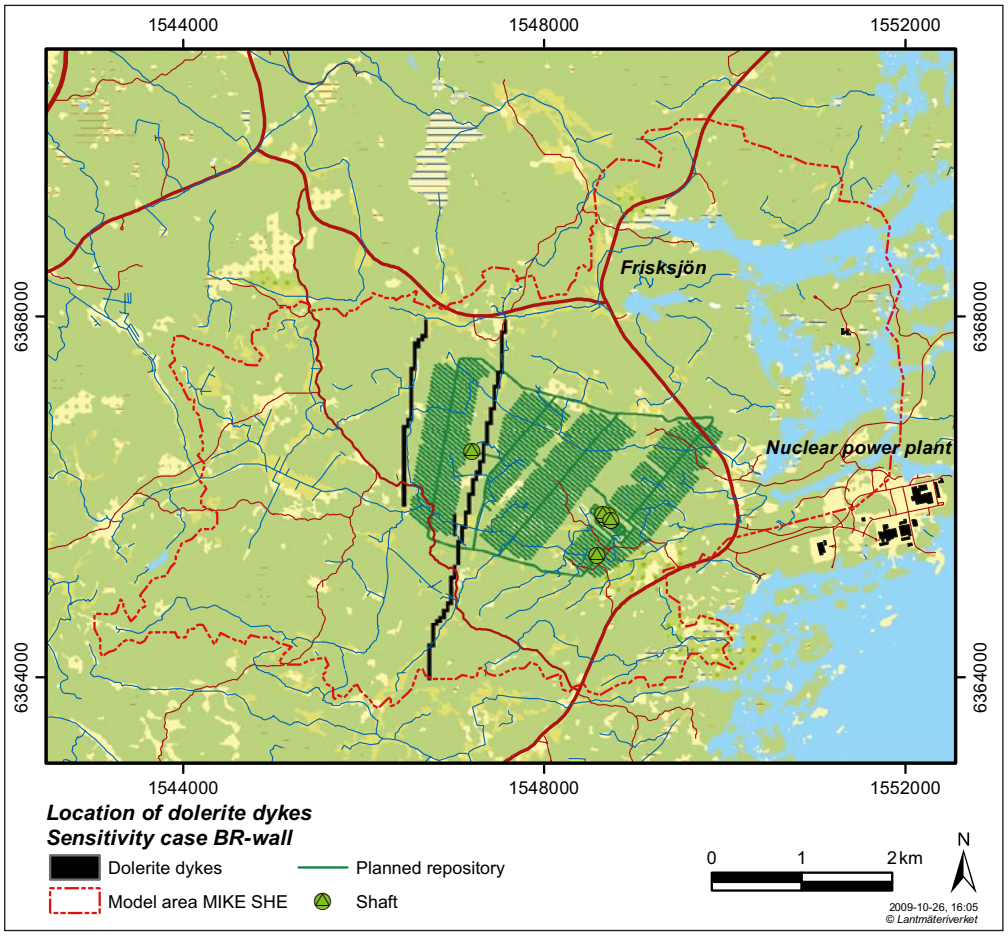

Figure 7-1. *Location of dolerite dykes in sensitivity case BR-wall.*

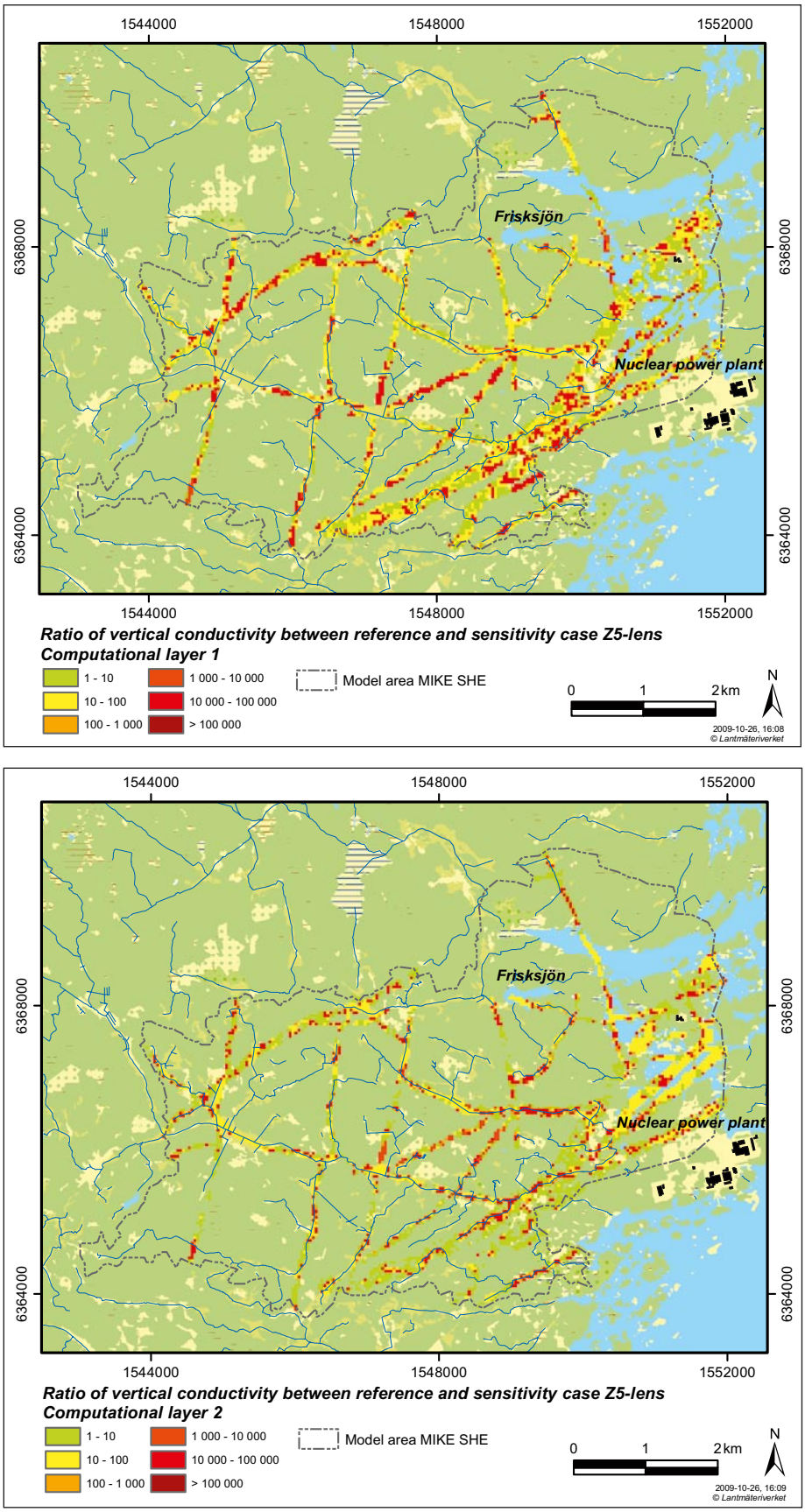

Figure 7-2. *Ratio of vertical conductivities in the reference case and sensitivity case Z5-lens for computational layer 1 (upper graph) and layer 2 (lower graph).*

The effect of the open repository on the groundwater table drawdown is substantial and the influence area reaches the model boundary, see e.g. Figure 5-10 in Section 5-4. Due to the no-flow boundary condition in each layer it is not possible for the repository to draw any water from the model boundary. This explains sensitivity case *BR-boundary* where all no-flow boundaries in the bedrock computational layers are changed to a fixed head boundary condition. Time varying head elevations for each layer are taken from the undisturbed reference simulation and used as input.

The names of the simulation cases are based on the following abbreviations: BR = bedrock, H = horizontal conductivity, V = vertical conductivity, Z3 = clay gyttja QD layer, Z5 = glacial clay QD layer, low = lower conductivity, high = higher conductivity, and S0 = no sediments.

In all cases, the period 2004 to 2006 is simulated (in accordance with Section 3.2.2). All of the sensitivity cases are modelled for both undisturbed conditions and for open repository conditions. The open repository conditions have been simulated with a grouting level of $K=1\cdot10^{-9}$ m/s in the deposition tunnels and $K=1\cdot10^{-8}$ m/s in all other tunnels and shafts. The reference case is based on these conditions and the updated version of the SDM-Site Laxemar model.

7.2 Results from the sensitivity analysis

7.2.1 Parameters in the evaluation

The simulation results from the different sensitivity cases have been analysed with respect to the inflow to the open repository, the impact on the surface water system, and the drawdown of the groundwater table.

The results are summarised in Table 7-2, where evaluation key parameters according to the list below are calculated and tabulated. The names of the key parameters are based on the following abbreviations: OR = open repository, Q = discharge, H = water level, S = surface water, G = groundwater.

In order to estimate how reasonable the changes in the hydraulic parameters are, the differences between observed data and simulated undisturbed conditions have also been analysed for each sensitivity case, see summary in Table 7-2. The deviations are analysed using parameters based on the following notation: R = correlation coefficient between observed and simulated value, ME = mean error between observed and simulated value, MAE = mean absolute error between observed and simulated value, PSM = surface water discharge monitoring station, SSM = groundwater monitoring well in QD, HLX = groundwater monitoring well (percussion-drilled borehole) in bedrock.

Table 7-2. Summary of results and key parameters, according to the definitions in the text, for the different sensitivity cases.

Parameter		Reference	BR-V-low	BR-H-low	BR-HV-low	BR-HV-high	BR-wall	S0	Z3Z5-HV-low	Z5-lens	BR-boundary
OR Q	(L/s)	74.4	27.5	46.2	13.7	129	73.2	76.8	72.1	72.5	74.6
OR G 0.3	(km^2)	15.7	14.1	9.0	7.3	17.9	15.1	13.4	17.9	17.6	14.5
OR G 1.0	(km^2)	13.5	9.7	8.0	4.5	15.7	12.8	11.0	15.5	15.4	12.2
OR S dH	(m)	0.07	0.04	0.03	0.03	0.17	0.07	0.05	0.06	0.07	0.06
OR S dQ	(%)	–7	–2	–4	–1	–4	–7	–13	–4	–5	–2
R PSM S	(–)	0.89	0.88	0.89	0.88	0.89	0.89	0.89	0.89	0.89	0.89
ME PSM S	(m)	0.10	0.11	0.11	0.12	0.09	0.10	0.09	0.11	0.09	0.09
MAE PSM S	(m)	0.10	0.11	0.11	0.12	0.09	0.10	0.09	0.11	0.09	0.09
ME SSM G	(m)	0.30	0.21	–0.06	0.03	0.31	0.28	0.31	0.27	0.18	0.26
MAE SSM G	(m)	0.98	0.94	0.83	0.84	1.00	0.97	1.01	1.02	0.96	0.96
ME HLX G	(m)	0.58	0.84	0.28	0.39	0.56	0.55	0.60	0.30	–0.15	0.52
MAE HLX G	(m)	0.87	0.99	0.96	0.85	0.96	0.89	0.91	0.87	0.99	0.89

The parameters in the evaluation are described as follows:

OR Q: Total inflow to the open repository tunnels, including access tunnels, transport tunnels, deposition tunnels and shafts, annual average for 2006.

OR G 0.3: Influence area with drawdown of groundwater table larger than 0.3 m, annual average for 2006. In the text below, this is referred to as the influence area.

OR G 1.0: Influence area with drawdown of groundwater table larger than 1.0 m, annual average for 2006.

OR S dH: Drawdown of surface water level in Lake Frisksjön, annual average for 2006.

OR S dQ: Relative difference in surface water discharge in the stream Laxemarån, comparing undisturbed conditions and open repository conditions, annual average for 2006.

R PSM S: Average correlation coefficient, comparing observed and simulated discharges, for the four surface water discharge monitoring stations, undisturbed conditions 2004–2006.

ME PSM S: Average mean error, comparing observed and simulated levels, for the surface water level monitoring station at the outlet from Lake Frisksjön (PSM000348), undisturbed conditions 2004–2006.

MAE PSM S: Average mean absolute error, comparing observed and simulated levels, for the surface water level monitoring station at the outlet from Lake Frisksjön (PSM000348), undisturbed conditions 2004–2006.

ME SSM G: Average mean error, comparing observed and simulated levels, for the SSM groundwater monitoring wells, undisturbed conditions 2004–2006.

MAE SSM G: Average mean absolute error, comparing observed and simulated levels, for the SSM groundwater monitoring wells, undisturbed conditions 2004–2006.

ME HLX G: Average mean error, comparing observed and simulated head elevations, for the HLX percussion boreholes, undisturbed conditions 2004–2006.

MAE HLX G: Average mean absolute error, comparing observed and simulated head elevations, for the HLX percussion boreholes, undisturbed conditions 2004–2006.

The upper part of Table 7-2 presents the parameters describing the influence of the open repository (cf. above). The lower part of Table 7-2 shows how reasonable the sensitivity cases are, by comparing the simulated undisturbed conditions with observed data in terms of the parameters defined above.

7.2.2 Sensitivity in terms of deviations from measured data

The sensitivity to changes of the parameters describing the hydrogeological properties of the bedrock and the QD is relatively high with regard to both groundwater table elevation and the head elevation in the bedrock. The effect on the surface discharges and the water level in Lake Frisksjön is small in all sensitivity cases.

All sensitivity cases, except cases *S0* and *BR-HV-high*, give better calibration results for the groundwater levels compared to the reference case. The best result for the head elevation in the bedrock is achieved in *Z5-lens* and the worst in *BR-V-low*. Case *BR-H-low* and *BR-HV-low* give the best overall calibration results.

7.2.3 Sensitivity to changed boundary conditions

From the results presented in Chapter 5, it could be expected that the inflow to the open repository would increase if the no-flow boundary condition is changed to a fixed head boundary in the bedrock. However, this is not the case; the inflow changes only very little. The influence area decreases, of course, as the fixed head boundary condition prevents the influence area to extend to the model boundary.

In Table 7-3, a summary of changes in flow components contributing to the open repository inflow is presented for the reference case and the sensitivity case *BR-boundary*. As can be seen, the flow components contributing to the open repository inflow remain more or less unchanged. The horizontal net inflow, i.e. the flow from the model boundary, only contributes with 3% of the total inflow to the open repository.

7.2.4 Sensitivity to the bedrock properties

Case *BR-V-low* gives a slightly reduced influence area, 10% smaller than in the reference case. With a decreased vertical conductivity, the influence area extends further in all directions compared to the reference, but the drawdown pattern is more scattered resulting in a smaller total influence area (see Figure 7-3). The inflow to the open repository is greatly affected; it decreases with 63% compared to the reference case. In the case where the horizontal conductivity is decreased with a factor of 10, *BR-H-low*, the influence area is reduced with over 40%, but the drawdown within this area is substantial (Figure 7-4). The inflow to the open repository decreases with 38% compared to the reference.

The combined effect of the first two sensitivity cases is shown in Figure 7-5. In this case, *BR-HV-low,* when both the vertical and horizontal conductivities are reduced with a factor of 10 the influence area is substantially reduced. It decreases with 54% compared to the reference case. An even larger effect is seen on the inflow to the open repository which decreases with 82%. The conclusion from the first three sensitivity cases is that the horizontal conductivity is the most sensitive parameter regarding the influence area, while the vertical conductivity will affect the inflow to the open repository to a greater extent.

The sensitivity to increased hydraulic conductivities in both the horizontal and the vertical directions is tested in sensitivity case *BR-HV-high*, where the conductivities are increased with a factor of 3 in the bedrock below 150 m.b.s.l. The result is shown in Figure 7-6. The influence area increases somewhat (+14%) but the largest effect is seen on the inflow to the open repository which increases with 73%, from an inflow of 74 L/s in the reference case to 129 L/s in case *BR-HV-high*. The effect on the water level in Lake Frisksjön is substantial and the drawdown increases with 10 cm compared to the reference case.

Table 7-3. Summary water balance for 2006 (L/s) showing the changes in flow components in the bedrock when introducing the open repository, in the reference case and the case with changed boundary condition (*BR-boundary*).

Changes in flow components due to the open repository:	*Reference case*		*BR-boundary case*	
	Flow in L/s	Relative contribution	Flow in L/s	Relative contribution
Vertical net inflow to bedrock in the influence area	45.63	61%	46.00	62%
Vertical net inflow to bedrock in the land area, excluding the influence area	6.02	8%	5.07	7%
Vertical net inflow to bedrock from the sea area	4.36	6%	4.06	5%
Horizontal net inflow to bedrock from the model boundary	0.00	0%	2.30	3%
Net inflow from river	1.76	2%	1.81	2%
Storage change in bedrock	–16.66	22%	–15.38	21%
Inflow to the open repository	74.43		74.63	

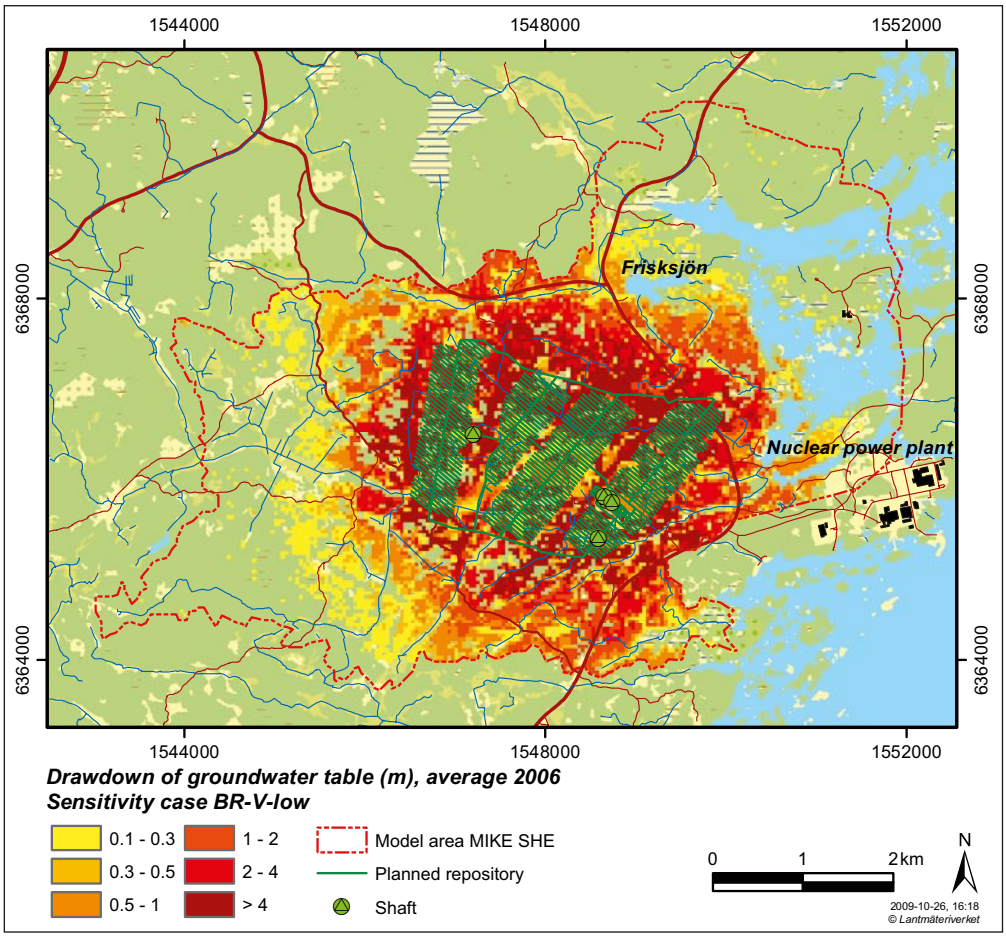

Figure 7-3. *Drawdown of the groundwater table as an average for 2006, sensitivity case BR-V-low with a grouting level of $K=1\cdot10^{-9}$ m/s in deposition tunnels and $K=1\cdot10^{-8}$ m/s in all other tunnels and shafts.*

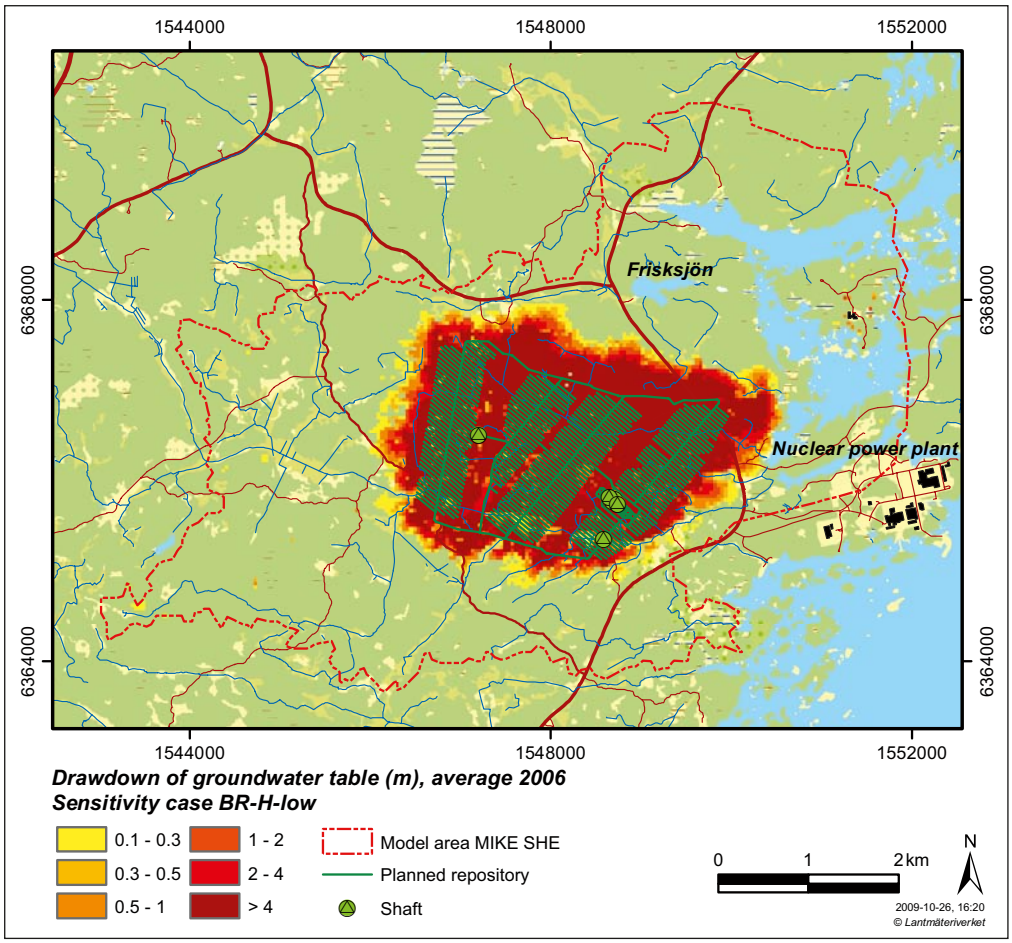

Figure 7-4. *Drawdown of the groundwater table as an average for 2006, sensitivity case BR-H-low with a grouting level of $K=1\cdot10^{-9}$ m/s in deposition tunnels and $K=1\cdot10^{-8}$ m/s in all other tunnels and shafts.*

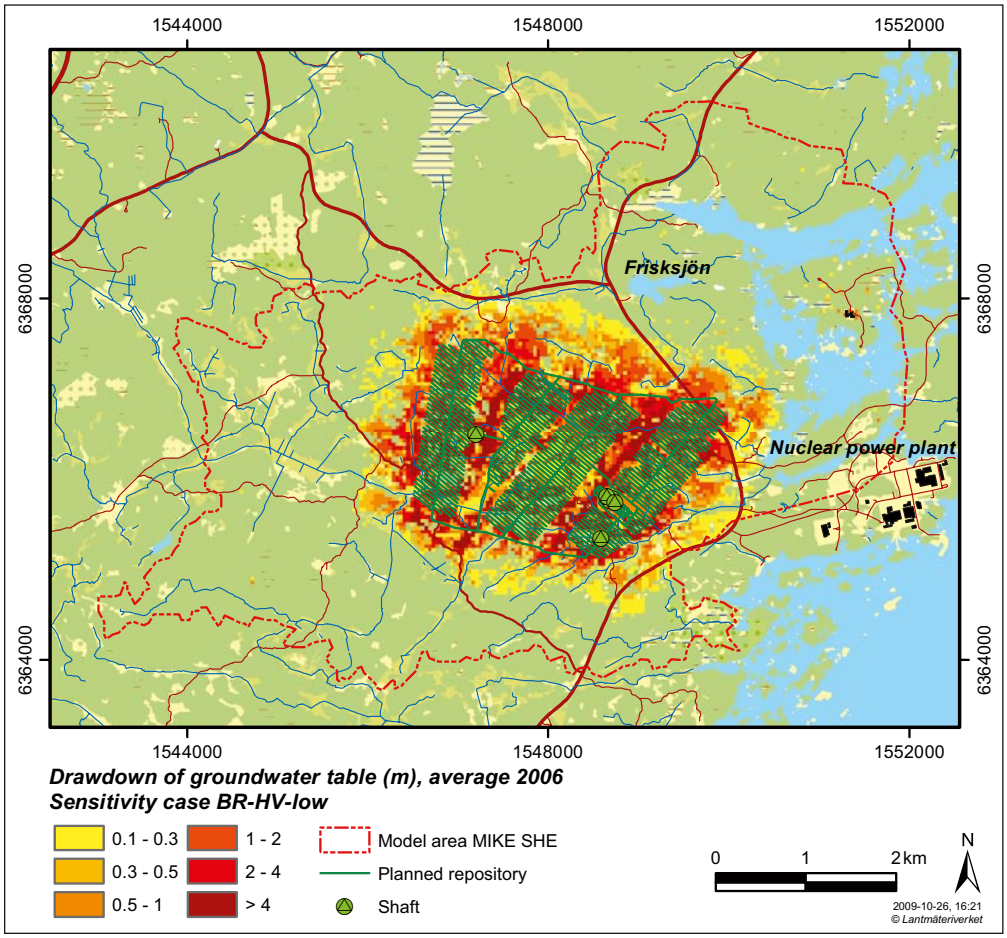

Figure 7-5. *Drawdown of the groundwater table as an average over 2006, sensitivity case BR-HV-low with a grouting level of $K=1\cdot10^{-9}$ m/s in deposition tunnels and $K=1\cdot10^{-8}$ m/s in all other tunnels and shafts.*

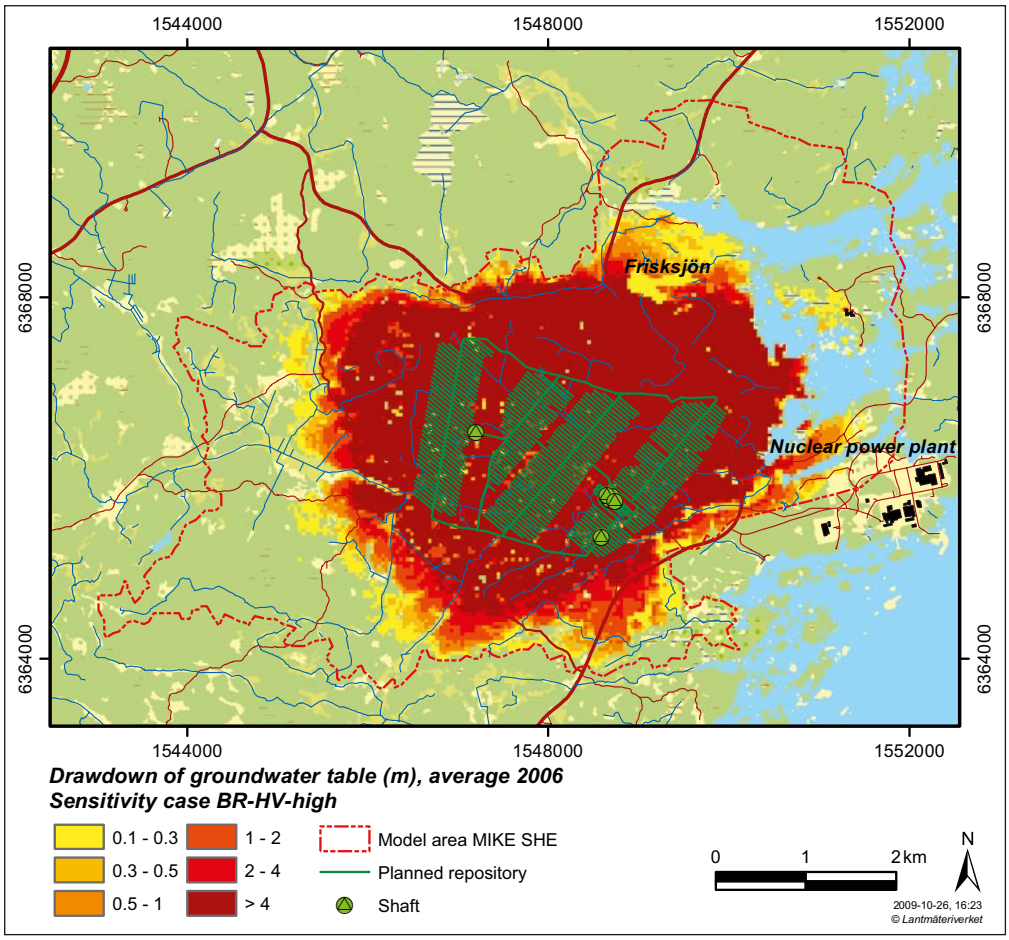

Figure 7-6. *Drawdown of the groundwater table as an average for 2006, sensitivity case BR-HV-high with a grouting level of $K=1\cdot10^{-9}$ m/s in deposition tunnels and $K=1\cdot10^{-8}$ m/s in all other tunnels and shafts.*

In sensitivity case *BR-wall* both the influence area and the inflow to the open repository decrease slightly. The "wall" does not affect the vertical groundwater flow, only the horizontal flow. This explains the small decrease in the inflow to the open repository. The effect of the dolerite dykes, which decrease the groundwater flow in the east-west direction, is shown in Figure 7-7. The drawdown decreases east of the dolerite dykes, but they do not affect the drawdown in the rest of the area.

7.2.5 Sensitivity to the properties of the Quaternary deposits

The sensitivity cases *Z3Z5-HV-low* and *Z5-lens*, which deal with the conductivity in the QD layers, show little sensitivity with regard to the inflow to the open repository, –3% and –2% compared to the reference case, respectively. The influence areas, however, are affected to a somewhat greater extent. The case *Z3Z5-HV-low* gives a slightly increased influence area, 14%, due to a decreased infiltration and recharge of groundwater as a consequence of the reduced conductivity in QD layers Z3 and Z5. The results are similar in case *Z5-lens* where the influence area increases with 12%.

The opposite effect compared to the two sensitivity cases above is seen in sensitivity case *S0* where the infiltration and recharge of the groundwater table increases when the low-permeable sediment layers under the sea are removed from the model. The inflow to the open repository increases and the influence area decreases. The changes compared to the reference case are, however, rather small with the largest change in the influence area which decreases with 15%. The reduction of the discharge in Laxemarån is 13% compared to 7% in the reference simulation.

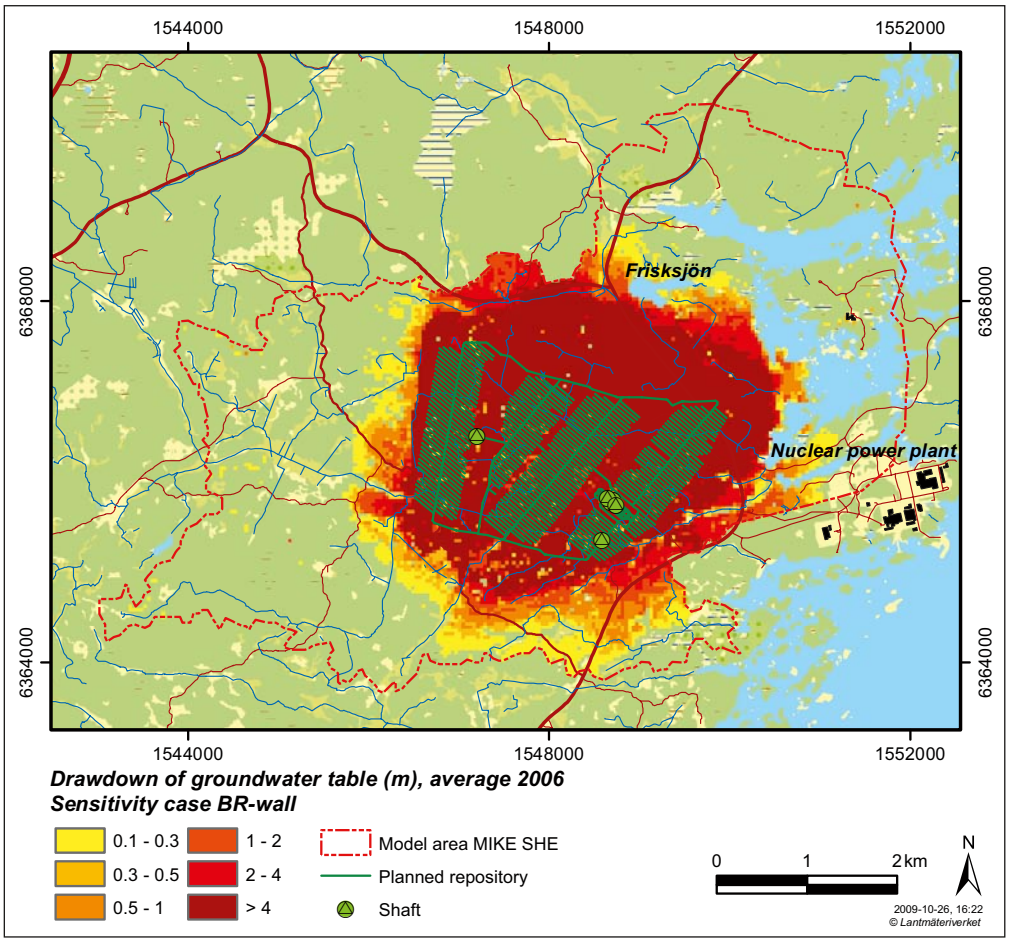

Figure 7-7. *Drawdown of the groundwater table as an average for 2006, sensitivity case BR-wall with a grouting level of $K=1\cdot10^{-9}$ m/s in deposition tunnels and $K=1\cdot10^{-8}$ m/s in all other tunnels and shafts.*

7.2.6 Conclusions of the sensitivity analysis

The following can be concluded from the sensitivity analysis of the hydraulic parameters with regard to the influence of the open repository:

- The most sensitive property with regard to the inflow to the open repository seems to be the vertical hydraulic conductivity of the bedrock. The horizontal conductivity seems to affect the groundwater table the most.
- The sensitivity to the hydraulic conductivity of the QD layers is rather small. Higher conductivity of the clay QD layers seems to decrease the influence area and opposite effect is seen when the sediment layers are removed.
- The inflow to the open repository is hardly affected by the tested change in the boundary conditions from a no-flow boundary to a time-varying prescribed head boundary.
- The influence on the surface water is small in all cases except in case *S0* (testing the effects of the sediment properties), which will affect the discharge in Laxemarån the most.

8 Conclusions

Unless otherwise stated, the conclusions below refer to results of modelling with the whole repository construction (all tunnels and shafts) open at the same time. As explained above, this is a hypothetical worst case. In reality, the open repository will be constructed and operated in five development phases, with different parts of the deep rock construction open in each phase.

8.1 Water balance and inflow to the open repository

The inflow of groundwater to the open repository affects the total turnover of water in the model area. Depending on the grouting level, the inflow to the repository is in the order of 35 to 55% of the total runoff for undisturbed conditions, considering the land part of the model area. Inside the influence area, the open repository creates a major change of the water balance, with an inflow to the repository of up to 97% of the total runoff for undisturbed conditions (depending on the grouting level).

In the MIKE SHE model, there are no horizontal boundary flows in the bedrock due to the no-flow boundary condition in all bedrock layers. When the repository is introduced the magnitudes of the vertical up- and downward flow change. For undisturbed conditions the vertical outflow from the bedrock to the QD is 34 L/s and the vertical inflow is 53 L/s (net inflow of 19 L/s). The corresponding flows with the repository vary between 15 and 19 L/s (outflow) and between 83 and 98 L/s (inflow) depending on the grouting level (net inflow between 64 and 83 L/s).

The inflow to tunnels and shafts varies between 55 and 88 L/s depending on the grouting level, where the higher inflow is for the case with $K=10^{-8}$ m/s in all tunnels and the lower is for a repository with $K=10^{-10}$ m/s around the deposition tunnels, and $K=10^{-8}$ m/s elsewhere. Between 65 and 80% of the repository inflow comes from increased vertical inflow from the land area, out of which 85–90% can be attributed to the influence area (here defined as the area in which the groundwater table drawdown exceeds 0.3 m in the simulation with a grouting level of $K=1\cdot10^{-8}$ m/s). The remaining contribution comes from increased vertical inflow from the sea, storage change in the bedrock and increased inflow from streams. When the model is run for a longer time period than that in the base case (nine years instead of three), the relative contribution from storage change in the bedrock decreases.

The meteorological conditions are hardly reflected in the calculated inflows to the repository, meaning that the inflow is more or less the same under dry conditions compared to wet conditions with large amounts of precipitation. Even in the second of two consecutive wet years, with a precipitation corresponding to a return time of 100 years, the inflow only increases with 5% compared to a year with normal precipitation.

The sensitivity analysis shows that the inflow to the repository is rather sensitive to changes of the analysed properties; the importance of the sediments under the sea as well as the sensitivity to changed boundary conditions and changes in hydrogeological properties of the bedrock and the Quaternary deposits have been tested. The most sensitive parameter seems to be the vertical hydraulic conductivity of the bedrock. The inflow decreased with approximately 63% when the vertical bedrock conductivity was decreased with a factor of 10.

The corresponding decrease in the horizontal hydraulic conductivity of the bedrock caused a decrease of "only" approximately 38% of the inflow to the repository. This implies that it is the properties of the bedrock that govern the inflow to the repository rather than the grouting conductivity or the meteorological conditions. The results from the sensitivity case where both the horizontal and vertical conductivities were increased with a factor of 3 in the bedrock below 150 m.b.s.l. further strengthens this hypothesis; in this case, the inflow increased with 73% compared to reference case.

8.2 Surface water

According to the model results, the water level in Lake Frisksjön would be affected by the repository and tunnel constructions. The calculated mean drawdown of the water level varies between 0.04 and 0.09 m depending on the level of grouting. During years with extremely dry conditions the groundwater discharge to Lake Frisksjön from the saturated zone is reversed leading to a large drawdown of the water-level.

The discharges in some streams, e.g. in Ekerumsbäcken, are to a large extent affected by the open repository, i.e. up to a decrease of 50% of the discharge. Laxemarån, the major water course in the area, is not affected to the same extent. This is mainly due to the fact that the catchment area to large extent is located outside the influence area. In the model, this part of the catchment area is represented by a specified inflow across the model boundary, which is not influenced by the repository. A grouting level of $K=1\cdot10^{-8}$ m/s results in a decrease of 8% of the average discharge in Laxemarån.

The sensitivity analysis shows that the discharges in the streams are rather insensitive to the bedrock properties. This was expected, as the surface water discharge is mainly controlled by the topographical conditions and the presence of a high conductive top soil layer, as long as the deeper till layers are less permeable than the top soil layers, which they are. However, when the sediment layers under the sea are removed the average discharge in Laxemarån decreases with 13% compared to undisturbed conditions; in the reference open repository simulation, with the sediments in the model, the corresponding decrease is 6%.

8.3 Groundwater table drawdown and head changes

The impact of the open repository on the groundwater table is extensive and reaches, irrespective of the grouting level, the model boundary. The influence area, here defined as a groundwater table drawdown larger than 0.3 m, is between 13.9 and 16.7 km^2. This corresponds to 40 to 50% of the total model area. The largest drawdown of the groundwater table is found above the central parts of the repository. The drawdown of the groundwater table, within this very limited area, is up to approximately 500 m. The average drawdown, within the influence area, varies between 20 and 25 m during 2006.

There are only slight differences in the head changes of the groundwater when considering different depths in the model. The influence area increases with depth and so does the change in head elevation. However, down to 310 m.b.s.l. the influence areas show the same overall pattern due to the isotropic bedrock, i.e. there is little difference between the horizontal and vertical hydraulic conductivities. Even though some high-permeable vertical fracture zones are present they will have little importance due the highly permeable surrounding bedrock, i.e. the difference in hydraulic conductivity between the fracture zones and the surrounding bedrock is small.

In the following comparisons, the influence area for the groundwater table has been defined as the area where the drawdown is larger than 0.3 m. A grouting level of $K=1\cdot10^{-8}$ m/s gives an influence area that is 6% larger (16.7 km^2) than that for a grouting level of $K=1\cdot10^{-9}$ m/s in the deposition tunnels and $K=1\cdot10^{-8}$ m/s elsewhere (15.7 km^2). The corresponding increase compared to the case with a grouting level of $K=1\cdot10^{-10}$ m/s in deposition tunnels and $K=1\cdot10^{-8}$ m/s elsewhere (13.9 km^2) is 20%. The overall pattern of the influence areas for the groundwater table is the same for all the three grouting levels.

The presented results are based on a three-year simulation period with meteorological input data for 2004–2006, where the years of 2004 and 2005 have been used as an initialisation period. However, in reality the repository would be open for many decades, and the groundwater table drawdown would have time to adjust to the inflow to the repository and reach new equilibrium conditions. When evaluating the effect of this by simulating a nine-year period, the influence area was found to be approximately 10% larger than that obtained after three years. This area was more or less reached after approximately six years.

This enlargement should be taken into account when considering the possible influence area. However, the temporal variation from the short-term variations of the meteorological and hydrological conditions during a year is larger, with an almost twice as large maximum influence area during the year, compared to the minimum influence area during the year (based on the results for 2006). Simulations with extremely high or low precipitation show that the influence area, for a drawdown exceeding 0.3 m, is approximately 25% larger for a dry year compared to a year characterised by wet conditions.

The closure of the repository was simulated by simply removing the repository from the model, and initialising the simulation from the situation with an open repository based on a grouting level of $K=1\cdot10^{-9}$ m/s in deposition tunnels and $K=1\cdot10^{-8}$ m/s elsewhere. The results from this simulation show that it takes approximately six years to a full recovery of the groundwater table. Two and a half years after repository closure the influence area is reduced to 44%, compared to the fully developed influence area with the whole repository open. Observe that these results do not consider the recovery of the groundwater head in the bedrock at the repository depth, which will take longer than that of the groundwater table.

Contrary to the inflow (see above), the sensitivity analysis shows that the groundwater table drawdown is most sensitive to the horizontal conductivity of the bedrock. The influence area of the groundwater table drawdown decreased by only 10% when the vertical hydraulic conductivity was reduced by a factor of 10 in the bedrock. The increase was as large as 40% when the corresponding change was made for the horizontal conductivity. The effect of the changes in the hydraulic conductivity of the QD layers on the influence area shows that the area increases with a decreased conductivity and vice versa. This is explained by a lower infiltration and recharge of the groundwater table when the conductivity is reduced.

9 References

Bosson E, 2006. Near-surface hydrogeological model of Laxemar. Open repository – Laxemar 1.2. SKB R-06-66, Svensk Kärnbränslehantering AB.

Bosson E, Sassner M, Gustafsson L-G, 2009. Numerical modelling of surface hydrology and near-surface hydrogeology at Laxemar-Simpevarp. Site descriptive modelling, SDM-Site Laxemar. SKB R-08-72, Svensk Kärnbränslehantering AB.

Brunberg A-K, Carlsson T, Brydsten L, Strömgren M, 2004. Oskarshamn site investigation. Identification of catchments, lake-related drainage parameters and lake habitats. SKB P-04-242, Svensk Kärnbränslehantering AB.

DHI Software, 2008a. MIKE SHE – User Manual. DHI Water, Environment & Health, Hørsholm, Denmark.

DHI Software, 2008b. MOUSE Pipe Flow – Reference Manual. DHI Water, Environment & Health, Hørsholm, Denmark.

Gustafsson L-G, Gustafsson A-M, Aneljung M, Sabel U, 2009. Effects on surface hydrology and near-surface hydrogeology of an open repository in Forsmark. Results of modelling with MIKE SHE. SKB R-08-121, Svensk Kärnbränslehantering AB.

Johansson P-O, 2008. Description of surface hydrology and near-surface hydrogeology at Forsmark. Site descriptive modelling, SDM-Site Forsmark. SKB R-08-08, Svensk Kärnbränslehantering AB.

Kristensen K J, Jensen S E, 1975. A model for estimating actual evapotranspiration from potential evapotranspiration. Nordic Hydrology, vol. 6, pp. 170–188.

Rhén I, Forsmark T, Hartley L, Jackson C P, Joyce S, Roberts D, Swift B, Marsic N, Gylling B, 2009. Bedrock hydrogeology: model testing and synthesis. Site descriptive modelling, SDM-Site Laxemar. SKB R-08-91, Svensk Kärnbränslehantering AB.

SKB, 2009. Site description of Laxemar at completion of the site investigation phase. SDM-Site Laxemar. SKB TR-09-01, Svensk Kärnbränslehantering AB.

Söderbäck B, Lindborg T (eds), 2009. Surface systems Laxemar, Site descriptive modelling, SDM-Site Laxemar. SKB R-09-01, Svensk Kärnbränslehantering AB.

Werner K, Öhman J, Holgersson B, Rönnback K, Marelius F, 2008. Meteorological, hydrological and hydrogeological monitoring data and near-surface hydrogeological properties data from Laxemar-Simpevarp. Site descriptive modelling, SDM-Site Laxemar. SKB R-08-73, Svensk Kärnbränslehantering AB.

Werner K, 2009. Description of surface hydrology and near-surface hydrogeology at Laxemar. Site descriptive modelling, SDM-Site Laxemar. SKB R-08-71, Svensk Kärnbränslehantering AB.

Appendix 1

The hydraulic conductivity of the grouted zone around the shafts is the same in all three grouting cases, $1 \cdot 10^{-8}$ m/s, which means that the conductance, C, is also the same in all grouting cases. The C values used for each shaft are listed in Table A1-1 to Table A1-6 below. The calculation of the conductance is described in Section 2.3.2.

Table A1-1. Geometry and conductivity for shaft SA01 when the grouting $K=1 \cdot 10^{-8}$ is applied to the walls of the shafts.

Calculation layer	Radius, m	Horiz. rock conductivity, Kh, m/s	Grid dx, m	Layer thickness dz, m	Grouting thickness, m	Grouting conductivity, Kgrout, m/s	Min[Kgrout, Kh]	Conductance, C, m^2/s
1	1.50	0.0022	40	2.00	5.00	1.00E–08	1.00E–08	8.57E–08
2	1.50	3.54E–05	40	2.84	5.00	1.00E–08	1.00E–08	1.22E–07
3	1.50	3.51E–07	40	1.00	5.00	1.00E–08	1.00E–08	4.28E–08
4	1.50	3.51E–07	40	2.00	5.00	1.00E–08	1.00E–08	8.57E–08
5	1.50	3.51E–07	40	35.26	5.00	1.00E–08	1.00E–08	1.51E–06
6	1.50	2.30E–07	40	40.00	5.00	1.00E–08	1.00E–08	1.71E–06
7	1.50	1.75E–07	40	40.00	5.00	1.00E–08	1.00E–08	1.71E–06
8	1.50	1.75E–07	40	40.00	5.00	1.00E–08	1.00E–08	1.71E–06
9	1.50	5.86E–08	40	40.00	5.00	1.00E–08	1.00E–08	1.71E–06
10	1.50	1.43E–08	40	40.00	5.00	1.00E–08	1.00E–08	1.71E–06
11	1.50	1.48E–08	40	40.00	5.00	1.00E–08	1.00E–08	1.71E–06
12	1.50	1.80E–08	40	40.00	5.00	1.00E–08	1.00E–08	1.71E–06
13	1.50	1.27E–09	40	40.00	5.00	1.00E–08	1.27E–09	2.18E–07
14	1.50	1.20E–09	40	40.00	5.00	1.00E–08	1.20E–09	2.06E–07
15	1.50	1.26E–09	40	40.00	5.00	1.00E–08	1.26E–09	2.16E–07
16	1.50	1.38E–09	40	40.00	5.00	1.00E–08	1.38E–09	2.37E–07
17	1.50	4.91E–11	40	25.70	5.00	1.00E–08	4.91E–11	5.41E–09

Table A1-2. Geometry and conductivity for shaft SA02 when the grouting $K=1 \cdot 10^{-8}$ is applied to the walls of the shafts.

Calculation layer	Radius, m	Horiz. rock conductivity, Kh, m/s	Grid dx, m	Layer thickness dz, m	Grouting thickness, m	Grouting conductivity, Kgrout, m/s	Min[Kgrout, Kh]	Conductance, C, m^2/s
1	1.50	0.00061	40	2.00	5.00	1.00E–08	1.00E–08	8.57E–08
2	1.50	4.00E–05	40	1.10	5.00	1.00E–08	1.00E–08	4.71E–08
3	1.50	6.41E–08	40	1.00	5.00	1.00E–08	1.00E–08	4.28E–08
4	1.50	6.41E–08	40	2.00	5.00	1.00E–08	1.00E–08	8.57E–08
5	1.50	6.41E–08	40	36.53	5.00	1.00E–08	1.00E–08	1.57E–06
6	1.50	7.22E–08	40	40.00	5.00	1.00E–08	1.00E–08	1.71E–06
7	1.50	6.78E–06	40	40.00	5.00	1.00E–08	1.00E–08	1.71E–06
8	1.50	5.59E–07	40	40.00	5.00	1.00E–08	1.00E–08	1.71E–06
9	1.50	1.69E–09	40	40.00	5.00	1.00E–08	1.69E–09	2.90E–07
10	1.50	4.91E–11	40	40.00	5.00	1.00E–08	4.91E–11	8.42E–09
11	1.50	4.91E–11	40	40.00	5.00	1.00E–08	4.91E–11	8.42E–09
12	1.50	4.06E–08	40	40.00	5.00	1.00E–08	1.00E–08	1.71E–06
13	1.50	7.81E–08	40	40.00	5.00	1.00E–08	1.00E–08	1.71E–06
14	1.50	4.20E–08	40	40.00	5.00	1.00E–08	1.00E–08	1.71E–06
15	1.50	8.91E–09	40	40.00	5.00	1.00E–08	8.91E–09	1.53E–06
16	1.50	1.71E–09	40	40.00	5.00	1.00E–08	1.71E–09	2.93E–07
17	1.50	5.14E–10	40	25.05	5.00	1.00E–08	5.14E–10	5.52E–08

Table A1-3. Geometry and conductivity for shaft SB00 when the grouting K=1·10^{-8} is applied to the walls of the shafts.

Calculation layer	Radius, m	Horiz. rock conductivity, Kh, m/s	Grid dx, m	Layer thickness dz, m	Grouting thickness, m	Grouting conductivity, Kgrout, m/s	Min[Kgrout, Kh]	Conductance, C, m^2/s
1	3.00	3.20E–04	40	2.23	5.00	1.00E–08	1.00E–08	1.43E–07
2	3.00	1.00E–08	40	1.00	5.00	1.00E–08	1.00E–08	6.41E–08
3	3.00	1.00E–08	40	1.00	5.00	1.00E–08	1.00E–08	6.41E–08
4	3.00	2.32E–08	40	1.00	5.00	1.00E–08	1.00E–08	6.41E–08
5	3.00	2.32E–08	40	38.44	5.00	1.00E–08	1.00E–08	2.46E–06
6	3.00	9.39E–08	40	40.00	5.00	1.00E–08	1.00E–08	2.56E–06
7	3.00	9.52E–08	40	40.00	5.00	1.00E–08	1.00E–08	2.56E–06
8	3.00	9.44E–08	40	40.00	5.00	1.00E–08	1.00E–08	2.56E–06
9	3.00	3.62E–09	40	40.00	5.00	1.00E–08	3.62E–09	9.28E–07
10	3.00	1.20E–09	40	40.00	5.00	1.00E–08	1.20E–09	3.07E–07
11	3.00	2.30E–09	40	40.00	5.00	1.00E–08	2.30E–09	5.89E–07
12	3.00	1.33E–09	40	40.00	5.00	1.00E–08	1.33E–09	3.41E–07
13	3.00	1.22E–09	40	40.00	5.00	1.00E–08	1.22E–09	3.13E–07
14	3.00	4.64E–09	40	40.00	5.00	1.00E–08	4.64E–09	1.19E–06
15	3.00	4.22E–09	40	40.00	5.00	1.00E–08	4.22E–09	1.08E–06
16	3.00	5.75E–09	40	40.00	5.00	1.00E–08	5.75E–09	1.47E–06
17	3.00	4.84E–09	40	40.00	5.00	1.00E–08	4.84E–09	1.24E–06
18	3.00	3.71E–09	40	6.05	5.00	1.00E–08	3.71E–09	1.44E–07

Table A1-4. Geometry and conductivity for shaft SC00 when the grouting K=1·10^{-8} is applied to the walls of the shafts.

Calculation layer	Radius, m	Horiz. rock conductivity, Kh, m/s	Grid dx, m	Layer thickness dz, m	Grouting thickness, m	Grouting conductivity, Kgrout, m/s	Min[Kgrout, Kh]	Conductance, C, m^2/s
1	2.50	5.90E–04	40	2.00	5.00	1.00E–08	1.00E–08	1.14E–07
2	2.50	1.00E–08	40	1.00	5.00	1.00E–08	1.00E–08	5.72E–08
3	2.50	3.81E–08	40	1.00	5.00	1.00E–08	1.00E–08	5.72E–08
4	2.50	4.11E–08	40	1.00	5.00	1.00E–08	1.00E–08	5.72E–08
5	2.50	4.11E–08	40	39.81	5.00	1.00E–08	1.00E–08	2.28E–06
6	2.50	2.75E–08	40	40.00	5.00	1.00E–08	1.00E–08	2.29E–06
7	2.50	9.74E–08	40	40.00	5.00	1.00E–08	1.00E–08	2.29E–06
8	2.50	1.14E–06	40	40.00	5.00	1.00E–08	1.00E–08	2.29E–06
9	2.50	3.81E–07	40	40.00	5.00	1.00E–08	1.00E–08	2.29E–06
10	2.50	3.77E–09	40	40.00	5.00	1.00E–08	3.77E–09	8.62E–07
11	2.50	2.62E–07	40	40.00	5.00	1.00E–08	1.00E–08	2.29E–06
12	2.50	5.20E–10	40	40.00	5.00	1.00E–08	5.20E–10	1.19E–07
13	2.50	1.56E–09	40	40.00	5.00	1.00E–08	1.56E–09	3.57E–07
14	2.50	4.40E–10	40	40.00	5.00	1.00E–08	4.40E–10	1.01E–07
15	2.50	1.51E–09	40	40.00	5.00	1.00E–08	1.51E–09	3.45E–07
16	2.50	6.49E–10	40	40.00	5.00	1.00E–08	6.49E–10	1.48E–07
17	2.50	2.33E–10	40	40.00	5.00	1.00E–08	2.33E–10	5.33E–08
18	2.50	5.51E–11	40	28.95	5.00	1.00E–08	5.51E–11	9.12E–09

Table A1-5. Geometry and conductivity for shaft SF00 when the grouting K=1·10^{-8} is applied to the walls of the shafts.

Calculation layer	Radius, m	Horiz. rock conductivity, Kh, m/s	Grid dx, m	Layer thickness dz, m	Grouting thickness, m	Grouting conductivity, Kgrout, m/s	Min[Kgrout, Kh]	Conductance, C, m^2/s
1	1.25	1.27E–03	40	2.00	5.00	1.00E–08	1.00E–08	7.81E–08
2	1.25	1.00E–08	40	1.00	5.00	1.00E–08	1.00E–08	3.90E–08
3	1.25	2.37E–08	40	1.00	5.00	1.00E–08	1.00E–08	3.90E–08
4	1.25	3.15E–08	40	1.00	5.00	1.00E–08	1.00E–08	3.90E–08
5	1.25	3.15E–08	40	38.56	5.00	1.00E–08	1.00E–08	1.51E–06
6	1.25	1.09E–07	40	40.00	5.00	1.00E–08	1.00E–08	1.56E–06
7	1.25	7.40E–08	40	40.00	5.00	1.00E–08	1.00E–08	1.56E–06
8	1.25	1.02E–08	40	40.00	5.00	1.00E–08	1.00E–08	1.56E–06
9	1.25	1.33E–09	40	40.00	5.00	1.00E–08	1.33E–09	2.08E–07
10	1.25	3.43E–09	40	40.00	5.00	1.00E–08	3.43E–09	5.36E–07
11	1.25	3.94E–09	40	40.00	5.00	1.00E–08	3.94E–09	6.15E–07
12	1.25	9.96E–10	40	40.00	5.00	1.00E–08	9.96E–10	1.56E–07
13	1.25	1.39E–10	40	40.00	5.00	1.00E–08	1.39E–10	2.17E–08
14	1.25	2.48E–09	40	40.00	5.00	1.00E–08	2.48E–09	3.87E–07
15	1.25	3.20E–09	40	40.00	5.00	1.00E–08	3.20E–09	5.00E–07
16	1.25	4.04E–09	40	33.66	5.00	1.00E–08	4.04E–09	5.31E–07

Table A1-6. Geometry and conductivity for shaft ST00 when the grouting K=1·10^{-8} is applied to the walls of the shafts.

Calculation layer	Radius, m	Horiz. rock conductivity, Kh, m/s	Grid dx, m	Layer thickness dz, m	Grouting thickness, m	Grouting conductivity, Kgrout, m/s	Min[Kgrout, Kh]	Conductance, C, m^2/s
1	1.75	1.08E–03	40	2.00	5.00	1.00E–08	1.00E–08	9.31E–08
2	1.75	4.00E–05	40	1.00	5.00	1.00E–08	1.00E–08	4.65E–08
3	1.75	5.14E–08	40	1.00	5.00	1.00E–08	1.00E–08	4.65E–08
4	1.75	5.14E–08	40	1.00	5.00	1.00E–08	1.00E–08	4.65E–08
5	1.75	5.14E–08	40	38.89	5.00	1.00E–08	1.00E–08	1.81E–06
6	1.75	1.10E–07	40	40.00	5.00	1.00E–08	1.00E–08	1.86E–06
7	1.75	4.23E–08	40	40.00	5.00	1.00E–08	1.00E–08	1.86E–06
8	1.75	2.70E–08	40	40.00	5.00	1.00E–08	1.00E–08	1.86E–06
9	1.75	3.75E–09	40	40.00	5.00	1.00E–08	3.75E–09	6.98E–07
10	1.75	9.49E–10	40	40.00	5.00	1.00E–08	9.49E–10	1.77E–07
11	1.75	1.17E–09	40	40.00	5.00	1.00E–08	1.17E–09	2.18E–07
12	1.75	3.63E–10	40	40.00	5.00	1.00E–08	3.63E–10	6.76E–08
13	1.75	1.70E–09	40	40.00	5.00	1.00E–08	1.70E–09	3.17E–07
14	1.75	3.08E–09	40	40.00	5.00	1.00E–08	3.08E–09	5.73E–07
15	1.75	5.55E–09	40	40.00	5.00	1.00E–08	5.55E–09	1.03E–06
16	1.75	5.49E–09	40	33.70	5.00	1.00E–08	5.49E–09	8.61E–07